



UNIVERSITY OF LEEDS

This is a repository copy of *A review of current techniques for the evaluation of powder mixing*.

White Rose Research Online URL for this paper:

<https://eprints.whiterose.ac.uk/id/eprint/130746/>

Version: Accepted Version

---

**Article:**

Asachi, M, Nourafkan, E [orcid.org/0000-0002-1898-5528](https://orcid.org/0000-0002-1898-5528) and Hassanpour, A [orcid.org/0000-0002-7756-1506](https://orcid.org/0000-0002-7756-1506) (2018) A review of current techniques for the evaluation of powder mixing. *Advanced Powder Technology*, 29 (7). pp. 1525-1549. ISSN 0921-8831

<https://doi.org/10.1016/j.appt.2018.03.031>

---

© 2018, The Society of Powder Technology Japan. Licensed under the Creative Commons Attribution-NonCommercial-NoDerivatives 4.0 International License (<http://creativecommons.org/licenses/by-nc-nd/4.0/>)

**Reuse**

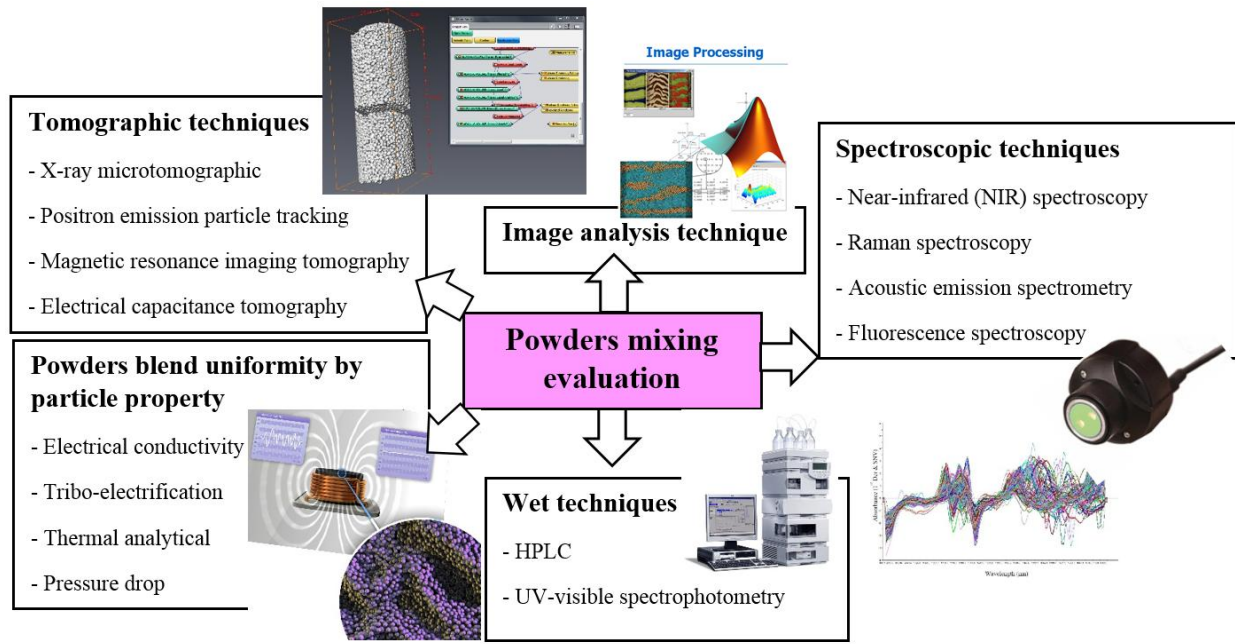
This article is distributed under the terms of the Creative Commons Attribution-NonCommercial-NoDerivatives (CC BY-NC-ND) licence. This licence only allows you to download this work and share it with others as long as you credit the authors, but you can't change the article in any way or use it commercially. More information and the full terms of the licence here: <https://creativecommons.org/licenses/>

**Takedown**

If you consider content in White Rose Research Online to be in breach of UK law, please notify us by emailing [eprints@whiterose.ac.uk](mailto:eprints@whiterose.ac.uk) including the URL of the record and the reason for the withdrawal request.



[eprints@whiterose.ac.uk](mailto:eprints@whiterose.ac.uk)  
<https://eprints.whiterose.ac.uk/>



## A review of current techniques for the evaluation of powder mixing

Maryam Asachi<sup>1</sup>, Ehsan Nourafkan<sup>1\*</sup>, Ali Hassanpour<sup>1\*</sup>

<sup>1</sup>School of Chemical and Process Engineering, University of Leeds, Leeds, LS2 9JT, UK

### ABSTRACT

Blending a mixture of powders to a homogeneous system is a crucial step in many manufacturing processes. To achieve a high quality of the end product, powder mixtures should be made with high content uniformity. For instance, producing uniform tablets depends on the homogeneous dispersion of active pharmaceutical ingredient (API), often in low level quantities, into excipients. To control the uniformity of a powder mixture, the first required step is to estimate the powder content information during blending. There are several powder homogeneity evaluation techniques which differ in accuracy, fundamental basis, cost and operating conditions. In this article, emerging techniques for the analysis of powder content and powder blend uniformity, are explained and compared. The advantages and drawbacks of all the techniques are reviewed to help the readers to select the appropriate equipment for the powder mixing evaluation. In addition, the paper highlights the recent innovative on-line measurement techniques used for the non-invasive evaluation of the mixing performance.

**Keywords:** Powder mixing evaluation, Powder blend homogeneity, Wet techniques, Dry techniques

\*Corresponding authors. Ali Hassanpour ([a.hassanpour@leeds.ac.uk](mailto:a.hassanpour@leeds.ac.uk), Tel.: (+44) 0113 343 2405); Ehsan Nourafkan ([e.nourafkan@leeds.ac.uk](mailto:e.nourafkan@leeds.ac.uk), Tel.: (+44) 0113 343 2407)

1  
2  
3  
4  
5  
6  
7  
8  
9  
10  
11  
12  
13  
14  
15  
16  
17  
18  
19  
20  
21  
22  
23  
24  
25  
26  
27  
28  
29  
30  
31  
32  
33  
34  
35  
36  
37  
38  
39  
40  
41  
42  
43  
44  
45  
46  
47  
48  
49  
50  
51  
52  
53  
54  
55  
56  
57  
58  
59  
60  
61  
62  
63  
64  
65

**Contents:**

1. Introduction.....

2. Wet techniques to assess powder blend uniformity .....

2.1. Ultra-Violet (UV)-visible absorbance spectrophotometry .....

2.2. HPLC (High-Performance Liquid Chromatography) .....

3. Dry techniques to assess powder blend uniformity.....

3.1. Image analysis technique .....

3.2. Assessment of powder blend uniformity by bulk particle properties.....

3.2.1 Pressure drop method.....

3.2.2. Electrical conductivity method .....

3.2.3. Tribo-electrification method .....

3.2.4. Thermal analytical method.....

3.3. Tomographic techniques .....

3.3.1. X-ray microtomographic method.....

3.3.2. Positron emission particle tracking (PEPT) method .....

3.3.3. Electrical capacitance tomography .....

3.3.4. Magnetic resonance imaging tomography .....

3.4. Spectroscopic techniques .....

3.4.1. Near-infrared spectroscopy .....

3.4.2. Raman spectroscopy .....

3.4.3. Acoustic emission spectrometry .....

3.4.4. Fluorescence spectroscopy.....

4. Conclusions.....

1  
2  
3  
4 **1. Introduction**  
5  
6

7 Powder mixing unit operation is a very common step in particulate processes and has  
8 significant impact on the quality of the end product; examples are in industries such as  
9 pharmaceutical, agro-food, cement and plastics [1-8]. The final characteristics of the powdered  
10 products nowadays are becoming more complex. In some cases, a mixture of up to 20 powder  
11 ingredients is necessary to meet acceptable quality standard of the final product. Powder  
12 segregation, a phenomenon which is described as the opposite of mixing, or reverse mixing,  
13 takes place as a result of powder in-homogeneity during blending process or during secondary  
14 processing steps such as packaging and transportation [9-11]. A batch of pharmaceutical tablets  
15 at a cost of thousands of dollars could be rejected due to powder in-homogeneities arising from  
16 segregation of active component. As another example, layer by layer deposition of the  
17 segregated powders before getting fused together by laser, could adversely affect the quality of  
18 products in 3D printing manufacturing.  
19  
20  
21  
22  
23  
24  
25  
26  
27  
28

29  
30 Mixing processes of granular materials often aim at producing a product with a suitable  
31 degree of homogeneity. There are two main types of equipment available for the mixing of  
32 granular materials. In the first group, the container is rotated around an axis to move around the  
33 materials inside to mix them with a dominant shear and diffusion mixing mechanisms. On the  
34 other hand, convection and/or shear could be the main mechanism in the second group in which  
35 the container is stationary and an internal rotor causes a mild or fast agitation. For the mixing of  
36 granular materials, the choice of mixer type is vital as the quality of the mixture highly depends  
37 on the mixer selection [12]. In addition, the quality of the mixture and the end-point of the  
38 process should be interpreted by evaluating the samples taken from the mixture. The goal of  
39 powder sampling is to collect a small amount of sample from a bulk powder in such a way that  
40 the sample represents the physical and chemical characteristics of the entire bulk. It should be  
41 noted that acquiring a representative sample from the bulk powder is crucial because further  
42 analyses and data interpretation regarding the mixing process performance depends on the  
43 sampling representativity [13].  
44  
45  
46  
47  
48  
49  
50  
51  
52  
53  
54  
55

56 It should be noted that developing a general guidance for obtaining a representative sampling  
57 is challenging and beyond the scope of this article since the conditions of mixing processes are  
58 different from case to case. However, a brief description of sample representativity procedure  
59  
60  
61  
62  
63  
64  
65

1  
2  
3  
4 has been provided here and the readers are referred to the additional sources on this topic [7, 14,  
5  
6 15].  
7

8  
9 To apply a proper sampling procedure on bulk powders, the population and sample size, sample  
10 collection and sample size reduction method, and statistical analysis confirming the stated level  
11 of acceptance of the sampling plan must be fully addressed [16, 17]. A general framework of the  
12 sampling used in powder mixing processes is illustrated in Fig. 1-a.  
13  
14

15  
16  
17 The scale of scrutiny according to the product specification is mainly used to determine the  
18 ideal size of samples. The taken samples having the required size of scale of scrutiny must be  
19 analysed for the composition evaluation [12]. Generally, sample size should be close to the size  
20 of the final product, e.g. tablet size in pharmaceutical industry. Moreover, the sample size should  
21 be larger than the minimum amount needed for the analytical analysis. It should be noted that if  
22 the scale of scrutiny is defined too small, the homogeneity of the blend would wrongly appear to  
23 be unacceptable. In contrast, if the sample size is considered too large, the homogeneity of the  
24 blend would wrongly appear to be acceptable resulting in an overestimation of the homogeneity  
25 (Fig. 1-b). If the scale of scrutiny is much smaller than the minimum amount of sample that the  
26 sampler provides, reliable sample reduction techniques, which have been fully reviewed by Allen  
27 [18], must be applied. The granules segregation during sample reduction process must be  
28 prevented to have representative sub-samples which meet the scale of scrutiny. Cone and  
29 quartering, scoop sampling, rotary riffler, chute riffler and table riffler are among the most well-  
30 known and applied methods for sample splitting. Allen reported the representivity of all the  
31 methods (based on standard deviation in size distribution observed between different subsamples  
32 generated from the same primary sample) and introduced the rotary riffler as the most  
33 representative method for sample size reduction [18].  
34  
35  
36  
37  
38  
39  
40  
41  
42  
43  
44  
45  
46  
47

48  
49 **Fig. 1.** (a) A general framework of sampling in powder mixing processes, (b) effect of the scale  
50 of scrutiny on mixing evaluation.  
51  
52

53  
54 Powder sampling in a dynamic mixing process (Fig. 1-a) must be performed based on Golden  
55 Rules as follows [19]:  
56

57  
58 -Rule 1: Powder mixtures should be sampled when in motion.  
59  
60  
61  
62  
63  
64  
65

1  
2  
3  
4 -Rule 2: The whole stream of the powder mixture should be taken for many short increments of  
5 time, rather than part of the stream being taken for the whole time.  
6  
7

8  
9 Acquisition of samples at the outlet of a continuous mixer should be performed at a regular  
10 frequency (starting at 3 times the residence time of the mixer when the system has reached a  
11 steady state). Full stream samplers at the outlet of the mixer are used in continuous mixers [19].  
12 In a batch mixer, the mixer needs to be stopped at different blending times and then the sampling  
13 is carried out at various locations (by dividing the space into equal regions). Regarding the  
14 location of sampling, the whole powder stream should be sampled for numerous short increments  
15 of time [19].  
16  
17  
18  
19  
20  
21

22  
23 The traditional samplers, e.g. thief and cross-cut, are most commonly used instruments for  
24 powder sampling [20]. Using samplers is mostly an invasive approach which causes disturbance  
25 in the mixture, hence special care and designs are needed to mitigate it [15, 21, 22]. However, in  
26 recent decades, non-invasive analytical technologies have been developed such as Near-Infrared  
27 spectroscopy (NIR), Raman spectroscopy and Electrical Capacitance Tomography with no  
28 interference with the blending process [23].  
29  
30  
31  
32  
33

34  
35 To control the uniformity of a mixture and reduce its inhomogeneity during blending, it is  
36 necessary to monitor the component concentration inside the mixer. This helps to achieve the  
37 optimum mixing conditions, such as end-point mixing time. Process monitoring can be achieved  
38 by performing routine testing of the process samples using off-line, at-line, inline and on-line  
39 instrumentations. Off-line analyser is a discontinuous, invasive, slow and time consuming  
40 traditional laboratory method that is performed in a controlled location by a technically trained  
41 person. For this purpose, the samples removed from the process are transported to a laboratory  
42 for further analysis. Its advantage lies in the fact that it provides the greatest flexibility in  
43 selecting the measurement method, sample preparation and the most accurate method [24].  
44 Procedure of at-line analyser is similar to that of off-line, however, the main difference is the  
45 time duration of the analysis. Usually, at-line analysis can be performed with automatic facilities  
46 quicker than off-line analysis by a mediocre operator. For at-line analysis, a defined device is  
47 placed close to the line to analyse the samples which may be occasionally or continuously  
48 extracted from the stream. Although the devices used in at-line analysis are mainly robust, they  
49 rely on standardized procedures and fixed parameter settings [24].  
50  
51  
52  
53  
54  
55  
56  
57  
58  
59  
60  
61

1  
2  
3  
4 In-line analysers are simple sensors or measuring devices that are placed directly into a  
5 process stream. Therefore, there is no need to extract a sample from the process for examination.  
6 In-line process measurement performs the analysis either invasively by using a probe positioned  
7 in the process stream or non-invasively in which the probe does not have physical contact with  
8 the sample [25]. However, using in-line method, achieving a representative sample might be  
9 difficult since the measurements could be influenced by immediate process fluctuations.  
10 Temperature, pH, pressure, and flowrate are the usual process parameters which are measured in-  
11 line. On-line analysers are fully automated systems used to closely monitor the parameters that  
12 are critical in the production process. On-line methods have this ability to control the mixing  
13 processes by automatically changing the status of devices, such as valves, as part of their  
14 analysis sequence. Using an on-line measurement, continuously extracted samples from the  
15 process stream (by the means of a bypass) are transported to a specialized analyser and then  
16 returned to the process stream. This eliminates many preparation possibilities (i.e., all forms of  
17 destructive testing methods) and allows a large fraction of the product stream to be analysed  
18 [24].  
19  
20  
21  
22  
23  
24  
25  
26  
27  
28  
29  
30  
31

32 Current research provides useful information on analytical methods for uniformity analysis of  
33 powder mixtures. Fast and accurate uniformity evaluation of powder blends is one of the  
34 challenges faced by many industries. This review article provides comprehensive background  
35 information on different powder mixing evaluation techniques and introduces the readers to the  
36 pros and cons of all the techniques in terms of cost, functionality, precision and operation  
37 conditions.  
38  
39  
40  
41  
42  
43  
44  
45  
46

## 47 **2. Wet techniques to assess powder blend uniformity**

### 48 **2.1. Ultra-Violet (UV)-visible absorbance spectrophotometry**

49  
50 By illuminating the sample with UV radiation and obtaining the absorbance, it is possible to  
51 estimate the concentration of a specimen. According to the Beer-Lambert law (Eq. 1), the  
52 absorbance information has a linear relationship with the concentration data [26, 27].  
53  
54  
55  
56

$$57 A = a(\lambda) \times b \times C \quad (1)$$

58  
59  
60  
61  
62  
63  
64  
65



1  
2  
3  
4 where A, b, C and  $a(\lambda)$  are the measured absorbance, path length, specimen concentration  
5 and wavelength dependant absorptivity coefficient, respectively. Thus, UV-visible  
6 spectrophotometry is able to determine the concentration of the absorber in a solution based on  
7 Beer-Lambert law after selection of a proper wavelength. Quantifying the trend of the  
8 absorbance values versus different standard concentrations is necessary for the measurement of  
9 the unknown concentrations. Before spectral analysis of the unknown samples, spectrum  
10 background correction using a buffer blank is needed. According to Fig. 2-a, the unknown  
11 sample is placed between a light source and a photodetector. The intensity of the beam of UV-  
12 visible light, before and after passing the light through the sample, is then used to measure the  
13 unknown concentration [28].  
14  
15  
16  
17  
18  
19  
20  
21  
22

23 Determination of the active ingredient content of powder mixture samples (especially in  
24 pharmaceutical products e.g. tablets and capsules) with UV-visible spectroscopy is a frequently  
25 useful technique [29, 30]. In a work done by Mendez et al. [20] pharmaceutical powder mixing  
26 was successfully evaluated in a V-blender during batch production using UV-visible  
27 spectrophotometry. The acetaminophen concentration of tablets, produced from samples from  
28 different regions of the blender at different times, was measured using UV-visible  
29 spectrophotometry (Agilent UV-VIS 8453E double-beam spectrophotometer at a wavelength of  
30 244 nm). 3 samples of approximately 3.0 g were collected each time using a thief probe at three  
31 different locations (right, left and the bottom of blender). To perform quantitative determination,  
32 different standard solutions of acetaminophen were prepared to build a calibration curve.  
33  
34  
35  
36  
37  
38  
39  
40

41 Moreover, the UV-visible spectrophotometer is widely used as reference method for the  
42 determination of active ingredient during powder mixture as it is fast and simple method [31-33].  
43 However, the disadvantages of this analytical method are as follow [34-36]:  
44  
45  
46

47 -The main disadvantage of UV-visible spectrophotometry is that the absorbance spectra of  
48 soluble components are measured all together. Therefore, the separate measurement of  
49 component fractions within a mixture is not applicable in most cases using this technique.  
50  
51

52 -The impurities could influence the absorption spectra of the target component. Therefore,  
53 UV-visible spectrophotometry could not properly discriminate between the sample of interest  
54 and the contaminants absorbing at the same wavelength. Moreover, the detectors of the  
55 spectrophotometers are sensitive to the light. If any impurity in the sample reflects the light, an  
56 erroneous reading may be recorded by the detectors.  
57  
58  
59  
60  
61

1  
2  
3  
4 -Absorption values could be influenced by parameters such as temperature and pH leading to  
5 inaccurate result analysis.  
6

7 -The sensitivity of a spectrophotometer is often inadequate at low concentrations.  
8  
9

## 10 11 12 13 **2.1. HPLC (High-Performance Liquid Chromatography)**

14  
15 High-pressure liquid chromatography (HPLC) is a traditional off-line wet technique to  
16 separate, identify, and quantify the components in a mixture (Fig. 2-b). HPLC differs from the  
17 standard column chromatography method by the fact that it applies pressure to force the solution  
18 through the column, and therefore provides quicker, and more accurate results [37, 38]. As  
19 shown in Fig. 2-b, the solvent flows through a column with the help of a high pressure (up to 400  
20 atm). The sample, injected to the mobile phase, is transported to the HPLC column for content  
21 determination as schematically shown in Fig. 2-b.  
22  
23  
24  
25  
26  
27  
28

29  
30 **Fig. 2.** (a) Schematic of UV-Visible spectrometer, (b) High-pressure liquid  
31 chromatography (with permission from University of Leeds).  
32

33  
34 The separation of components takes place in a stationary phase, fixed inside the HPLC  
35 column, because of difference in relative affinities of the constituents. Different retention times  
36 of the constituents in the outlet of HPLC column enables the estimation of different component  
37 fractions by a detector [39, 40]. A broad range of detectors such as UV/Vis, fluorescence (FL),  
38 Evaporative Light Scattering (ELSD) and Photo Diode Array (PDA) are available for the  
39 detection of different types of constituents in the mobile phase. The description of different  
40 detector types is beyond the scope of this article and the readers are referred to the additional  
41 sources on this topic [26, 37]. For the content analysis of the unknown samples, the standard  
42 solutions are first analysed by HPLC to obtain the calibration plot, from which it is possible to  
43 measure the chromatogram areas as a linear function of the concentrations of each constituent.  
44 After analysing the chromatogram of the unknown sample (Fig. 2-b), the concentration of each  
45 constituents could be specified [41].  
46  
47  
48  
49  
50  
51  
52  
53  
54

55 For content uniformity testing of tablets, HPLC method was used by Walsh et al. [42] for the  
56 determination of naftazone component. For this purpose, separation was performed using a  
57 Merck Hitachi L-7100 Chromatograph. A Nucleosil 100-5 phenyl column and a mobile phase  
58  
59  
60  
61  
62  
63  
64  
65

1  
2  
3  
4 comprising methanol-sodium dihydrogen phosphate mixture were used. Quantification of  
5 naftazone was performed by making a calibration curve obtained from different standards  
6 containing different concentrations of naftazone. Good correlation over the concentration range  
7 of 0.1-10.0  $\mu\text{g/mL}$  has been shown by this method with a lower detection and quantification  
8 limits of 0.032 and 0.096  $\mu\text{g/mL}$ , respectively. Tanaka et al. [43] compared the efficiency of  
9 resonant acoustic mixing (RAM) technology for with ordinary mixing method for  
10 pharmaceutical blending process. The mixing of theophylline powder and lactose or magnesium  
11 oxide and lactose were carried out in a modified V-shaped mixing device and the APIs content  
12 uniformity in the mixture was quantified by HPLC method (LC-10vp series, Shimadzu). The  
13 API and lactose powders were mixed for 0.5 h at 30 rpm by ordinary method, and the powders  
14 were mixed for 0.01 h and 0.03 h at 100 G, 60 Hz by the resonant acoustic method. The  
15 coefficient of variation (CV) value of ordinary method was the largest and indicated non-  
16 uniformity. However, the CV values of resonant acoustic were smaller than ordinary mixing. The  
17 results showed that the resonant acoustic method could obtain content uniformity approximately  
18 900 times more rapidly compared with ordinary methods [43].

19  
20 Overall, as stated earlier UV-visible spectrophotometer method has its own limitation  
21 regarding the concentration measurement of each constituent in the mixture separately [42].  
22 However, HPLC is frequently used for the separation, identification and quantification of  
23 different constituents in a mixture. Moreover, HPLC resolves the problem of the interference of  
24 active impurities and thus provides more accurate analysis compared to the UV-visible  
25 spectrophotometer method [44, 45]. Eraga et al. [46] analysed the content of ibuprofen  
26 ingredient, in ibuprofen tablets by UV-visible and HPLC method (Agilent Infinity 1260, Agilent  
27 Technologies Inc., USA). The standard samples was prepared by dissolving 100 mg of  
28 ibuprofen powder reference standard in a 100 mL volumetric flask with 0.1 mol/L NaOH  
29 solution. A 1 mL aliquot of the solution was further diluted to 100 mL to give the desired  
30 concentration. The main samples were prepared by dissolving of 100 mg of crushed ibuprofen  
31 tablets in water with similar procedure of standard sample preparation. The results showed that  
32 the HPLC method is more sensitive and reliable assay for ibuprofen detection compare to UV-  
33 visible spectroscopy and hence the HPLC technique suggested to be used for verification of the  
34 UV-visible method.

1  
2  
3  
4 Beside several advantages of HPLC, there are several disadvantages for this analytical  
5 analysis technique. HPLC is time consuming as it requires two steps of 1-finding the optimum  
6 conditions (mobile phase composition, flowrate, injection volume and detector type) and 2-  
7 performing sample analysis at optimum conditions. Moreover, the complete package of HPLC  
8 facilities is expensive.  
9

10  
11  
12  
13 It should be noted that there are several issues with the above-mentioned traditional wet-based  
14 analytical methods. First, wet analytical methods are deemed tedious and time-consuming. Also,  
15 the material is lost by these methods because they the solid needs to be dissolved, hence, the  
16 studied material is not recoverable. Moreover, they are not classed as green method since they  
17 are wet-based techniques [47]. Therefore, other methods for analysing powder content are  
18 required which are briefly reviewed below.  
19  
20  
21  
22  
23  
24  
25  
26  
27

### 28 **3. Dry techniques to assess powder blend uniformity**

#### 29 **3.1. Image analysis technique**

30  
31  
32 With image processing of a captured photo from a powder mixture, it is possible to assess the  
33 uniformity of particles, providing that particles differ in colour. The 2D photo taken from the  
34 mixture of powders can be divided into several sections, where a component of interest can be  
35 quantitatively analysed using a potential image processing method. Then the fraction distribution  
36 of the desired component can be estimated in order to evaluate its homogeneity throughout the  
37 mixture [48, 49].  
38  
39  
40  
41  
42

43 Rosas and Blanco [50] applied image processing technique to evaluate the mixing  
44 homogeneity of coloured sand ( $\text{SiO}_2$ ) of different particle sizes in a blender. Two different set-  
45 ups were used to take the images during the mixing processes. Set-up 1 was based on at-line  
46 mode in which the samples were manually taken and photographed (using a Video meter Lab  
47 camera) and set-up 2 was based on a non-invasive image recording mode (Fig. 3-a). Different  
48 stages for the evaluation of the mixing quality of the captured photos are shown in Fig. 3-b. The  
49 quality of the raw image was first improved by some preliminary image pre-processing. After  
50 obtaining the segmented images using Matlab software, they were split into small subsections.  
51 Different mixing indices such as modified Lacey index,  $M_L$  (0 for totally segregated and 1 for  
52 totally random), modified Poole index,  $M_p$  (tends to unity in totally random images),  
53  
54  
55  
56  
57  
58  
59  
60  
61

1  
2  
3  
4 homogeneity ratio defined by  $H_L$  and  $H_P$  % (100 for near-random and homogeneous mixture)  
5  
6 were measured to investigate the quality of the powder mixtures. The homogeneity ratio was  
7  
8 defined as the ratio of the mixing index ( $M_{\text{image}}$ ) for an image and its randomized version  
9  
10 ( $M_{\text{random\_image}}$ ). The mathematical correlation of different mixing indices has been presented in  
11  
12 the study by Rosas and Blanco [50] in detail. Moreover, a review of different mixing indices  
13  
14 used for the evaluation of powder mixing performance has been provided by Poux et al. [10].  
15

16  
17 **Fig. 3.** (a) Schematic of two setups applied for capturing images during mixing process and (b)  
18  
19 different required steps for homogeneity assessment of images, (Reprinted from Rosas and  
20  
21 Blanco [50]).  
22  
23

24  
25 In a recent work, mixing of couscous particles of nearly spherical shape (with specific size  
26  
27 ranges) in a continuous system has been assessed by on-line image-processing during steady and  
28  
29 unsteady state regimes [51]. Using the on-line image-processing technique **described** by  
30  
31 Ammarcha et al. [51], homogeneity of mixtures was evaluated by capturing all images of  
32  
33 particles at the discharge of the continuous pilot-scale mixer (Fig. 4). The Charge Coupled  
34  
35 Device (CCD, one pixel width-5000 pixels length) camera of the set-up was placed vertically  
36  
37 with respect to the belt to film the passing mixture at different times. Each pixel represented a  
38  
39  $60 \times 60 \mu\text{m}^2$  surface on the belt which was much smaller than the size of each particle. The  
40  
41 pictures were captured by grouping 200 consecutive one-pixel-width lines ( $500 \times 200 \text{ pixel}^2$  image  
42  
43 or  $30 \times 1.2 \text{ cm}^2$  surface). Quality of the mixtures was evaluated by the concept of coefficient of  
44  
45 variation obtained for the key ingredient.

46  
47 There **have** been numerous reported **works** on this topic and Table 1 summarises some recent  
48  
49 works based on image analysis technique for the evaluation of powder mixing performance.  
50

51  
52 **Fig. 4.** The combined mixer/image-processing for on-line monitoring of continuous mixing,  
53  
54 (Reprinted from G. Ammarcha et al. [51]).  
55  
56

57  
58 **Table 1.** Research works based on image analysis for powder blend uniformity evaluation.  
59  
60  
61  
62  
63  
64  
65

1  
2  
3  
4 In all the above-mentioned research studies, only the surfaces of mixtures were scanned for  
5 homogeneity characterisation. Slicing samples while preserving its properties, (e.g. using  
6 solidification of a mixture by a binder such as gelatin as solidifier and then refrigeration), could  
7 provide more content information from a discretized mixture. Measurement of the composition  
8 of a mixture, containing two coloured particles of granite stone, was performed by Realpe et al.  
9 [60] using a combination of slicing technique and image processing. Homogeneity of the mixture  
10 was assessed with image processing of the samples collected after slicing. After image  
11 processing of the captured pictures of the entire sliced samples (Fig. 5), mixing quality of the  
12 mixture could be evaluated. This technique could be beneficial to a broad range of industries  
13 such as metallurgy, pharmaceuticals, food processing and ceramics. Based on slicing technique,  
14 the internal structure of a mixture can be characterised off-line or at-line. In addition, the best  
15 binder should be investigated in such a way that it does not destroy the chemical structure while  
16 the internal physical properties are preserved.  
17  
18  
19  
20  
21  
22  
23  
24  
25  
26  
27  
28  
29

30 **Fig. 5.** The top view of the sliced samples after solidification of a homogenised mixture,  
31 (Reprinted from A. Realpe et al. [60]).  
32  
33  
34

35 Image analysis method is widely used for powder homogeneity evaluation due to its relative  
36 simplicity and low cost compared to the other techniques. However, this technique cannot be  
37 easily applied for the differentiation of components of similar colours. As the lighting conditions  
38 may not be always stable through the images, further background correction is also required for  
39 the analysis of the raw images. Moreover, unless slicing technique is used, image processing will  
40 provide only the surface properties of the mixture.  
41  
42  
43  
44  
45  
46  
47  
48  
49

### 50 **3.2. Assessment of powder blend uniformity by bulk particle properties**

51 Bulk powder property can be a good indicator of powder homogeneity status during the  
52 mixing process. With determination of the bulk powder properties during blending, (e.g.  
53 monitoring pressure drop, conductivity, interaction charges or thermal behaviour), it could be  
54 possible to evaluate the mixing performance, which is briefly reviewed below.  
55  
56  
57  
58  
59  
60  
61  
62  
63  
64  
65

### 3.2.1. Pressure drop method

Segregation of binary mixture of silica sand and silica gel was investigated by Olivieri et al. [61] in a Fluidization system. The pressure was monitored at different locations along the bed using pressure transducers to investigate the segregation pattern (Fig. 6-a). The plot of pressure gradient against the gas superficial velocity was used to discover the occurrence of segregation (Fig. 6-b). Velocity ( $U$ ) between 2.2 and 9.1  $cm/s$  demonstrated the bubble formation and the onset of segregation of sand particles at the bottom of the bed. The decreasing pattern of pressure gradient in upper region of the bed at this range of velocity, was reported to be as a result of the progressive accumulation of low density silica-gel particles in this region. A uniform pattern could be observed at  $U > 9.1$   $cm/s$ .

In other work performed by Yudin et al. [62], different distributor configurations, such as perforated plate, circular edged slotted type ( $90^\circ$ ) and novel swirling type ( $45^\circ$ ), were used for the investigation of the mixing performance of a fluidized bed system using the pressure drop concept. The differential pressure readings across the column were logged using AZ Instrument™ 82012 differential digital manometer (resolution of  $\pm 1$   $mmH_2O$  and  $\pm 1.0\%$  accuracy). Excellent particulate mixing was reported to be achieved by the novel swirling distributor without the need to apply mechanical rotation.

**Fig. 6.** (a) Schematic of fluidized bed equipped with pressure transducer (PT) and (b) pressure gradient versus gas superficial velocity at different heights of the bed, (Reprinted from Olivieri et al. [61]).

Using pressure drop information of a system, segregation patterns can be predicted only qualitatively and the technique could be potentially used to identify trend changes. Robust and precise quantitative analysis is needed for content analysis and mixing performance evaluation which will be described later.

### 3.2.2. Electrical conductivity method

Shenoy et al. [63] developed an at-line powder uniformity assessment method based on measuring the conductivity of powder samples. The effects of particle density, size and shape on the mixture uniformity in a lab-scale paddle mixer were investigated. The binary mixtures containing salt and other food seasoning powders were prepared and then the conductivity of

1  
2  
3  
4 different taken samples was measured by a conductivity meter instrument (SG78, Mettler  
5 Toledo). Using a conductivity calibration curve of salt obtained from analysis of different known  
6 standard concentrations, the unknown salt concentration of each sample could be determined.  
7  
8

9  
10 In another study, Shenoy et al. [64] compared the image processing with salt conductivity  
11 method for the quality analysis of food powder mixtures. The powder mixtures were first located  
12 next to each other inside of the mixer, representing a fully segregated medium. Using a bent  
13 spoon (a kind of thief probe sampler), nine samples were extracted at five different mixing times.  
14 The extracted samples were then positioned in small containers (4 cm diameter and 1 cm height).  
15 Digital colour imaging (DCI) and salt conductivity method were used for measuring the salt  
16 concentration of each sample. It was demonstrated that the image processing technique could be  
17 a better option for mixing evaluation of multicomponent samples when the components had  
18 different colours. Using conductivity method, mixing performance of components could only be  
19 assessed in binary mixtures, containing conductive component (e.g. salt) and other non-  
20 conductive food components. For multicomponent food samples, only the mixing quality of salt  
21 would be determined. On the other hand, it was found that the image processing technique could  
22 not be a good indicator of mixing performance of components in the case of strongly segregated  
23 mixture of oregano and salt as it could not effectively detect the salt particles of samples which  
24 were sieved through the voids of oregano. In this case, conductivity method was reported to be a  
25 better candidate as it is volume sensitive.  
26  
27  
28  
29  
30  
31  
32  
33  
34  
35  
36  
37  
38

39 In general, the conductivity method is a simple and inexpensive tool to study the powder  
40 mixture uniformity. This technique only needs a conductivity meter to measure the conductivity  
41 of samples in order to evaluate the mixing. The deficiency of this method is that it can only be  
42 applied for the differentiation of a component with high conductivity mixed with other low  
43 conductivity components.  
44  
45  
46  
47  
48  
49  
50  
51

### 52 **3.2.3. Tribo-electrification method**

53 Contact friction between particles causes a phenomenon called tribo-electrification or particle  
54 charging. The tribo-electrification phenomenon is due to particle-particle and/or particle-surface  
55 interactions, usually creating bi-polar charging, which allows the creation of attractive or  
56 repulsive forces between individual particles. Hao et al. [65] investigated the relationship  
57  
58  
59  
60  
61  
62  
63  
64  
65



1  
2  
3  
4 between the electrostatic properties of different pharmaceutical powder formulations and the  
5 blending homogeneity in a V-blender. A Faraday Cup was used for the measurement of the  
6 electrostatic charge of particles (Fig. 7-a). The electrometer was zeroed after warming up when it  
7 was connected to the Faraday Cup. A glass beaker instead of metallic scoop/sampling thief was  
8 applied for transferring the samples to the container in order to mitigate the charge transfer from  
9 the operator and the container. Nearly 2 g of sample was enough to entirely coat the floor of the  
10 Faraday Cup.  
11  
12  
13  
14  
15  
16  
17

18 The plot of particle charge versus blending time for six different samples taken from six  
19 different spots (three spots from each side) inside of the V-blender is shown in Fig. 7-b. The  
20 measured charge quantities were close to each other at 4 and 12 *min* (highlighted in red)  
21 indicative of a better uniformity of extracted powder samples under these conditions. Based on  
22 the observed results, existence of the cyclic nature of the charge change events which occurred  
23 with certain periodicity patterns upon continuous powder blending was reported.  
24  
25  
26  
27  
28  
29

30 **Fig. 7.** (a) A simple schematic of Faraday Cup and (b) charge versus blend time plotted for  
31 Blend 1 (200 g batch, 98.75% Avicel PH200, 0.50% Cab-o-sil, 0.75% Magnesium Stearate,  
32 Reprinted from Hao et al. [65]).  
33  
34  
35  
36

37 Measurement of the bulk electric charge of samples may offer a desirable and economical  
38 method for qualitatively assessing the powder mixing uniformity. However, it could be an  
39 unreliable tool for evaluating the mixing performance because the measurement is also affected  
40 by the variations of humidity, temperature and other environment factors [66].  
41  
42  
43  
44  
45

#### 46 **3.2.4. Thermal analytical method**

47 Effusivity has been used recently to evaluate the degree of homogeneity of powder mixtures  
48 by analysing the extracted samples of different locations of a mixer. This technique is based on  
49 evaluating the ability of powders to transfer heat, which depends on the particle size, shape,  
50 porosity and the composition of a mixture as well as the phase surrounding the particles.  
51 Effusivity has a proportional relationship with thermal conductivity ( $k$ ), heat capacity ( $C_p$ ) and  
52 density ( $\rho$ ) of a substance as defined by Eq. 2. The sensor for this technique must be able to track  
53  
54  
55  
56  
57  
58  
59  
60  
61  
62  
63  
64  
65

1  
2  
3  
4 the temperature changes within the powder samples in order to obtain the effusivity information  
5  
6 [67].  
7  
8

$$Effusivity = \sqrt{k\rho C_p}$$

2

10  
11  
12  
13 Leonard et al. [68] investigated the uniformity of pharmaceutical powders at-line by the  
14 effusivity technique. Experiments were carried out on three pharmaceutical binary mixtures  
15 (containing active and excipient ingredients) mixed in a V-blender. The sampling operation at  
16 different times was carried out using a thief probe after stopping the blender and collecting three  
17 samples of approximately 5 g from different corners of the blender. The concentration of active  
18 ingredient in the samples was estimated using standard calibration curves obtained from multiple  
19 blends of known active concentrations. Powder effusivity was measured using a BT-01™ unit  
20 from Mathis Instruments (Fredericton, NB, Canada, Fig. 8-a), working based on the hot wire  
21 technology and tracking temperature changes within a sample during a given time interval. The  
22 uniformity patterns of active ingredient of different blends can be observed in Fig. 8-b.  
23 According to Fig. 8-b, all curves reached a plateau after a period between 6 and 8 min, indicating  
24 the end-point of mixing. The estimated error of this technique was reported to be ±3.4 % which  
25 was higher than that obtained from UV-visible spectrophotometry (±0.7 %). The work reports  
26 that more accurate analysis can be performed by UV-visible spectrophotometry, however, it is  
27 destructive, time consuming and not applicable as an in-line measurement mode. On the other  
28 hand, effusivity technique could potentially be used as an effective and fast tool for determining  
29 the end-point time of powder blending processes.  
30  
31  
32  
33  
34  
35  
36  
37  
38  
39  
40  
41  
42  
43  
44

45  
46 **Fig. 8.** (a) Schematic of BT-01™ unit and (b) evaluation of Acetaminophen homogeneity at  
47 three sampling positions of a V-blender using effusivity measurement, (Reprinted from Leonard  
48 et al. [68]).  
49  
50  
51  
52

53  
54 Differential Scanning Calorimetry (DSC) is another method for the evaluation of powder  
55 uniformity which works based on heat transfer phenomena. This method uses enthalpy values to  
56 predict the sample content and offers a simple and cost-effective means of monitoring powder  
57 blending [69]. Bharvada et al. [70] evaluated the mixing of binary pharmaceutical mixtures,  
58  
59  
60  
61  
62  
63  
64  
65

1  
2  
3  
4 containing Microcrystalline cellulose (MCC) and active component of Atenolol, in a high shear  
5 mixer using the DSC technique. For the analysis of the mixing performance, different samples  
6 (equal to  $3 \times$  the quantity of drug) were extracted from different locations of the mixer (top,  
7 middle and bottom) using a sampling thief. The enthalpy of samples was measured by an Indium  
8 calibrated Auto DSC (TA Instruments, USA). The relative standard deviation (*RSD*) of unknown  
9 samples (Figs. 9-a and 9-b) extracted from several positions of the blender was estimated using  
10 standard calibration curve, obtained from analysing several known active component fractions  
11 with known enthalpies. The *RSD* was found to be low after 15 *min*, indicating the optimum time  
12 of mixing for the binary system of MCC-Atenolol blend. From the comparison of the results of  
13 DSC technique with HPLC method, it was concluded that the relative standard deviation  
14 measured by DSC was higher than that obtained using HPLC for lower levels of drug, i.e. 0.5%,  
15 1% and 2%. However, the results of DSC and HPLC techniques were nearly similar for the  
16 concentrations above 5%.  
17  
18  
19  
20  
21  
22  
23  
24  
25  
26  
27  
28  
29

30 **Fig. 9.** (a) Average enthalpy changes of top, middle and bottom samples in the mixer and (b) %  
31 *RSD* of top, middle and bottom samples of microcrystalline cellulose-Atenolol blend at different  
32 time points, (Reprinted from Bharvada et al. [70]).  
33  
34  
35

36 The above-mentioned methods based on thermal characterisation are convenient and simple  
37 for the evaluation of powder uniformity. However, a sampling operation, using thief probe is  
38 needed for the extraction and analysis of thermal behaviour of samples which might disturb the  
39 powder bed, and therefore results may be biased [10, 15]. Although the uniformity assessment  
40 results derived from thermal characterisation methods shown earlier seem to be reliable and  
41 accurate, these methods should be applied to more powder systems with complex thermal  
42 behaviour.  
43  
44  
45  
46  
47  
48  
49  
50  
51  
52

### 53 **3.3. Tomographic techniques**

54 There are several tomographic techniques [71] such as X-ray, positron emission particle  
55 tracking, electrical capacitance and magnetic resonance imaging, used for the evaluation of  
56 powder blend uniformity which are reviewed in this section.  
57  
58  
59  
60  
61  
62  
63  
64  
65

### 3.3.1. X-ray microtomographic method

X-ray computed microtomography ( $\mu$ CT) is a non-invasive technique performed for the evaluation of powder homogeneity which could provide high resolution images (typically 50 microns or less) [72]. By projecting an X-ray beam through the material and the measurement of the energy debilitation of the beam received on a detector, a three-dimensional structure of an object could be constructed. Liu et al. [73] used X-ray microtomography to evaluate the mixing and segregation of a binary system containing spherical and non-spherical particles at different times of vibration inside a cylindrical container. Since the size of the container (9 mm in diameter and 28 mm in height) was too large for the image acquisition process, different samples at the upper, middle and lower levels of the cylindrical container were exposed to the X-ray light beam (Fig. 10-a) and the total projected images were reconstructed at different vibration times (Fig. 10-b). The pixel size, the exposure time and the sample-to-detector distance were 13.0  $\mu$ m, 1.0 s and 25.0 cm, respectively. The uniformity of mixture was analysed using a numerical index,  $S'$ , based on the sphericity of particles, estimated by following equations:

$$\sigma^2 = \frac{\sum_{i=1}^{N_l} (s_i - \bar{s})^2}{(N_l - 1)} \quad 3$$

$$\bar{s} = \frac{\sum_{i=1}^{N_p} s_i}{N_p} \quad 4$$

$$S' = \frac{\sigma}{\bar{s}} \quad 5$$

where  $\bar{s}$ ,  $N_p$ ,  $s_i$  and  $N_l$  are the mean sphericity measured over the totality of the particles in all three levels of the container, particles in the upper, middle and lower levels in total, the  $i^{\text{th}}$  value of  $s$  which represents a sphericity of the particle and particles in one level, respectively.

Components were displayed with different colours depending on the sphericity of the particles. The increased degree of coincidence of the normalized frequency distributions with vibration time obtained for the upper, middle and lower levels indicated a better uniformity at higher vibration times (Fig. 10-c).

1  
2  
3  
4 **Fig. 10.** (a) The schematic of mixing process, (b) images taken at different times of rotation and  
5  
6 (c) evaluation of the mixing performance by normalized frequency distribution, (Reprinted from  
7  
8 Liu et al. [73]).  
9

10  
11 Surface imaging tools such as Scanning Electron Microscope (SEM) are only able to scan the  
12  
13 outer surface of objects and therefore they cannot be applied for full-scale evaluation of powder  
14  
15 mixtures. On the other hand,  $\mu$ CT has a great potential for deep understanding of the structural  
16  
17 properties of particulate materials [74, 75]. Precise data analysis could be provided from  
18  
19 rendered high resolution images using this technique. However, material with similar structural  
20  
21 properties cannot be easily differentiated using this technique. Also, this method is an expensive  
22  
23 tool for the evaluation of powder homogeneity.  
24

### 25 26 **3.3.2. Positron emission particle tracking (PEPT) method**

27  
28 Positron emission particle tracking tomography is an imaging technique that produces a three-  
29  
30 dimensional image of a process by detecting pairs of gamma rays emitted by a positron-emitting  
31  
32 radio nuclide (tracer) into the system [76-79]. The **spatial accuracy** in a range of 0.5 mm  
33  
34 (observed at 500 times per second) was reported for particle velocity of 1 m/s [80]. The accuracy  
35  
36 reduces as particle velocity is increased because the particle moves further and therefore more  
37  
38 detectors are needed to spot the tracer [80]. Also, the accuracy of this method depends on the  
39  
40 measurement conditions, specifically the mass of material between the tracer particle and the  
41  
42 detectors. The size and density of the tracer are considered to be approximately the same as the  
43  
44 components inside the mixer. Therefore, it would be possible to assume that the movement of the  
45  
46 tracer closely follows the components in the mixer. Marigo et al. [81] studied the mixing  
47  
48 behaviour of glass spheres inside a cylindrical **Turbula** mixer with the use of PEPT technique.  
49  
50 Glass particle tracer as well as two detectors for tracking the gamma rays of the tracer were  
51  
52 applied. By the measurement of axial and radial diffusion of the tracer (Eqs. 6 and 7,  
53  
54 respectively), the mixing efficiency was evaluated for different operating conditions in axial and  
55  
56 radial directions (Fig. 11-a).  
57

$$58 \quad D_x = \frac{1}{N'-1} \sum_{k=1}^{N'-1} \frac{(x^{k+1} - x^k)^2}{(t^{k+1} - t^k)} \quad 6$$

$$D_r = \frac{1}{N' - 1} \sum_{k=1}^{N'-1} \frac{(r^{k+1} - r^k)^2}{(t^{k+1} - t^k)} \quad 7$$

where  $x^k$  and  $x^{k+1}$ ,  $N'$ ,  $r^k$  and  $r^{k+1}$  are the axial positions of the particle at time  $t^k$  and at time  $t^{k+1}$ , the total shaft rotation and the radial positions of the particle at time  $t^k$  and at time  $t^{k+1}$ , respectively.

The tracer motion was further discussed by occupancy concept which is defined as the ratio of time that the tracer spends at a given position to the total tracking time. By increasing the speed of cylindrical **Turbula** mixer up to 46 *rpm*, a clear core-shell pattern was observed in the transverse and axial direction (Fig. 11-b). This event represented the tendency of the tracer particle to stay in two core regions of the bed in the axial direction which hindered the tracer particle to cross the middle point. This core-shell pattern represented the inadequate mixing operation, leading to a decrease in the mixing efficiency in the axial direction.

**Fig. 11.** (a) Comparison of dispersion coefficients,  $D_x$  and  $D_r$ , as a function of rotation speed and (b) occupancy plots for 20 *min* measurement time, (Reprinted from Marigo et al. [81]).

Gundogdu [82] described a technique based **on a clustering** method to track multiple particles rather than single tracer particle, enabling exploration of more comparative information about the mixing in a system. The study of Gundogdu offers a unique solution to track more than one particle. He found that  $^{18}\text{F}$  radioactive particles provided better results than  $^{22}\text{Na}$  particles. All experiments of Gundogdu were carried out in open air and calculations were performed in off-line mode. It should be noted here that more intensive investigation of this method is needed due to the complexity of its procedure [82].

PEPT is a non-invasive technique for evaluating the flow processes by **tracking** the motion of a radioactive tracer particle. This method allows looking through opaque systems without interfering with flow [83]. However, erroneous locations may also be calculated using this technique due to scattering of gamma rays. In addition, in order to obtain reliable data long run experiments have to be carried out, allowing the tracer (s) occurrence in different regions of a mixer, except in the stagnant sections [84].

### 3.3.3. Electrical capacitance tomography

Electrical capacitance tomography (ECT) provides a non-intrusive cross-sectional view of a stream which can be obtained by the measurement of variations in dielectric properties (relative permittivity) of the materials inside the vessel. The main advantage of this technique is that it could provide a cross-sectional view of a stream, containing liquid, solid and/or gas, in a non-intrusive way. However, as compared to X-ray,  $\gamma$ -ray, as well as Magnetic Resonance Imaging (MRI), this low-resolution technique (spatial resolution typically 3-10 % of a pipe diameter) has limited application to powder mixtures that require an analysis at very fine scale. Ehrhardt et al. [85] used an electrical capacitance sensor consisting of two copper electrodes placed around a glass tube to assess the segregation problems of discharging silicon carbide (SiC) and sugar mixture (sugar at the bottom and SiC at the top) through two funnels (Fig. 12-a). The sensor was connected to a capacitance meter and further to a computer through an analogue/digital converter to estimate the capacity of particles. It is found that in the lower funnel, silicon carbide was mixed with sugar at the beginning of the experiment, whereas segregation was observed after a while (Fig. 12-b). This was reported to be as a result of density segregation of silicon carbide.

**Fig. 12.** (a) Schematic of the experimental rig comprising the initial mixture (1), vibrating channel (2), upper funnel (3), sensors (4), static mixer (5), lower funnel (6), belt conveyor (7) and capacimeter (8), (b) discharge profiles through a funnel, (Reprinted from Ehrhardt et al. [85]).

In new research done by Huang et al. [86], a new measurement method for the mixing of binary mixtures was developed based on capacitance probe in a bubbling fluidized bed. A capacitance measurement instrument (MTI Accumeasure) was used to measure the signals of capacitance probes from different measurement points of the fluidized bed (Fig. 13-a). A linear relationship between the signal of the probe and fraction distribution of solids in binary mixtures was considered (Eqs. 8-10).

$$C_1 + C_2 + C_a = 1 \tag{8}$$

$$C_1 * v_1 + C_2 * v_2 + C_a * v_a = v \tag{9}$$

$$C_1 = \frac{v}{v_1 - v_2} + \frac{v_2(1 - C_a) - C_a v_a}{v_1 - v_2} \tag{10}$$

1  
2  
3  
4 where  $v$ ,  $v_1$ ,  $v_2$ ,  $v_a$ ,  $C_1$ ,  $C_2$  and  $C_a$  are the measured probe voltage signal, voltage signal  
5 corresponding to pure substance of solid 1, solid 2, air, the volume fraction of solid 1, solid 2 and  
6 air in the mixtures, respectively.  
7

8  
9 **The fraction** of quartz sand particles at different bed heights **of a binary** mixture of  
10 polypropylene plastic and quartz particles is shown in Fig. 13-b. It can be observed that the  
11 fraction of quartz in the lower part of fluidized bed ( $30\text{ cm}$ ) is high, while a decrease at heights  
12 above  $30\text{ cm}$  is observed. A successful segregation measurement of binary mixture in the  
13 fluidized bed using capacitance probe was confirmed using this method.  
14  
15  
16  
17  
18  
19  
20  
21

22 **Fig. 13.** (a) Schematic of fluidization experiment and the structure of capacitance probe and (b)  
23 fraction distribution of sand in polypropylene plastic and quartz sand mixture, (Reprinted from  
24 Huang et al. [86]).  
25  
26  
27  
28  
29

30 ECT shows great potential in many harsh conditions such as high-pressure or high  
31 temperature. However, this technique has a relatively low spatial resolution. Moreover, it is only  
32 applicable for the materials with noticeable variations in dielectric properties.  
33  
34  
35  
36  
37  
38

### 39 **3.3.4. Magnetic resonance imaging tomography**

40  
41 Magnetic resonance imaging (MRI) is a tomography system that provides a non-invasive 3D  
42 images of a mixture using strong magnetic field generated by the surrounding powerful magnets  
43 [87]. The signal intensity of one voxel in MRI is proportional to the atomic nuclei number of  
44 observable elements such as hydrogen, phosphorus or fluorine. Hardy et al. [88] studied the  
45 mixing performance of oil-filled melamine microcapsules (hence visible to MRI) and solid  
46 melamine spheres in a cylindrical container using **a MRI method. A tomographic system (Bruker**  
47 **Avance 200 SWB, Bruker Biospin MRI GmbH, Ettlingen, Germany)** was used to track the  
48 visible particle signal intensity. A  $1\text{ cm}^3$  mixture volume was imaged with an isotropic spatial  
49 resolution of  $235\ \mu\text{m}$ . The effectiveness **of the MRI** technique for quantitative characterization of  
50 fine powder mixtures (size range of about  $10\ \mu\text{m}$ ) has been shown in this article. Three  
51 orthogonal slices through the 3D mixture data set at each mixing step are shown in Fig. 14.  
52  
53  
54  
55  
56  
57  
58  
59  
60  
61  
62  
63  
64  
65



1  
2  
3  
4 Bright and dark regions represent the presence of MRI active particles and non-visible particles,  
5 respectively. It is evident from Fig. 14 that the uniformity was achieved at higher time steps,  
6 referring to the end-point of mixing identified using the MIR method.  
7  
8  
9

10  
11 **Fig. 14.** MRI slices through a cylindrical powder sample at different time steps, (Reprinted from  
12 Hardy et al. [88]).  
13  
14

15  
16 The limitation of MRI method lies in the fact that the particles mainly need to be coated by  
17 substances, such as oil, to be visible by MRI. Coating of particles may change the powder flow  
18 characteristic which could influence their mixing behaviour [89-91]. Also, the spatial resolution  
19 is less than the  $\mu$ CT method [92]. A summary of research work based on tomographic  
20 techniques for powder homogeneity assessment is presented in Table 2.  
21  
22  
23  
24  
25  
26

27 **Table 2.** Summary of different tomographic techniques for powder mixing assessment.  
28  
29  
30  
31  
32  
33  
34

### 35 **3.4. Spectroscopic techniques**

36  
37 Spectroscopic techniques have already found a wide range of applications in industrial sectors  
38 [91]. In particular, component composition of samples could be determined using their spectral  
39 information and used to evaluate the mixing performance. In this regard, different spectroscopic  
40 methods along with their functionalities are explained in the following sections.  
41  
42  
43  
44  
45

#### 46 **3.4.1. Near-infrared spectroscopy**

47  
48 NIR spectroscopy is a molecular vibrational spectroscopic method for the detection of  
49 vibrational transitions in the molecules that can be performed either by diffuse reflectance or  
50 transmission mode. The intensity ratio of the scattered light from the sample compared to the  
51 light reflected from a reference surface can be measured by the diffuse reflectance mode. On the  
52 other hand, decrease by radiation intensity can be detected by the transmission mode when  
53 radiation passes through the sample [92].  
54  
55  
56  
57  
58  
59  
60  
61  
62  
63  
64  
65

1  
2  
3  
4 There are numerous research works investigating the powder uniformity using Near-Infrared  
5 (NIR) spectroscopy (Table 3).  
6  
7  
8  
9

10 **Table 3.** Current researches investigating the powder blend uniformity using NIR system.  
11  
12  
13  
14

15 In order to monitor the mixing of powders, a segregation tester device was developed by  
16 Johanson [116] which works based on a relationship between the mixture NIR spectral intensity  
17 and the spectral intensity of pure components. Based on a similar concept, Asachi et al. [117]  
18 and Oka et al. [118] evaluated the mixing performance of powders, where component fractions  
19 are determined by minimization of the difference between the computed intensity curve of the  
20 mixture (Eq. 11) and one measured using a spectroscopy tool as shown in Eq. 12 [117]. The  
21 distribution of component fractions through the mixture could then be used for the evaluation of  
22 powder mixing uniformity.  
23  
24  
25  
26  
27  
28  
29

$$FS_{mix}(\lambda) = \sum_{i=1}^{n_{comp}} (x_i \cdot FS_i(\lambda)) \quad 11$$

$$Error = \sum_{k=1}^{n_{wave}} (FS_{mix}(\lambda_k) - F_{mix}(\lambda_k))^2 \quad 12$$

30  
31  
32  
33  
34  
35  
36  
37 where  $FS_{mix}(\lambda)$ ,  $FS_i(\lambda)$  and  $x_i$  are average intensity of the mixture, average intensity of pure  
38 components and fraction of components, respectively.  
39  
40

41 Asachi et al. [117] investigated the effect of using different pre-processing methods on the  
42 measured component fractions according to the above-mentioned approach; scatter correction  
43 and the combined smoothing-derivatives. The second derivative of the smoothing technique of  
44 Norris-Williams method was reported to be the best pre-processing method for the quantification  
45 of low content level enzyme granules (1.85 % w/w) in the mixture of washing powders; the  
46 percentage error for the quantification of segregation of low content level enzyme in a heap of  
47 powder mixtures was reported to be around 10 %.  
48  
49  
50  
51  
52  
53  
54

55 Concentration profiles of three types of bird seed in a pile of powders, estimated using the  
56 segregation tester, are shown in Fig. 15-a. Spectra of the pure components and those obtained for  
57 the mixture are shown in Fig. 15-b. Good agreement between the actual values and the predicted  
58 values is observed in Fig. 15-b. The smallest representative size (view port) of each sample, was  
59  
60  
61  
62  
63  
64  
65

1  
2  
3  
4 deduced by plotting the segregation intensity factors as a function of view port size (Fig. 15-c).  
5 According to Fig. 15-c, a view port size of about 4500  $\mu m$  was suitable for sand with an average  
6 particle size of 1500  $\mu m$ . The expected error of this method was reported to be within 7% and  
7 0.5% for a badly segregating and moderately segregating materials, respectively. Moreover,  
8 suitable range of particle size for this device was reported to be between up to 3 mm.  
9

10  
11  
12  
13  
14  
15 **Fig. 15.** (a) Concentration profiles of segregation for a mixture of three bird seeds and (b) spectra  
16 of pure components and mixture and (c) segregation intensity as a function of viewport size,  
17  
18 (Reprinted from Johanson [116]).  
19  
20  
21

22 Koller et al. [119] applied a FT-NIR spectroscopy with a fiber optical reflection probe in a  
23 four- bladed mixer to assess the mixing process in pharmaceutical powder mixtures. The NIR  
24 spectra were recorded using a PerkinElmer FT-NIR400 Spectrometer. A penetration depth of  
25 approximately 0.3-0.5 mm and a spot diameter of 4 mm (sampling volume of approximately  
26 6 mm<sup>3</sup>) was reported for the studied probe. Fiber optical probe of the spectrometer was  
27 introduced in direct contact with the powder bed during mixing process (Fig. 16-a). The pure and  
28 mixture spectra were analysed by Partial Least Squares Regression (PLSR) to estimate the  
29 concentration change in the mixtures (Fig. 16-b). It is shown that locating a NIR probe in powder  
30 beds is a suitable method to determine the end-point time of blending. The Root-Mean-Square  
31 Error of Prediction (RMSEP) was reported to be in the order of 2 to 3 % for the API content.  
32  
33  
34  
35  
36  
37  
38  
39  
40  
41

42 **Fig. 16.** (a) Experimental of an in-line NIR setup with a four-bladed mixer connected to a  
43 controllable mixing device and (b) blending plots for the mixer, light grey represents acetyl  
44 salicylic acid (ASA) and dark grey shows  $\alpha$ -lactose Monohydrate, (Reprinted from Koller et al.  
45  
46 [119]).  
47  
48  
49  
50

51 Other configurations of NIR set-ups have also been applied to monitor greater quantities of  
52 samples. By placing several NIR probes at several positions of a blend, it is possible to monitor  
53 the entire blend [32, 120]. Scheibelhofer et al. [121] applied multiple NIR probes, connected to a  
54 Fourier-transform NIR spectrometer, to quasi-simultaneously investigate the pharmaceutical  
55 blend uniformity at multiple positions (Fig. 17-a). In contrast to thief sampling, the samples are  
56  
57  
58  
59  
60  
61  
62  
63  
64  
65

1  
2  
3  
4 analysed here by applying probes. In this work, it is shown that the size of sample volume  
5 (defined as the number of particles contained in the sample) was dependent on the particle speed  
6 in front of the sensor window and the number of accumulated spectra (Fig. 17-b). The measured  
7 volume, at optimum case, was reported to be about  $16 \text{ mm}^3$  which was less than the final dosage  
8 form ( $75 \text{ mm}^3$ ). Standard deviation of the model predictions was estimated to be about  $\pm 5\%$   
9 using this set-up. In a recent work, the potential of NIR spectroscopy for continuous monitoring  
10 of powder flow was demonstrated by Alam et al. [122]. The information from the bulk phase of  
11 the powder stream could be obtained using transmission NIR spectroscopy (NIR spectrometer  
12 with a diode array detector). According to the analysis, the proposed NIR device could detect the  
13 NIR signal intensity of powder beds up to  $5 \text{ mm}$  in thickness. The analysed volume of each  
14 sample using this transmission NIR method was estimated to be around  $0.25 \text{ mm}^3$ . Quantitative  
15 determination of API concentration in the developed continuous stream of powder was carried  
16 out at different process parameters (such as powder flow rate and tube angle). A schematic  
17 of on-line monitoring of continuous stream using transmission NIR is illustrated in Fig. 17-c. As  
18 shown in Fig. 17-c, a tube connected to the powder feeder was used to deliver the samples to the  
19 NIR spectrometer, where the spectra could be recorded in a non-contact manner.  
20  
21  
22  
23  
24  
25  
26  
27  
28  
29  
30  
31  
32  
33

34  
35 **Fig. 17.** (a) Schematic of multi-probe spectroscopy setup, (b) dependence of the sample volume  
36 size to the number of accumulated spectra and the moving speed in front of the sensor window ( $f$   
37  $= 1$  is the tip speed of the blade,  $f = 0.5$  is half of this speed) and (c) continuous blend monitoring  
38 of powder streams using transmission NIR, (Reprinted from Scheibelhofer et al. [121] and  
39 Reprinted from Alam et al. [122]).  
40  
41  
42  
43  
44  
45  
46  
47

48 NIR offers a fast chemical imaging of multicomponent mixtures and continuous monitoring  
49 of samples at different modes of at-line, in-line and/or on-line [123]. However, it is difficult to  
50 obtain a very high-resolution visualization to the internal field of particulate systems using this  
51 method. Furthermore, overlapped spectra of different components could pose difficulty and  
52 challenge when using the NIR technique to assess homogeneity of a mixture.  
53  
54  
55  
56  
57  
58

### 59 3.4.2. Raman spectroscopy

60  
61  
62  
63  
64  
65

1  
2  
3  
4 The irradiation of materials cause different phenomena including scattering, absorption and  
5  
6 fluorescence (Fig. 17). The Raman effect is a scattering process that alters the frequency of an  
7  
8 incoming monochromatic light beam, mainly from a laser in the visible, Near-Infrared, or near  
9  
10 Ultraviolet range [124].  
11

12  
13  
14  
15 **Fig. 18.** IR and NIR absorption, the Raman effect and fluorescence, (Reprinted from De Beer et  
16  
17 al. [25]).  
18  
19

20  
21 Allan et al. [125] used an on-line Kaiser Raman spectrometer with a non-contact optic to  
22  
23 obtain the spectra of powder mixture in a high shear convective blender (Fig. 19-a). A sampling  
24  
25 depth of over 3.5 mm and an estimated sampling volume of about 11.095 cm<sup>3</sup> (equated to a mass  
26  
27 of 4.99 g) was reported for the measurement of aspirin in Avicel using this system. The mixing  
28  
29 end-point of different amounts of aspirin and Avicel was investigated using this technique (Fig.  
30  
31 19-b). As shown in Fig. 19-b, by increasing the amount of aspirin, more time was needed to  
32  
33 achieve a homogeneous state. The detection limit of aspirin in Avicel using the proposed Raman  
34  
35 system (2<sup>nd</sup> derivative at 1606 cm<sup>-1</sup>) was reported to be around 1.1 % (w/w).  
36

37 **Fig. 19.** (a) Schematic of Raman probe and sample set-up and (b) Raman probe mixing profiles  
38  
39 at 1606 cm<sup>-1</sup> for the case of the addition of different amounts of aspirin to Avicel, (Reprinted  
40  
41 from Allan et al. [125]).  
42  
43

44  
45 In a recent work, Wang et al. [126] developed a custom-designed macro-Raman based system  
46  
47 for homogeneity analysis of multi-component bulk of pharmaceutical powders (Fig. 20-a). The  
48  
49 studied spectroscopy system was equipped with a motorized translational sample stage (Fig. 20-  
50  
51 a). For the quantitative analysis of component fraction, a correlation based on spectral  
52  
53 information was applied as follows:

$$\frac{Y_i}{Y_j} = c_j^i \cdot \frac{I_i}{I_j} \quad 13$$

54  
55  
56  
57 where  $I$  and  $Y$  are the spectral intensity of the component  $i$  or  $j$  at all wavenumbers to the  
58  
59 measured raw spectrum of the mixture and the mass fraction of components, respectively.  
60  
61

1  
2  
3  
4 In the first part of the analysis, a direct relationship between the errors of the measured  
5 compositions and the analysed sample volume and sampling methods was demonstrated. Larger  
6 sample volume scanning, across cavity or groove (Fig. 20-b), was shown to be more suitable for  
7 bulk composition analysis of inhomogeneous samples. Therefore, more representative bulk  
8 compositions of inhomogeneous samples were analysed by the cavity or groove scanning  
9 methods. A large error was reported for the single spot sampling method (sample volume of  
10  $0.4 \mu\text{L}$ ) which was mostly due to its relatively smaller sample volume. Binary mixtures of  
11 leucine and mannitol with equal masses were mixed for different times using a wrist action  
12 shaking machine. From analysis of several samples at different times, a cumulative distribution  
13 of mass fraction of leucine was obtained as shown in (Fig. 20-c). According to Fig. 20-c, mixing  
14 deteriorates in the binary mixture of leucine and mannitol during blending (as standard deviation  
15 of the measurements was increased by time).  
16  
17  
18  
19  
20  
21  
22  
23  
24  
25  
26

27  
28 **Fig. 20.** (a) Dispersive macro-Raman Set-up, (b) different sampling methods: single spot (I),  
29 scanning across the cavity (II), scanning along the groove (III) and (c) cumulative distributions  
30 of the measured leucine mass fraction during mechanical mixing, (Reprinted from Wang et al.  
31 [126]).  
32  
33  
34  
35  
36

37 Raman imaging has less overlapped spectra and higher spatial resolution as compared to the  
38 NIR and therefore it has a better sensitivity to detect minor components [127, 128]. Thus, Raman  
39 eliminates the limitation of NIR in which the overlapped spectra make it difficult to perform low  
40 dose quantitative analysis. However, this technique is more expensive than NIR. In addition,  
41 substantial interferences in Raman spectra can be produced by fluorescence when the molecule is  
42 excited to an elevated state [25, 47, 129]. For the elimination of the fluorescence contribution,  
43 some researchers proposed stimulated Raman scattering (SRS) [25, 130, 131]. The advantage of  
44 SRS is that it removes the non-resonant background via heterodyne detection. Therefore, SRS is  
45 free of non-resonant background and fluorescence contribution and it allows selective imaging of  
46 the molecules.  
47  
48  
49  
50  
51  
52  
53  
54  
55  
56

### 57 **3.4.3. Acoustic emission spectrometry**

58  
59  
60  
61  
62  
63  
64  
65

1  
2  
3  
4 The impact of particles on the inner surface of a vessel, which generates the acoustic  
5 emission, can be used to non-invasively monitor the particulate process. The attachment of a  
6 transducer to the outside of a vessel is the most common method to detect acoustic emission of  
7 particles. It is also possible to estimate the size of particles from the acoustic emission signals  
8 created from particle–particle collisions. Allan et al. [132] investigated the blend process  
9 monitoring of aspirin or Avicel added to Avicel particles in a scaled-down convective mixer with  
10 the use of powder acoustic emission (AE). Mixing profiles which were produced from the  
11 measurement of AE spectra in this system, are represented in Fig. 21-a. No change could be  
12 observed in the mixing profile when Avicel was added to Avicel particles. However, the AE  
13 signal increases in the case of the addition of aspirin, and after a while it reaches a plateau as the  
14 mixture becomes homogeneous (about 700 s). In another part of this study, the effect of impeller  
15 speed on the AE response was investigated. It was found that at low impeller speeds (<50 rpm),  
16 the movement and velocity of powders near the glass wall was not sufficient, thus a small  
17 acoustic signal was produced.

18  
19  
20  
21  
22  
23  
24  
25  
26  
27  
28  
29  
30 Following the previous research, Allan et al. [125] carried out a comparison between different  
31 techniques of NIR, acoustic emission and Raman spectroscopy for obtaining mixing profiles.  
32 The end-point identified for the blending process as well as the trends of the mixing profiles  
33 were similar for the three techniques (Fig. 21-b). However, the detection limit for aspirin in  
34 Avicel using the acoustic emission (AE) system was reported to be around 5.2 % (w/w) which  
35 was poorer than that reported for the Raman and NIR systems.

36  
37  
38  
39  
40  
41  
42 **Fig. 21.** (a) Acoustic emission mixing profiles and (b) mixing profiles for the addition of 30 g  
43 aspirin to 75 g Avicel, (Reprinted from Allan et al. [125, 132]).  
44  
45  
46

47  
48 Acoustic emission has the advantage of being a non-invasive monitoring method for powder  
49 mixing. Unlike many techniques, such as NIR, which needs an optically transparent window in  
50 the process vessel, this method is able to collect the spectral information of blends behind any  
51 type of wall material. Also, the cost of an AE measurement system is less than NIR  
52 spectroscopy. However, some authors [125, 132] reported that this method would only be  
53 representative for powder composition at the interface rather than in the bulk material as AE  
54 spectra only could be obtained by the collisions of particles with the vessel wall [125, 132]. The  
55  
56  
57  
58  
59  
60  
61  
62  
63  
64  
65

1  
2  
3  
4 depth information for AE spectrometry is reported to be less than other spectroscopic techniques  
5 such as NIR (typically 2-3 mm). Moreover, the sensitivity of AE is found to be poorer than NIR  
6 and Raman spectroscopy.  
7  
8  
9

#### 10 11 **3.4.4. Fluorescence spectroscopy**

12  
13 Materials that absorb ultraviolet or visible light energy, may dissipate a part of the energy as  
14 heat or electromagnetic radiation. The latter phenomenon is called fluorescence. The  
15 fluorescence detection of materials can be useful to study the behaviour of processes and  
16 therefore is a potential tool for the assessment of content blend uniformity [133, 134]. Domike et  
17 al. [135] used a light induced fluorescence (LIF) instrument to evaluate the total content of  
18 fluorescent active pharmaceutical ingredient (API) in tablets. Ten tablets from three batches  
19 containing different weights of triamterene have been tested using this technique and the results  
20 were compared with those obtained by UV-visible spectrophotometry. The position of tablet  
21 relative to the LIF instrument is shown in Fig. 22-a. The concentration of the API of tablets was  
22 obtained by plotting the calibration curve of LIF signal against different standard API  
23 concentrations. Figure 22-b shows a relatively good agreement between the results of  
24 fluorescence spectroscopy and UV-visible spectrophotometry analysis. The Root Mean Standard  
25 Error of Prediction (RMSEP) for LIF was reported to be in the range of 4.40-7.93%.  
26  
27  
28  
29  
30  
31  
32  
33  
34  
35  
36  
37  
38

39 **Fig. 22.** (a) LIF instrument and (b) triamterene concentration obtained using LIF and UV  
40 analysis, (Reprinted from Domike et al. [135]).  
41  
42  
43

44 In another study, Karumanchi et al. [136] used a LIF sensor (with a sample volume of  
45 approximately  $0.117\text{ cm}^3$ ) to evaluate and monitor the blend homogeneity of fluorescent API.  
46 For this purpose, the data obtained from LIF sensor placed on the surface of collected samples  
47 containing fluorescent API was analysed. A stainless-steel grain type sampling thief was used for  
48 extracting the samples. The excitation wavelength of the fluorescent API was reported to be  
49 around 330-360 nm. Five LIF measurements were made on each sample. Using fluorescence  
50 reference standards, the calibration of LIF sensor to estimate the final API concentration was  
51 performed. The results showed that the blend met the  $\%RSD \leq 4\%$  criterion at 2-20 min,  
52 indicating to an acceptable mixing status during this blending interval. A linear relationship  
53  
54  
55  
56  
57  
58  
59  
60  
61  
62  
63  
64  
65



1  
2  
3  
4 ( $R^2 = 0.97, p < 0.0001$ ) was observed between LIF %RSD and HPLC %RSD, suggesting that LIF  
5  
6 can be successfully used to qualitatively evaluate the blend homogeneity.

7  
8 Sensitivity of fluorescence is greater than absorption spectroscopic methods because it uses  
9  
10 both excitation and emission wavelengths. It is available with relatively low cost and it is fast  
11  
12 and sensitive to differentiate active content at low concentrations. However, fluorescence  
13  
14 intensity is sensitive to fluctuations in pH and temperature. Also, the applicability of this  
15  
16 technique depends on the strength of fluorescence of the component to be investigated relative to  
17  
18 the fluorescence of other components within the mixture.

#### 20 21 **4. Conclusions**

22  
23 To obtain a high-end product quality, mixture of powders should be made with high content  
24  
25 uniformity to reduce powder segregation and product failure. Numerous uniformity assessment  
26  
27 methods for particulate systems have been developed and studied over the last few decades. In  
28  
29 this study, different techniques for the assessment of blend uniformity have been examined.  
30  
31 Spectroscopic approaches such as NIR and Raman have been broadly used for the assessment of  
32  
33 powder mixture uniformity. These techniques attracted more attention due to the fact that the  
34  
35 uniformity of several components can be monitored either at-line, in-line and/or on-line using  
36  
37 these techniques. However, using tomography systems or methods based on particle properties,  
38  
39 such as conductivity, one or two ingredients could be monitored usually in an at-line mode.  
40  
41 Among different spectroscopic tools, Raman and fluorescence showed a high sensitivity to detect  
42  
43 minor components, therefore they can be applied for the evaluation of powder uniformity with  
44  
45 higher accuracy. However, NIR spectroscopy is more commonly used for the evaluation of  
46  
47 powder homogeneity due to its relatively low cost as compared to other spectroscopic  
48  
49 instruments. In general, the suitable technique must be chosen according to the application,  
50  
51 material and device specifications, budget as well as the required precision and sensitivity. The  
52  
53 advantages and disadvantages of all the reviewed techniques are briefly summarised in Table 4.

54 **Table 4.** Powder uniformity assessment techniques with their advantages and disadvantages.

55  
56  
57 In certain circumstances, different techniques could lead to **false conclusions**. For example,  
58  
59 wrong choice of dilution technique may lead to inaccurate results obtained by HPLC and/or UV-

1  
2  
3  
4 visible absorbance spectrophotometry [69, 137]. Improper light condition, dirty camera lenses, a  
5 low-resolution camera and unreliable image-processing softwares could influence the accuracy  
6 and reliability of the image analysis. For instance, Abdelrahman et al. [138] evaluated the flow  
7  
8 detection of particles using optical imaging. It was shown that changing the camera focus on the  
9 point of interest could affect the accuracy of the particle detection. In spectroscopic techniques,  
10 scanning cannot be achieved properly when a sticky lump of powders adheres to an optical  
11 sensor during the process. In addition, the efficiency of spectral acquisition and the related data  
12 analysis is highly dependent on the distance of the probe from the powder mixture. For example,  
13 3 mm is reported to be the most efficient distance for the MicroNIR1700® probe in the related  
14 study of Asachi et al. [117]. Other factors which influence the light absorption such as porosity,  
15 particle morphology, particle size distribution and powder layer thickness must be precisely  
16 considered during spectral analysis [139]. Environmental conditions, such as humidity and  
17 temperature, must also be taken into consideration for an accurate result analysis in different  
18 techniques such as NIR spectroscopy, tribo-electrification and electrical conductivity [140-143].  
19  
20  
21  
22  
23  
24  
25  
26  
27  
28  
29  
30  
31  
32  
33

### 34 **Nomenclature**

36 AE	Acoustic emission
37 API	Active pharmaceutical ingredient
38 ASA	Acetyl salicylic acid
39 CCD	Charge coupled device
40 CV	Coefficient of variation
41 DSC	Differential Scanning Calorimetry
42 ECT	Electrical capacitance tomography
43 FT	Fourier-transform
44 HPLC	High-Performance Liquid Chromatography
45 LIF	Light induced fluorescence
46 MCC	Microcrystalline cellulose
47 MRI	Magnetic resonance imaging
48 NIR	Near-Infrared

1		
2		
3		
4	PEPT	Positron emission particle tracking
5		
6	PLSR	Partial least squares regression
7		
8	PT	Pressure transducer
9		
10	RAM	Resonant acoustic mixing
11	RSC	Royal society of chemistry
12		
13	<i>RSD</i>	Relative standard deviation
14		
15	SEM	Scanning electron microscope
16		
17	SiC	Silicon carbide
18		
19	SRS	Stimulated Raman scattering
20		
21	U	Velocity
22	UV	Ultra-Violet
23		
24	$\mu$ CT	X-ray computed microtomography
25		
26		
27		
28		
29	<b>Reference</b>	
30		
31		
32	[1] B. Remy, J.G. Khinast, B.J. Glasser, Discrete element simulation of free flowing grains in a	
33	four-bladed mixer, <i>AIChE J.</i> 55 (2009) 2035-2048.	
34		
35		
36	[2] S.I. Badawy, T.J. Lee, M.M. Menning, Effect of drug substance particle size on the	
37	characteristics of granulation manufactured in a high-shear mixer, <i>AAPS Pharm. Sci. Tech.</i> 1	
38	(2000) 55-61.	
39		
40		
41		
42	[3] R.K. Thakur, C. Vial, K.D.P. Nigam, E.B. Nauman, G. Djelveh, Static mixers in the process	
43	industries-A review, <i>Chem. Eng. Res. Des.</i> 81 (2003) 787-826.	
44		
45		
46		
47	[4] H. Hoornahad, E.A.B. Koenders, Towards simulation of fresh granular-cement paste material	
48	behavior, <i>Adv. Mater. Res.</i> 295 (2011) 2171-2177.	
49		
50		
51	[5] X.Y. Zhou, G.J. He, Y.L. Fan, Y. Xiao, S.K. Kunnath, G. Monti, <i>Advances in Civil</i>	
52	<i>Infrastructure Engineering</i> , pp. 1287-1294, Trans Tech Publications Ltd, 2013.	
53		
54		
55		
56	[6] J.K. Prescott, T.P. Garcia, A solid dosage and blend uniformity trouble shooting diagram,	
57	<i>Pharm. Technol.</i> 25 (2001) 68-87.	
58		
59		
60		
61		
62		
63		
64		
65		

- 1  
2  
3  
4 [7] A.N. Huang, H.P. Kuo, Developments in the tools for the investigation of mixing in  
5 particulate systems-A review, *Adv. Powder Technol.* 25 (2014) 163-173.  
6  
7  
8 [8] P. Tang, V.M. Puri, Methods for Minimizing Segregation: A Review, *Particulate Science and*  
9 *Technology, Part. Sci. Technol.* 22 (4) (2004) 321-337.  
10  
11  
12 [9] M.E. Aulton, *Aulton's pharmaceuticals: the design and manufacture of medicines*, Chapter 12  
13 written by Andrew Twitchell, pp. 152-167, 3rd Edition., Edinburgh, Churchill Livingstone,  
14 2007.  
15  
16  
17 [10] M. Poux, P. Fayolle, J. Bertrand, D. Bridoux, J. Bousquet, Powder mixing: some practical  
18 rules applied to agitated systems. *Powder Technol.* 68 (1991) 213-34.  
19  
20  
21 [11] A. Levy, C. Kalman, *Handbook of Conveying and Handling of Particulate Solids*, Chapter  
22 7, pp. 589-603, Volume 10, 1st Edition, Elsevier Science, 2001.  
23  
24  
25 [12] J. Bridgwater, Mixing of powders and granular materials by mechanical means-A  
26 perspective, *Particuology.* 10 (2012) 397-427.  
27  
28  
29 [13] H.G. Brittain, Particle-Size Distribution II: The Problem of Sampling Powdered Solids,  
30 *Pharm. Tech.* 2 (2002) 67-73.  
31  
32  
33 [14] E.Z. Dahmash, A.R. Mohammed, Review Foundation: Characterisation and surface-  
34 profiling techniques for composite particles produced by dry powder coating in pharmaceutical  
35 drug delivery, *Drug Discov. Today.* 21 (2016) 550-561.  
36  
37  
38 [15] F.J. Muzzio, P. Robinson, C. Wightman, D. Brone, Sampling practices in powder blending,  
39 *Int. J. Pharm.* 155 (1997) 153-178.  
40  
41  
42 [16] R.W. Gerlach, J.M. Nocerino, Guidance for Obtaining Representative Laboratory Analytical  
43 Subsamples from Particulate Laboratory Samples. U.S. Environmental Protection Agency,  
44 EPA/600/R-03/027, 2003.  
45  
46  
47 [17] Applying to Standards, Tests, Assays, and Other Specifications of the United States  
48 Pharmacopeia, Bulk Powder Sampling Procedures, 523-536, Copyright © The United States  
49 Pharmacopeial Convention, ISBN: 978-1-936424-41-2, 2015  
50  
51  
52  
53  
54  
55  
56  
57  
58  
59  
60  
61  
62  
63  
64  
65

- 1  
2  
3  
4 [18] T. Allen, Particle size measurement, Powder sampling and particle size Measurement,  
5 Volume 1, 5th Edition, Springer, 1968.  
6  
7  
8 [19] E.L. Paul, V.A. Atiemo-Obeng, S.M. Kresta, Handbook of industrial mixing, science and  
9 practice, Volume 15, pp. 887-987, Wiley-Blackwell Publication, 2003.  
10  
11  
12 [20] A.S.L. Mendez, G. de Carli, C.V. Garcia, Evaluation of powder mixing operation during  
13 batch production: Application to operational qualification procedure in the pharmaceutical  
14 industry, Powder Technol. 198 (2010) 310-313.  
15  
16  
17 [21] F.J Muzzio, C.L. Goodridge, A. Alexander, P. Arratia, H. Yang, O. Sudah, G. Mergen,  
18 Sampling and characterization of pharmaceutical powders and granular blends, Int. J. Pharm.  
19 250 (2003) 51-64.  
20  
21  
22 [22] L. Susana, P. Canu, A.C. Santomaso, Development and characterization of a new thief  
23 sampling device for cohesive powders, Int. J. Pharm. 416 (2011) 260-267.  
24  
25  
26 [23] C. Benedetti, N. Abatzoglou, J.S. Simard, L. McDermott, G. Leonard, L. Cartilier,  
27 Cohesive, multi component, dense powder flow characterization by NIR, Int. J.  
28 Pharm. 336 (2007) 292-301.  
29  
30  
31 [24] S. Laske, A. Paudel, O. Scheibelhofer and the Author Team, A review of PAT strategies in  
32 secondary solid oral dosage manufacturing of small molecules, J. Pharm. Sci. 106 (2017) 667-  
33 712.  
34  
35  
36 [25] T. De Beer, A. Burggraeve, M. Fonteyne, L. Saerens, J.P. Remon, C. Vervaet, Near infrared  
37 and Raman spectroscopy for the in-process monitoring of pharmaceutical production processes,  
38 Int. J. Pharm. 417 (2011) 32-47.  
39  
40  
41 [26] D.A. Skoog, F.J. Holler, S.R. Crouch, Principles of Instrumental Analysis, 6th ed., Brooks  
42 Cole, 2007.  
43  
44  
45 [27] D. Harvey, Modern analytical chemistry, Chapter 10, pp. 368-461, McGraw-Hill Higher  
46 Education, 1999.  
47  
48  
49  
50  
51  
52  
53  
54  
55  
56  
57  
58  
59  
60  
61  
62  
63  
64  
65

- 1  
2  
3  
4 [28] D.G. Watson, *Pharmaceutical Analysis: A Textbook for Pharmacy Students and*  
5 *Pharmaceutical Chemists*, 4th Edition, Elsevier, 2016.  
6  
7  
8  
9 [29] S. Gorog, *Ultraviolet-Visible Spectrophotometry in Pharmaceutical Analysis*, CRC Press,  
10 2018.  
11  
12  
13 [30] A.C. Tella, O.M. Olabemiwo, M.O. Salawu, G.K. Obiyenwa, Developing a  
14 Spectrophotometric method for the estimation of Albendazole in solid and suspension forms, *Int.*  
15 *J. Phys. Sci.* 5 (2010) 379-382.  
16  
17  
18 [31] M. Jamrogiewicz, K. Cal, M. Gruszecka, A. Ciesielski, Determination of API content in a  
19 pilot-scale blending by near-infrared spectroscopy as a first step method to process line  
20 implementation, *Acta. Poloniae. Pharmaceutica.* 70 (2013) 419-29  
21  
22  
23 [32] A.S. El-Hagrasy, H.R. Morris, F. D'Amico, R.A. Lodder, J.K. Drennen, Near-infrared  
24 spectroscopy and imaging for the monitoring of powder blend homogeneity, *J. Pharm. Sci. Sep.*  
25 90 (2001) 1298-307.  
26  
27  
28 [33] H. Ma, C.A. Anderson, Characterization of Pharmaceutical Powder Blends by NIR  
29 Chemical Imaging, *J. Pharm. Sci.* 97 (2008) 3305-3320.  
30  
31  
32 [34] S.L. Upstone, *Ultraviolet/visible light absorption spectrophotometry in clinical chemistry,*  
33 *Encyclopedia of Analytical Chemistry*, John Wiley and Sons Ltd., 2013.  
34  
35  
36 [35] Y.K. Jung, M.J. Kim, Y.J. Kim, J.Y. Kim, Limitation of UV-Vis Absorption Analysis for  
37 Determination of Aqueous Colloidal Fullerene (nC60) at High Ionic Strength, *KSCE J. Civ. Eng.*  
38 17 (2013) 51-59.  
39  
40  
41 [36] S. Krukowski, M. Karasiewicz, W. Kolodziejcki, Convenient UV-spectrophotometric  
42 determination of citrates in aqueous solutions with applications in the pharmaceutical analysis of  
43 oral electrolyte formulations, *J. Food. Drug. Anal.* 25 (2017) 717-722.  
44  
45  
46 [37] S. Moldoveanu, V. David, *Selection of the HPLC Method in Chemical Analysis*, 1st  
47 Edition, Elsevier, 2016.  
48  
49  
50  
51  
52  
53  
54  
55  
56  
57  
58  
59  
60  
61  
62  
63  
64  
65

- 1  
2  
3  
4 [38] M. Thammana, A Review on High Performance Liquid Chromatography (HPLC), RRJPA.  
5  
6 5 (2016) 22-28.  
7  
8  
9 [39] I.D. Kamalanathan, P.J. Martin Competitive adsorption of surfactant-protein mixtures in a  
10 continuous stripping mode foam fractionation column, Chem. Eng. Sci. 146 (2016) 291-301.  
11  
12  
13 [40] X. Liu, M. Tracy, C. Pohl, New Development in Surfactant Analysis by HPLC, Technical  
14 report. Dionex Corporation, Sunnyvale, CA USA, 2014.  
15  
16  
17  
18 [41] E. Nourafkan, Z. Hu, D. Wen, Controlled delivery and release of surfactant for enhanced oil  
19 recovery by nanodroplets, Fuel. 218 (2018) 396-405.  
20  
21  
22 [42] M.I. Walash, F. Belal, N. El-Enany, M. Eid, and R.N. El-Shaheny, Stability-Indicating  
23 HPLC Method for Determination of Naftazone in Tablets. Application to Degradation Kinetics  
24 and Content Uniformity Testing, J. Chromatogr. Sci. 49 (2011) 495-501.  
25  
26  
27  
28 [43] R. Tanaka, N.Takahashi, Y.Nakamura, Y. Hattori, K. Ashizawa, M. Otsuka, Verification of  
29 the mixing processes of active pharmaceutical ingredient, excipient and lubricant in a  
30 pharmaceutical formulation using a resonant acoustic mixing technology, RSC Adv. 6 (2016)  
31 87049-87057.  
32  
33  
34  
35 [44] S.M. Dhole, P.B. Khedekar, N.D. Amnerkar, Comparison of UV spectrophotometry and  
36 high performance liquid chromatography methods for the determination of repaglinide in tablets,  
37 Pharm. Methods. 3 (2012) 68-72.  
38  
39  
40  
41 [45] F. Eeni, Use of high-performance liquid chromatography in the pharmaceutical industry, J.  
42 Chromatogr. A. 507 (1990) 141-149.  
43  
44  
45  
46 [46] S.O. Eraga, M.I. Arhewoh, R.N. Chibuogwu, M.A. Iwuagwu, A comparative UV-HPLC  
47 analysis of ten brands of ibuprofen tablets, Asian Pac. J. Trop. Biomed. 5 (2015) 880-884.  
48  
49  
50  
51 [47] V. Baeten, Spectroscopy: developments in instrumentation and analysis, J. Grasas. Y.  
52 aceites. 53 (2002) 45-63.  
53  
54  
55  
56  
57  
58  
59  
60  
61  
62  
63  
64  
65

- 1  
2  
3  
4 [48] V. Mizonov, I. Balagurov, H. Berthiaux, C. Gatumel, Intensification of vibration mixing of  
5 particulate solids by means of multi-layer loading of components, *Adv. Powder Technol.* 28  
6 (2017) 3049-3055.  
7  
8  
9  
10 [49] M. Yamamoto, S. Ishihara, J. Kano, Evaluation of particle density effect for mixing  
11 behavior in a rotating drum mixer by DEM simulation, *Adv. Powder Technol.* 27 (2016) 864-  
12 870.  
13  
14  
15 [50] J.G. Rosas, M. Blanco, A criterion for assessing homogeneity distribution in hyperspectral  
16 images. Part 1: Homogeneity index bases and blending processes, *J. Pharm. Biomed. Anal.* 70  
17 (2012) 680-690.  
18  
19  
20 [51] C. Ammarcha, C. Gatumel, J.L. Dirion, M. Cabassud, H. Berthiaux, Continuous powder  
21 mixing of segregating mixtures under steady and unsteady state regimes: Homogeneity  
22 assessment by real-time on-line image analysis, *Powder Technol.* 315 (2017) 39-52.  
23  
24  
25 [52] J. Cho, Y. Zhu, K. Lewkowicz, S. Hee Lee, T. Bergman, B. Chaudhuri, Solving granular  
26 segregation problems using a biaxial rotary mixer, *Chem. Eng. Process.* 58 (2012) 42-50.  
27  
28  
29 [53] C.R. Jung, R.S. Ortiz, R. Limberger, P. Mayorga, A new methodology for detection of  
30 counterfeit Viagra<sup>1</sup> and Cialis<sup>1</sup> tablets by image processing and statistical analysis, *Forensic Sci.*  
31 *Int.* 216 (2012) 92-96.  
32  
33  
34 [54] O.O. Olaofe, K.A. Buist, N.G. Deen, M.A. van der Hoef, J.A.M. Kuipers, Improved digital  
35 image analysis technique for the evaluation of segregation in pseudo-2D beds, *Powder Technol.*  
36 244 (2013) 61-74.  
37  
38  
39 [55] J.G. Benito, I. Ippolito, A.M. Vidales, Novel aspects on the segregation in quasi 2D piles,  
40 *Powder Technol.* 234 (2013) 123-131.  
41  
42  
43 [56] D. Pihler-Puzovic, T. Mullin, The timescales of granular segregation in horizontally shaken  
44 monolayers, *Proc. R. Soc.* 469 (2013) 1-20.  
45  
46  
47 [57] X. Liu, C. Zhang, J. Zhan, Quantitative comparison of image analysis methods for particle  
48 mixing in rotary drums, *Powder Technol.* 282 (2015) 32-36.  
49  
50  
51  
52  
53  
54  
55  
56  
57  
58  
59  
60  
61  
62  
63  
64  
65



- 1  
2  
3  
4 [58] H. Mio, R. Higuchi, W. Ishimaru, A. Shimosaka, Y. Shirakawa, J. Hidaka, Effect of paddle  
5 rotational speed on particle mixing behavior in electrophotographic system by using parallel  
6 discrete element method, *Adv. Powder Technol.* 20 (2009) 406-415.  
7  
8  
9  
10 [59] R.K. Soni, R. Mohanty, S. Mohanty, B.K. Mishra, Numerical analysis of mixing of particles  
11 in drum mixers using DEM, *Adv. Powder Technol.* 27 (2016) 531-540.  
12  
13  
14  
15 [60] A. Realpe, K. Barrios, M. Rozo, Assessment of homogenization degree of powder mixing in  
16 a cylinder rotating under cascading regime, *Int. J. Eng. Technol.* 7 (2015) 394-404.  
17  
18  
19 [61] G. Olivieri, A. Marzocchella, P. Salatino, Segregation of fluidized binary mixtures of  
20 granular solids, *AIChE J.* 50 (2004) 3095-3106.  
21  
22  
23  
24 [62] A.S.M. Yudin, S. Anuar, A.N. Oumer, Improvement on particulate mixing through inclined  
25 slotted swirling distributor in a fluidized bed: An experimental study, *Adv. Powder Technol.* 27  
26 (2016) 2102-2111.  
27  
28  
29  
30 [63] P. Shenoy, M. Viau, K. Tammel, F. Innings, J. Fitzpatrick, L. Ahrne, Effect of powder  
31 densities, particle size and shape on mixture quality of binary food powder mixtures, *Powder*  
32 *Technol.* 272 (2015) 165-172.  
33  
34  
35  
36 [64] P. Shenoy, F. Innings, K. Tammel, J. Fitzpatrick, L. Ahrne, Evaluation of a digital colour  
37 imaging system for assessing the mixture quality of spice powder mixes by comparison with a  
38 salt conductivity method, *Powder Technol.* 286 (2015) 48-54.  
39  
40  
41  
42 [65] T. Hao, J. Tukianen, A. Nivorozhkin, N. Landrau, Probing pharmaceutical powder blending  
43 uniformity with electrostatic charge measurements, *Powder Technol.* 245 (2013) 64-69.  
44  
45  
46  
47 [66] S.V. Hammond, F.J. Muzzio, K.C. Pingali, T. Shinbrot, An observed correlation between  
48 flow and electrical properties of pharmaceutical blends, *Powder Technol.* 192 (2009) 157-165.  
49  
50  
51  
52 [67] L. Mathews, C. Chandler, S. Dipali, P. Adusumilli, S. Lech, S. Daskalakis, N. Mathis,  
53 Monitoring blend uniformity with effusivity, *Pharm. Technol.* (2002) 80-84.  
54  
55  
56  
57 [68] G. Leonard, F. Bertrand, J. Chaouki, P.M. Gosselin, An experimental investigation of  
58 effusivity as an indicator of powder blend uniformity, *Powder Technol.* 181 (2008) 149-159.  
59  
60  
61  
62  
63  
64  
65

- 1  
2  
3  
4 [69] S. Mahmood, N.N.B. Hilmi, N.K.B. Husain, B. Chatterjee, U. K. Mandal, Differential  
5 scanning calorimetric characterization of pharmaceutical powder blend uniformity in a  
6 laboratory-scale V-blender, *Powder Technol.* 287 (2016) 152-159.  
7  
8  
9  
10 [70] E. Bharvada, V. Shah, M. Misra, Exploring mixing uniformity of a pharmaceutical blend in  
11 a high shear mixture granulator using enthalpy values obtained from DSC, *Powder Technol.* 276  
12 (2015) 103-111.  
13  
14  
15  
16 [71] J. Jamaludin, M.Z. Zawahir, R.A. Rahim, F.R.M. Yunus, N.M.N. Ayob, M.S.R. Aw, N.S.  
17 Fadzil, Z. Zakaria, M.H.F. Rahiman, A Review of Tomography System, *Jurnal. Teknologi.* 64  
18 (2013) 47-51.  
19  
20  
21  
22 [72] M.J. Paulus, S.S. Gleason, S.J. Kennel, P.R. Hunsicker, D.K. Johnson, High Resolution X-  
23 ray Computed Tomography: An Emerging Tool for Small Animal Cancer Research, *Neoplasia.* 2  
24 (2000) 62-70.  
25  
26  
27  
28 [73] R. Liu, X. Yin, H. Li, Q. Shao, P. York, Y. He, T. Xiao, J. Zhang, Visualization and  
29 quantitative profiling of mixing and segregation of granules using synchrotron radiation X-ray  
30 microtomography and three dimensional reconstruction, *Int. J. Pharm.* 445 (2013) 125-133.  
31  
32  
33  
34 [74] S. Poutiainen, J. Pajander, A. Savolainen, J. Ketolainen, K. Jarvinen, Evolution of granule  
35 structure and drug content during fluidized bed granulation by X-ray microtomography and  
36 confocal Raman spectroscopy, *J. Pharm. Sci.* 100 (2011) 5254-5269.  
37  
38  
39  
40 [75] I. Akseli, S. Iyer, H.P. Lee, A.M. Cuitino, A quantitative correlation of the effect of density  
41 distributions in roller-compacted ribbons on the mechanical properties of tablets using  
42 ultrasonics and X-ray tomography, *AAPS Pharm. Sci. Tech.* 12 (2011) 834-853.  
43  
44  
45  
46 [76] D.L. Bailey, D.W. Townsend, P.E. Valk, M.N. Maisey, *Positron Emission Tomography:*  
47 *Basic Sciences*, Springer, 2005.  
48  
49  
50  
51 [77] P.M. Portillo, A.U. Vanarase, A. Ingram, J.K. Seville, M.G. Ierapetritou, F.J. Muzzio,  
52 Investigation of the effect of impeller rotation rate, powder flow rate, and cohesion on powder  
53 flow behavior in a continuous blender using PEPT, *Chem. Eng. Sci.* 65 (2010) 5658-5668.  
54  
55  
56  
57  
58  
59  
60  
61  
62  
63  
64  
65

- 1  
2  
3  
4 [78] H.P. Kuo, P.C. Knight, D.J. Parker, M.J. Adams, J.P.K. Seville, Discrete element  
5 simulations of a high-shear mixer, *Adv. Powder Technol.* 15 (2004) 297-309.  
6  
7  
8  
9 [79] D.J. Parker, A.E. Dijkstra, T.W. Martin, J.P.K. Seville, Positron emission particle tracking  
10 studies of spherical particle motion in rotating drums, *Chem. Eng. Sci.* 52 (1997) 2011-2022.  
11  
12  
13 [80] C.T. Crowe, *Multiphase Flow Handbook*, volume 14, CRC Press Taylor and Francis, 2006.  
14  
15  
16 [81] M. Marigo, M. Davies, T. Leadbeater, D.L. Cairns, A. Ingram, E.H. Stitt, Application of  
17 Positron Emission Particle Tracking (PEPT) to validate a Discrete Element Method (DEM)  
18 model of granular flow and mixing in the Turbula mixer, *Int. J. Pharm.* 446 (2013) 46-58.  
19  
20  
21 [82] O. Gundogdu, Positron Emission Tomography Particle tracking using cluster analysis, *Nucl.*  
22 *Instrum. Methods. A.* 534 (2004) 562-576.  
23  
24  
25 [83] D.J. Parker, C.J. Broadbent, P. Fowles, M.R. Hawkesworth, P. McNeil, Positron emission  
26 particle tracking-a technique for studying flow within engineering equipment, *Nucl. Instrum.*  
27 *Methods.* 326 (1993) 592-607.  
28  
29  
30 [84] M. Pasha, A.Hassanpour, H.Ahmadian, H.S.Tan, A.Bayly, M.Ghadiri, A comparative  
31 analysis of particle tracking in a mixer by discrete element method and positron emission particle  
32 tracking, *Powder Technol.* 270 (2015) 569-574.  
33  
34  
35 [85] N. Ehrhardt, M. Montagne, H. Berthiaux, B. Dalloz-Dubrujeaud, C. Gatumel., Assessing the  
36 homogeneity of powder mixtures by on-line electrical capacitance, *Chem. Eng. Process.* 44  
37 (2005) 303-313.  
38  
39  
40 [86] J. Huang, Y. Lu, H. Wang, new quantitative measurement method for mixing and  
41 segregation of binary-mixture fluidized bed by capacitance probe, *Chem. Eng. J.* 326 (2017) 99-  
42 108.  
43  
44  
45 [87] A.J. Sederman, L.F. Gladden, M.D. Mantle, Application of magnetic resonance imaging  
46 techniques to particulate systems, *Adv. Powder Technol.* 18 (2007) 23-38.  
47  
48  
49 [88] E.H. Hardy, J. Hoferer, G. Kasper, The mixing state of fine powders measured by magnetic  
50 resonance imaging, *Powder Technol.* 177 (2007) 12-22.  
51  
52  
53  
54  
55  
56  
57  
58  
59  
60  
61  
62  
63  
64  
65

- 1  
2  
3  
4 [89] R. Stannarius, Magnetic resonance imaging of granular materials, *Rev. Sci. Instr.* 88 (2017)  
5 051806.  
6  
7  
8  
9 [90] L. Pernenkil, C.L. Cooney, A review on the continuous blending of powders, *Chem. Eng.*  
10 *Sci.* 61 (2006) 720-742.  
11  
12  
13 [91] M. Nakagawa, S.A. Altobelli, A. Caprihan, E. Fukushima, E.K. Jeong, Noninvasive  
14 measurements of granular flows by magnetic-resonance imaging, *Exp. Fluids.* 16 (1993) 54-60.  
15  
16  
17 [92] M.M. Khalil, J.L. Tremoleda, T.B. Bayomy, W. Gsell, Molecular SPECT imaging: An  
18 Overview, *Int. J. Mol. Imag.* 2011 (2011) 1-15.  
19  
20  
21 [93] N. Sommier, P. Porion, P. Evesque, B. Leclerc, P. Tchoreloff, G. Couarraze, Magnetic  
22 resonance imaging investigation of the mixing-segregation process in a pharmaceutical blender,  
23 *Int. J. Pharm.* 222 (2001) 243-258.  
24  
25  
26 [94] P. Porion, N. Sommier, A.M. Faugere, P. Evesque, Dynamics of size segregation and  
27 mixing of granular materials in a 3D-blender by NMR imaging investigation, *Powder Technol.*  
28 141 (2004) 55-68.  
29  
30  
31 [95] M. Niedostatkiewicz, J. Tejchman, Z. Chaniecki, K. Grudzien, Determination of bulk solid  
32 concentration changes during granular flow in a model silo with ECT sensors, *Chem. Eng. Sci.*  
33 64 (2009) 20-30.  
34  
35  
36 [96] C. Rautenbach, M.C. Melaaen, B.M. Halvorsen, Possible identification of size difference  
37 segregation using electrical capacitance tomography and statistical analysis, *Eur. J. Sci. Res.* 116  
38 (2013) 351-364.  
39  
40  
41 [97] W. Bai, N.K.G. Keller, T.J. Heindel, R.O. Fox, Numerical study of mixing and segregation  
42 in a biomass fluidized bed, *Powder Technol.* 237 (2013) 355-366.  
43  
44  
45 [98] O. Mihailova, V. Lim, M.J. McCarthy, K.L. McCarthy, S. Bakalis, Laminar mixing in a  
46 SMX static mixer evaluated by positron emission particle tracking (PEPT) and magnetic  
47 resonance imaging (MRI), *Chem. Eng. Sci.* 137(2015)1014-1023.  
48  
49  
50  
51  
52  
53  
54  
55  
56  
57  
58  
59  
60  
61  
62  
63  
64  
65

- 1  
2  
3  
4 [99] Z. Csoban, B. Kallai-Szabo, N. Kallai-Szabo, T. Takacs, T. Hurtony, P. Gordon, R. Zelko, I.  
5 Antal, Assessment of distribution of pellets in tablets by non-destructive microfocus X-ray  
6 imaging and image analysis technique, Powder Technol. 301 (2016) 228-233.  
7  
8  
9  
10 [100] A. Kohler, A. Rasch, D. Pallares, F. Johnsson, Experimental characterization of axial fuel  
11 mixing in fluidized beds by magnetic particle tracking, Powder Technol. 316 (2017) 492-499.  
12  
13  
14  
15 [101] A.A. Gowen, C. Donnell, P. Cullen, S. Bell, Recent Applications of chemical imaging to  
16 pharmaceutical process monitoring and quality control, Eur. J. Pharm. Biopharm. 69 (2008) 10-  
17 22.  
18  
19  
20  
21 [102] B. Stuard, Infrared spectroscopy: fundamentals and applications, John Wiley & Sons,  
22 2004.  
23  
24  
25  
26 [103] Y. Sulub, M. Konigsberger, J. Cheney, Blend uniformity end-point determination using  
27 near-infrared spectroscopy and multivariate calibration, J. Pharm. Biomed. Anal. 55 (2011) 429-  
28 434.  
29  
30  
31  
32 [104] D.R. Ely, M. Teresa Carvajal, Determination of the scale of segregation of low dose tablets  
33 using hyperspectral imaging, Int. J. Pharm. 414 (2011) 157-160.  
34  
35  
36  
37 [105] X. He, X. Han, N. Ladyzhynsky, R. Deanne, Assessing powder segregation potential by  
38 near infrared (NIR) spectroscopy and correlating segregation tendency to tableting performance,  
39 Powder Technol. 236 (2013) 85-99.  
40  
41  
42  
43 [106] K. Jarvinen, W. Hoehe, M. Jarvinen, S. Poutiainen, M. Juuti, S. Borchert, In line  
44 monitoring of the drug content of powder mixtures and tablets by near-infrared spectroscopy  
45 during the continuous direct compression tableting process, Eur. J. Pharm. Sci. 48 (2013) 680-  
46 688.  
47  
48  
49  
50  
51 [107] A.U. Vanarase, M. Jarvinen, J. Paaso, F.J. Muzzio, Development of a methodology to  
52 estimate error in the on-line measurements of blend uniformity in a continuous powder mixing  
53 process, Powder Technol. 241 (2013) 263-271.  
54  
55  
56  
57  
58  
59  
60  
61  
62  
63  
64  
65

- 1  
2  
3  
4 [108] P.R. Wahl, G. Fruhmann, S. Sacher, G. Straka, S. Sowinski, J.G. Khinast, PAT for  
5 tableting: Inline monitoring of API and excipients via NIR Spectroscopy, Eur. J. Pharm.  
6 Biopharm. 87 (2014) 271-278.  
7  
8  
9  
10 [109] J.G. Osorio, G. Stuessy, G.J. Kemeny, F.J. Muzzio, Characterization of pharmaceutical  
11 powder blends using in situ near-infrared chemical imaging, Chem. Eng. Sci. 108 (2014) 244-  
12 257.  
13  
14  
15  
16 [110] B. Bakri, M. Weimer, G. Hauck, G. Reich, Assessment of powder blend uniformity:  
17 Comparison of real-time NIR blend monitoring with stratified sampling in combination with  
18 HPLC and at-line NIR Chemical Imaging, Eur. J. Pharm. Biopharm. 97 (2015) 78-89.  
19  
20  
21  
22 [111] Y. Lin, W. Li, J. Xu, P. Boulas, Development of a NIR-based blend uniformity method for  
23 a drug product containing multiple structurally similar actives by using the quality by design  
24 principles, Int. J. Pharm. 488 (2015) 120-126.  
25  
26  
27  
28 [112] J.G. Osorio, F.J. Muzzio, Evaluation of resonant acoustic mixing performance, Powder  
29 Technol. 278 (2015) 46-56.  
30  
31  
32  
33 [113] Z. Shi, K.C. McGhehey, I.M. Leavesley, L.F. Manley, On-line monitoring of blend  
34 uniformity in continuous drug product manufacturing process-The impact of powder flow rate  
35 and the choice of spectrometer: Dispersive vs. FT, J. Pharm. Biomed. Anal. 118 (2016) 259-266.  
36  
37  
38  
39 [114] L.K. Bittner, S.A. Schönbichler, M. Schmutzler, O.M.D. Lutz, C.W. Huck, Vibrational  
40 spectroscopic methods for the overall quality analysis of washing powders, Talanta. 148 (2016)  
41 329-335.  
42  
43  
44  
45 [115] L.B. Schlegel, M. Schubert-Zsilavec, M. Abdel-Tawab, Quantification of active  
46 ingredients in semi-solid pharmaceutical formulations by near infrared spectroscopy, J. Pharm.  
47 Biomed. Anal. 142 (2017) 178-189.  
48  
49  
50  
51 [116] K. Johanson, Review of new segregation tester method by Dr. Kerry Johanson, Powder  
52 Technol. 257 (2014) 1-10.  
53  
54  
55  
56  
57  
58  
59  
60  
61  
62  
63  
64  
65

- 1  
2  
3  
4 [117] M. Asachi, A. Hassanpour, M. Ghadiri, A. Bayly, Assessment of Near-Infrared (NIR)  
5 spectroscopy for segregation measurement of low content level ingredients, Powder Technol.  
6 320 (2017) 143-154.  
7  
8  
9  
10 [118] S. Oka, A. Sahay, W. Meng, F. Muzzio, Diminished segregation in continuous powder  
11 mixing, Powder Technol. 309 (2017) 79-88.  
12  
13  
14  
15 [119] D.M. Koller, A. Posch, G. Hörl, C. Voura, S. Radl, N. Urbanetz, S.D. Fraser, W. Tritthart,  
16 F. Reiter, M. Schlingmann, J.G. Khinast, Continuous quantitative monitoring of powder mixing  
17 dynamics by near-infrared spectroscopy, Powder Technol. 205 (2011) 87-96.  
18  
19  
20  
21 [120] Z. Shi, R.P. Cogdill, S.M. Short, C.A. Anderson, Process characterization of powder  
22 blending by near-infrared spectroscopy: blend end-points and beyond, J. Pharm. Biomed. Anal.  
23 47 (2008) 738-745.  
24  
25  
26  
27 [121] O. Scheibelhofer, N. Balak, D.M. Koller, J.G. Khinast, Spatially resolved monitoring of  
28 powder mixing processes via multiple NIR-probes, Powder Technol. 243 (2013) 161-170.  
29  
30  
31  
32 [122] M.A. Alam, Z. Shi, J.K. Drennen, C.A. Anderson, In-line monitoring and optimization of  
33 powder flow in a simulated continuous process using transmission near infrared spectroscopy,  
34 Int. J. Pharm. 526 (2017) 199-208.  
35  
36  
37  
38 [123] L. Zhang, M.J. Henson, S.S. Sekulic, Multivariate data analysis for Raman imaging of a  
39 model pharmaceutical tablet, Anal. Chim. Acta. 545 (2005) 262-278.  
40  
41  
42  
43 [124] E. Smith, Modern Raman spectroscopy-A practical approach, John Wiley & Sons,  
44 Manchester, 2005.  
45  
46  
47  
48 [125] P. Allan, L.J. Bellamy, A. Nordon, D. Littlejohn, J. Andrews, P. Dallin, In situ monitoring  
49 of powder blending by non-invasive Raman spectrometry with wide area illumination, J. Pharm.  
50 Biomed. Anal. 76 (2013) 28-35.  
51  
52  
53  
54 [126] H. Wang, D. Barona, S. Oladepo, L. Williams, S. Hoe, D. Lechuga-Ballesteros, R.  
55 Vehring, Macro-Raman spectroscopy for bulk composition and homogeneity analysis of multi-  
56 component pharmaceutical powders, J. Pharm. Biomed. Anal. 141 (2017) 180-191.  
57  
58  
59  
60  
61  
62  
63  
64  
65

- 1  
2  
3  
4 [127] S.J. Hudak, K. Haber, G. Sando, L.H. Kidder, E.N. Lewis, Practical limits of spatial  
5 resolution in diffuse reflectance NIR chemical imaging, *NIR news*. 18 (2007) 6-8.  
6  
7  
8  
9 [128] J.M. Amigo, C. Ravn, Direct quantification and distribution assessment of major and  
10 minor components in pharmaceutical tablets by NIR-chemical imaging, *Eur. J. Pharm. Sci.* 37  
11 (2009) 76-82.  
12  
13  
14  
15 [129] S. Svanberg, Atomic and molecular spectroscopy: basic aspects and practical applications,  
16 3rd ed., Chapter 10, pp. 389-454, Springer-Verlag, Berlin Heidelberg, 2001.  
17  
18  
19 [130] C.J. Strachan, M. Windbergs, H.L. Offerhaus, Pharmaceutical applications of non-linear  
20 imaging, *Int. J. Pharm.* 417 (2011) 163-172.  
21  
22  
23  
24 [131] M.N. Slipchenko, H. Chen, D.R. Ely, Y. Jung, M.T. Carvajal, J.X. Cheng, Vibrational  
25 imaging of tablets by epi-detected stimulated Raman scattering microscopy, *Analyst*. 135 (2010)  
26 2613-2619.  
27  
28  
29  
30 [132] P. Allan, L.J. Bellamy, A. Nordon, D. Littlejohn, Non-invasive monitoring of the mixing  
31 of pharmaceutical powders by broadband acoustic emission, *Analyst*. 135 (2010) 518-524.  
32  
33  
34  
35 [133] C.K. Lai, C.L. Cooney, Application of a fluorescence sensor for miniscale on-line  
36 monitoring of powder mixing kinetics, *J. Pharm. Sci.* 93 (2004) 60-70.  
37  
38  
39  
40 [134] C.K. Lai, D. Holt, J.C. Leung, G.K. Raju, P. Hansen, C.L. Cooney, Real time and  
41 noninvasive monitoring of dry powder blend homogeneity, *AIChE J.* 47 (2001) 2618-22.  
42  
43  
44 [135] R. Domike, S. Ngai, C.L. Cooney, Light induced fluorescence for predicting API content  
45 in tablets: sampling and error, *Int. J. Pharm.* 391 (2010) 13-20.  
46  
47  
48  
49 [136] V. Karumanchi, M.K. Taylor, K.J. Ely, W.C. Stagner, Monitoring powder blend  
50 homogeneity using light-induced fluorescence, *AAPS Pharm. Sci. Tech.* 12 (2011) 1031-1037.  
51  
52  
53 [137] A.S. El-Hagrasy, F.D. Amico, J.K. Drennen, A process analytical technology approach to  
54 near-infrared process control of pharmaceutical powder blending. Part I: D-optimal design for  
55 characterization of powder mixing and preliminary spectral data evaluation, *J. Pharm. Sci.* 95  
56 (2006) 392-406.  
57  
58  
59  
60  
61  
62  
63  
64  
65



- 1  
2  
3  
4 [138] M. Abdelrahman, E.W. Reutzel, A.R. Nassar, T.L.Starr, Flaw detection in powder bed  
5 fusion using optical imaging, *Addit. Manuf.* 15 (2017) 1-11.  
6  
7  
8  
9 [139] A. Rinnan, F.V.D. Berg, S.B. Engelsen, Review of the most common pre-processing  
10 techniques for near-infrared spectra, *Trends Anal. Chem.* 28 (2009) 1201-1222.  
11  
12  
13 [140] J. Zumba, J. Rodgers, M. Indest, Impact of temperature and relative humidity on the near  
14 infrared spectroscopy measurements of cotton fiber micronaire, *J. Text. Res.* DOI:  
15 10.1177/0040517517720499, (2017) 1-13.  
16  
17  
18  
19 [141] Y.E. Prawatya, M.B. Neagoe, T. Zegloul, L. Dascalescu, Optimization of continuous  
20 triboelectrification process for polymeric materials in dry contact, 13th International Conference  
21 on Tribology, IOP Publishing, 174 (2017) 012067.  
22  
23  
24  
25 [142] W.D. Greason, Investigation of a test methodology for triboelectrification, *J. Electrostat.*  
26 49, (2000) 245-256.  
27  
28  
29  
30 [143] A. K. Kamra, C. G. Deshpande, V. Gopalakrishnan, Effect of relative humidity on the  
31 electrical conductivity of marine air, *Q. J. Roy. Meteor. Soc.* 123 (1997) 1295-1305.  
32  
33  
34  
35  
36  
37  
38  
39  
40  
41  
42  
43  
44  
45  
46  
47  
48  
49  
50  
51  
52  
53  
54  
55  
56  
57  
58  
59  
60  
61  
62  
63  
64  
65

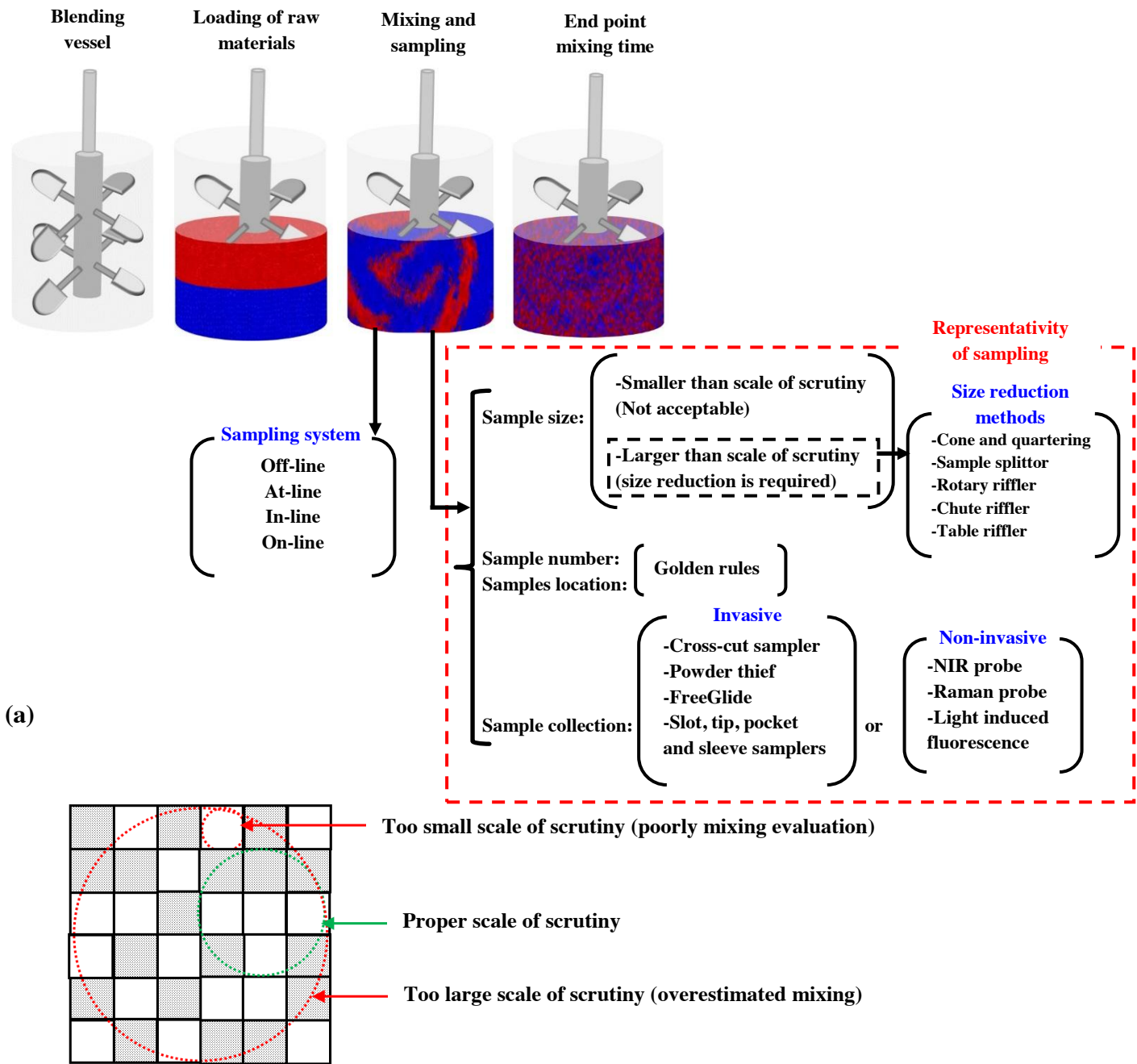
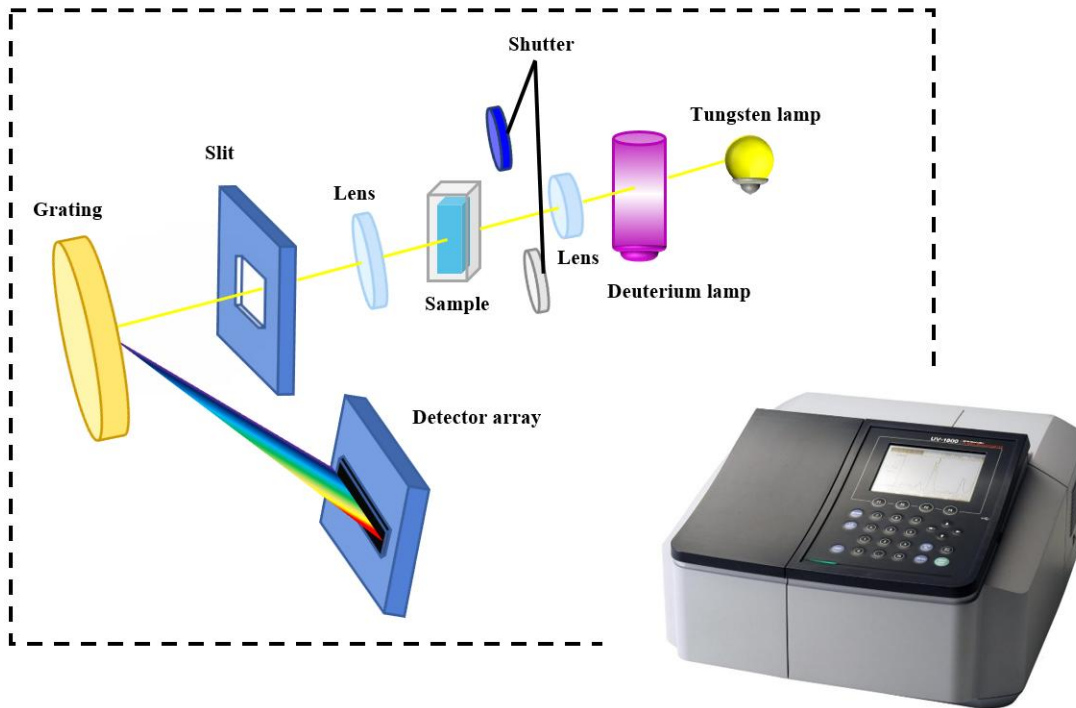
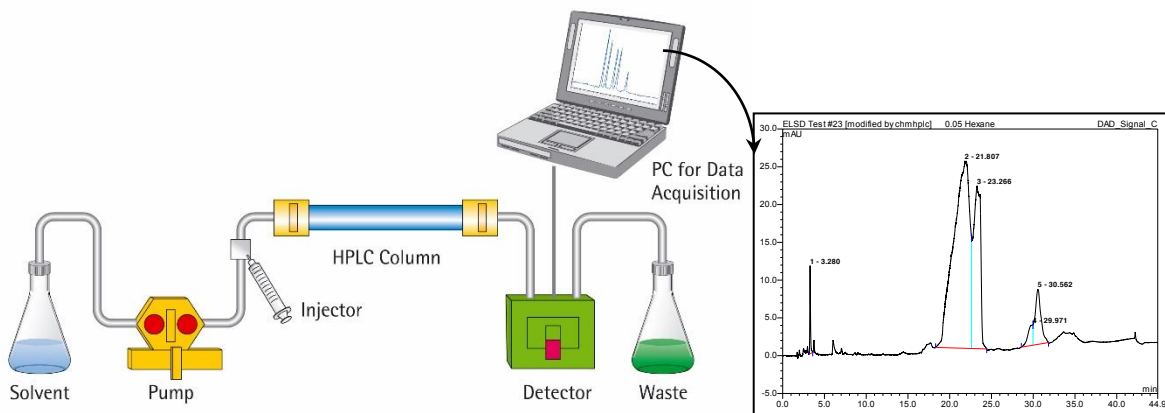


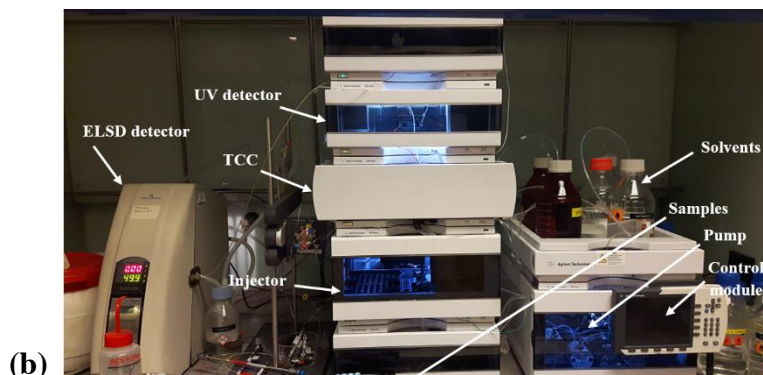
**Fig. 1.** (a) A general framework of sampling in powder mixing processes, (b) effect of the scale of scrutiny on mixing evaluation.



(a)

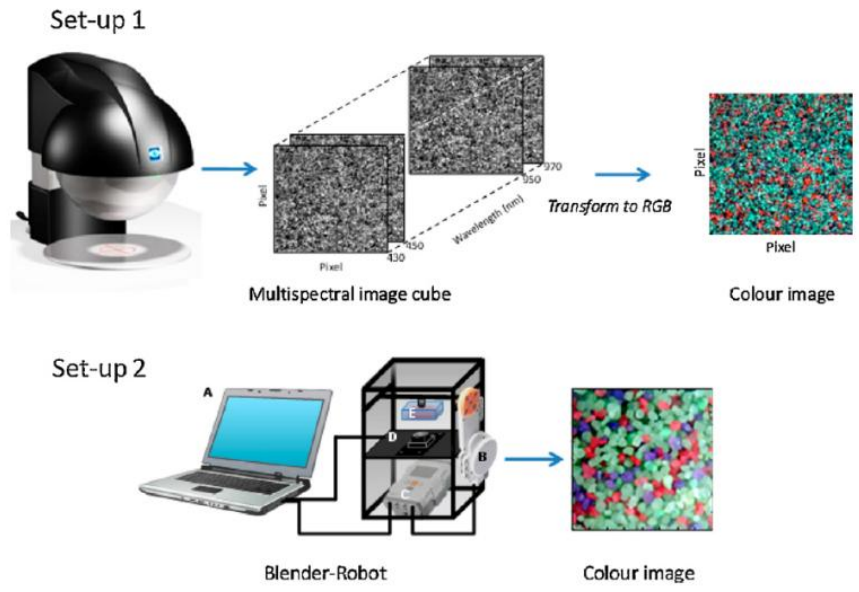


Chromatogram of HPLC

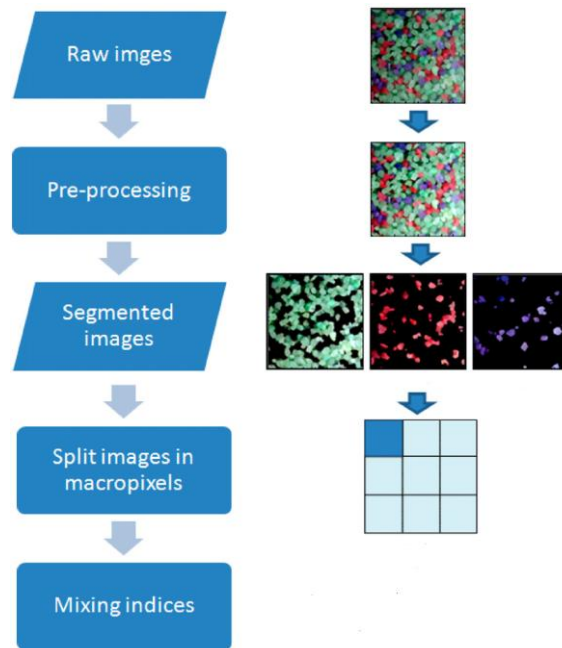


(b)

**Fig. 2.** (a) Schematic of UV-Visible spectrometer, (b) High-pressure liquid chromatography (with permission from University of Leeds).



(a)



(b)

**Fig. 3.** (a) Schematic of two setups applied for capturing images during mixing process and (b) different required steps for homogeneity assessment of images, (Reprinted from Rosas and Blanco [50]).

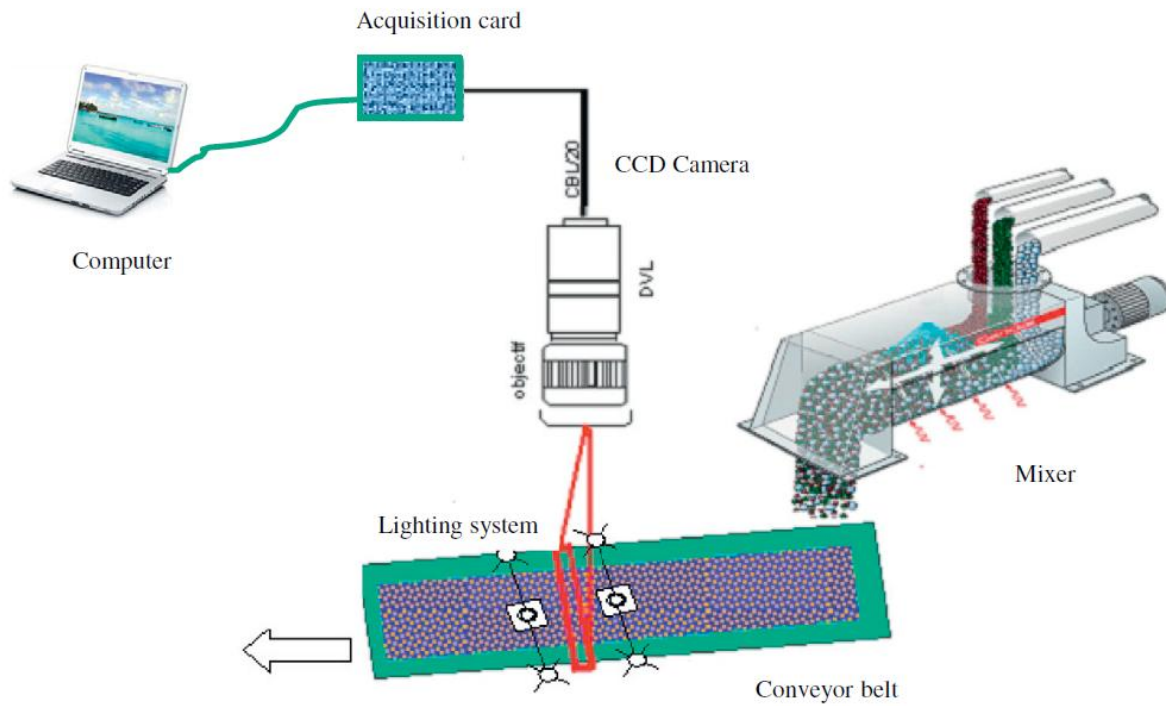


**Fig. 4.** The combined mixer/image-processing for on-line monitoring of continuous mixing, (Reprinted from G. Ammarcha et al. [51]).

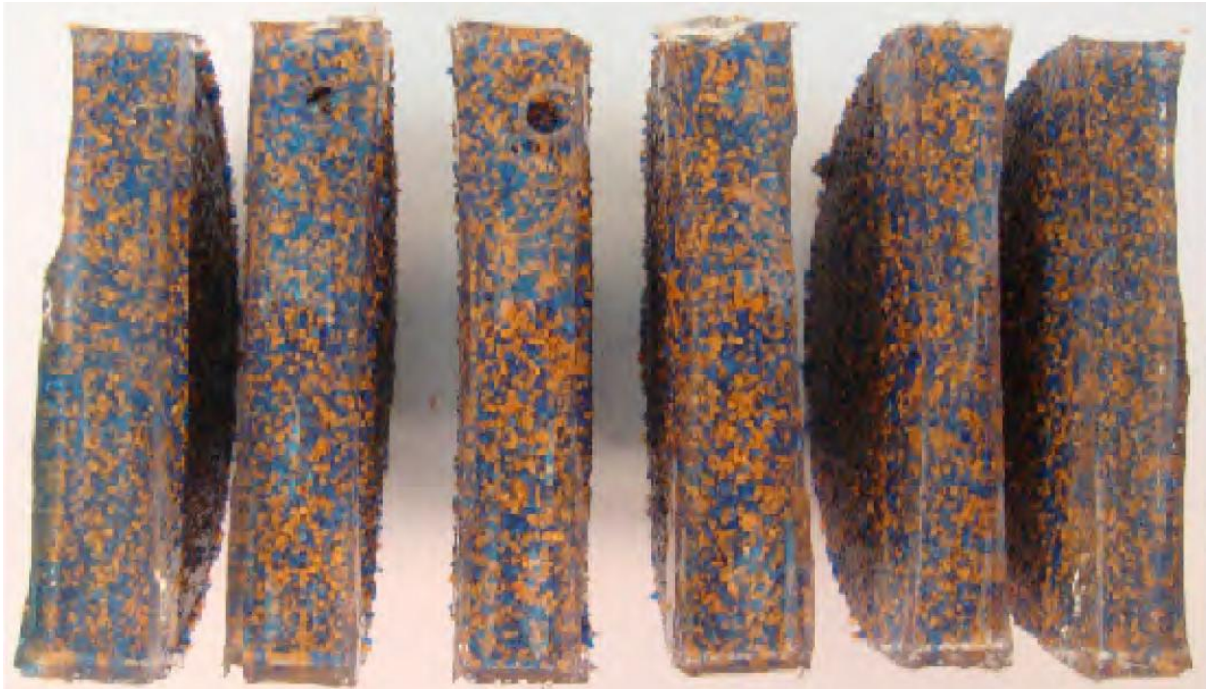
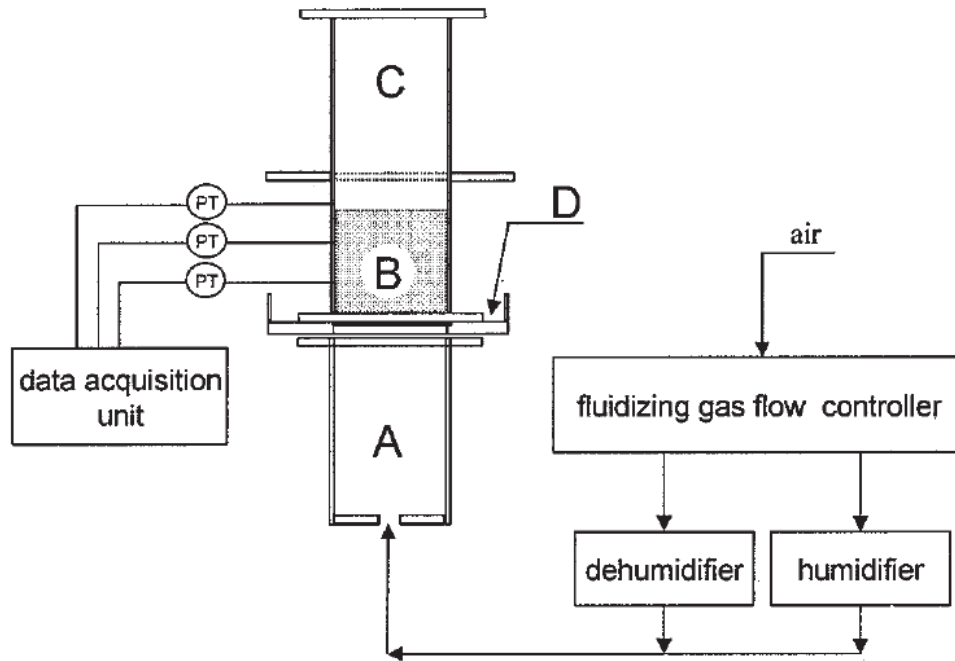
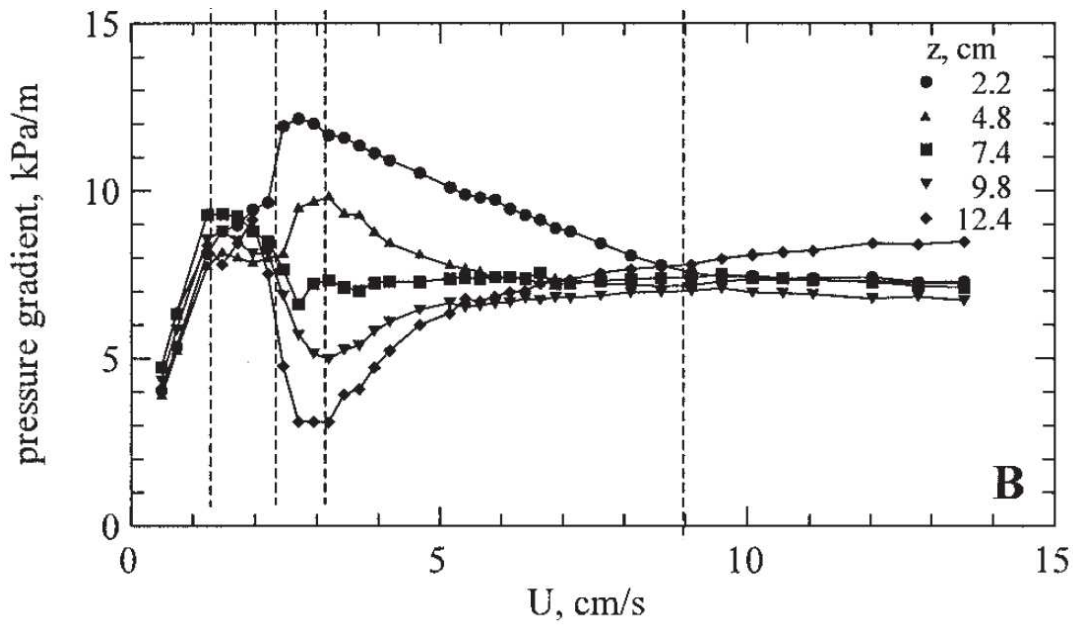


**Fig. 5.** The top view of the sliced samples after solidification of a homogenised mixture, (Reprinted from A. Realpe et al. [60]).



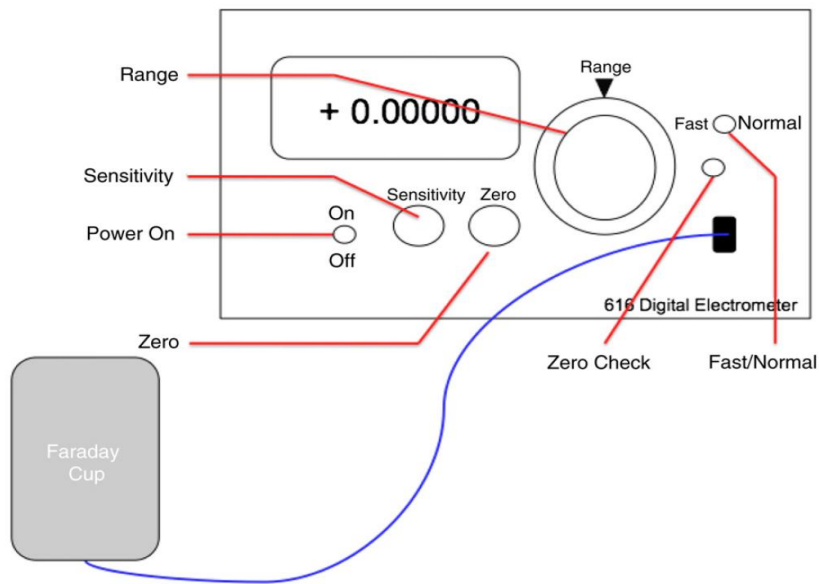
(a)



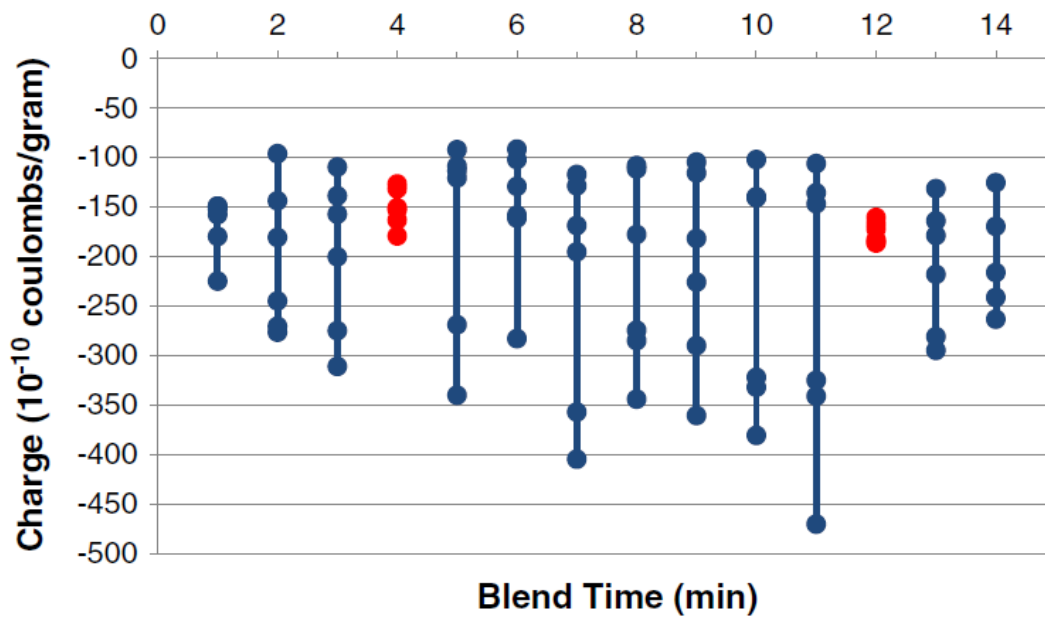
(b)

**Fig. 6.** (a) Schematic of fluidized bed equipped with pressure transducer (PT) and (b) pressure gradient versus gas superficial velocity at different heights of the bed, (Reprinted from Olivieri et al. [61]).





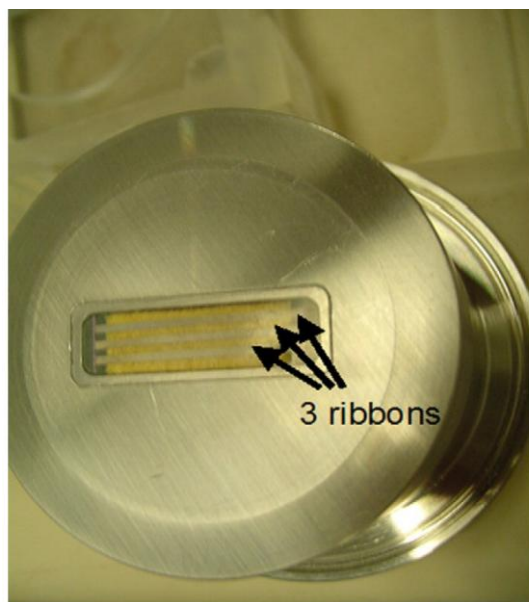
(a)



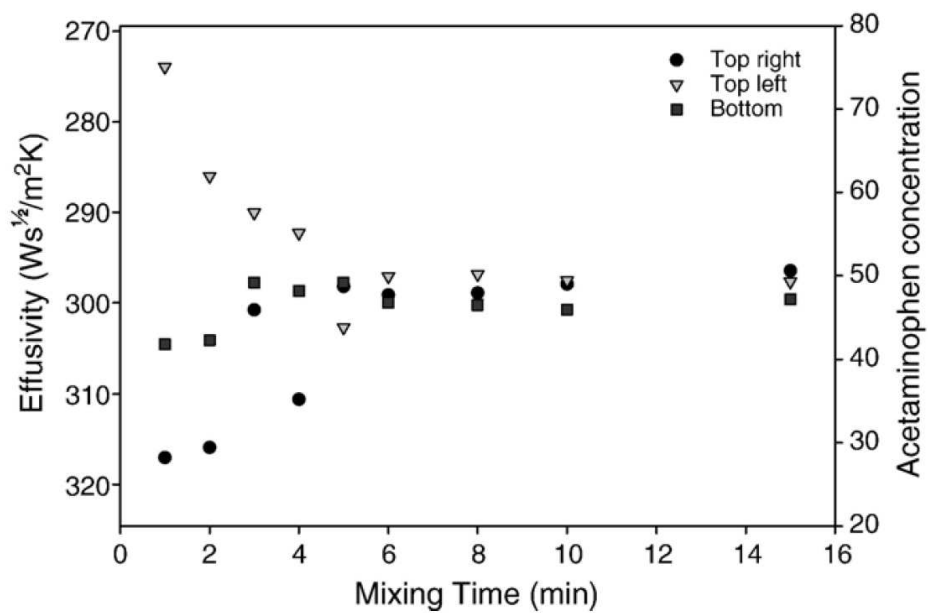
(b)

**Fig. 7.** (a) A simple schematic of Faraday Cup and (b) charge versus blend time plotted for Blend 1 (200 g batch, 98.75% Avicel PH200, 0.50% Cab-o-sil, 0.75% Magnesium Stearate, Reprinted from Hao et al. [65]).



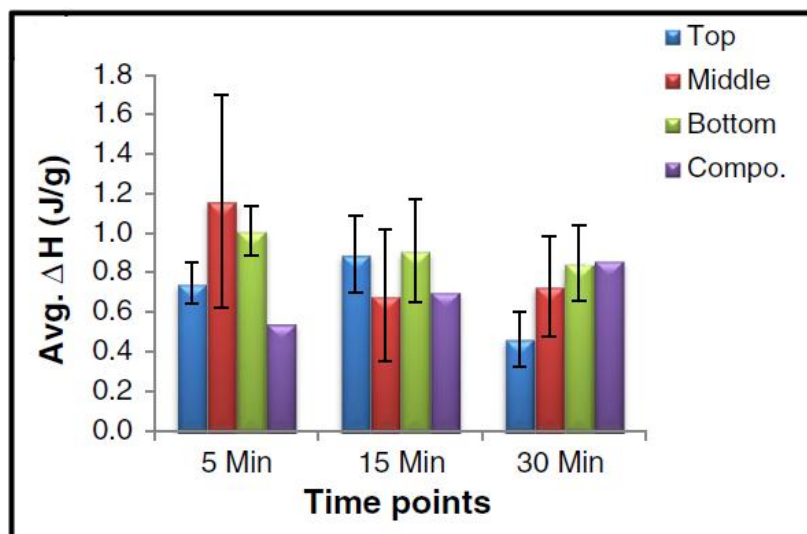


(a)

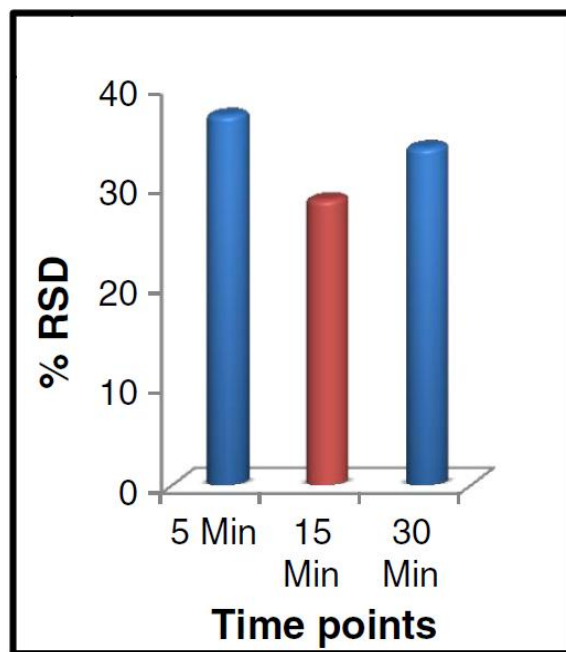


(b)

**Fig. 8.** (a) Schematic of BT-01™ unit and (b) evaluation of Acetaminophen homogeneity at three sampling positions of a V-blender using effusivity measurement, (Reprinted from Leonard et al. [68]).

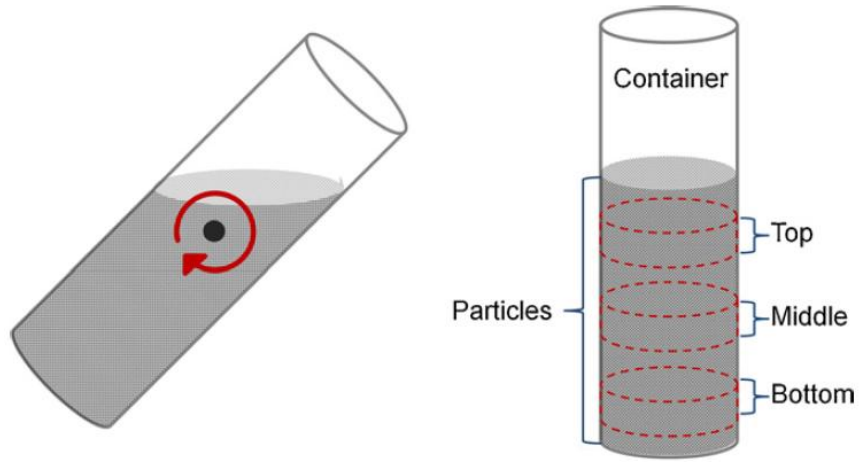


(a)

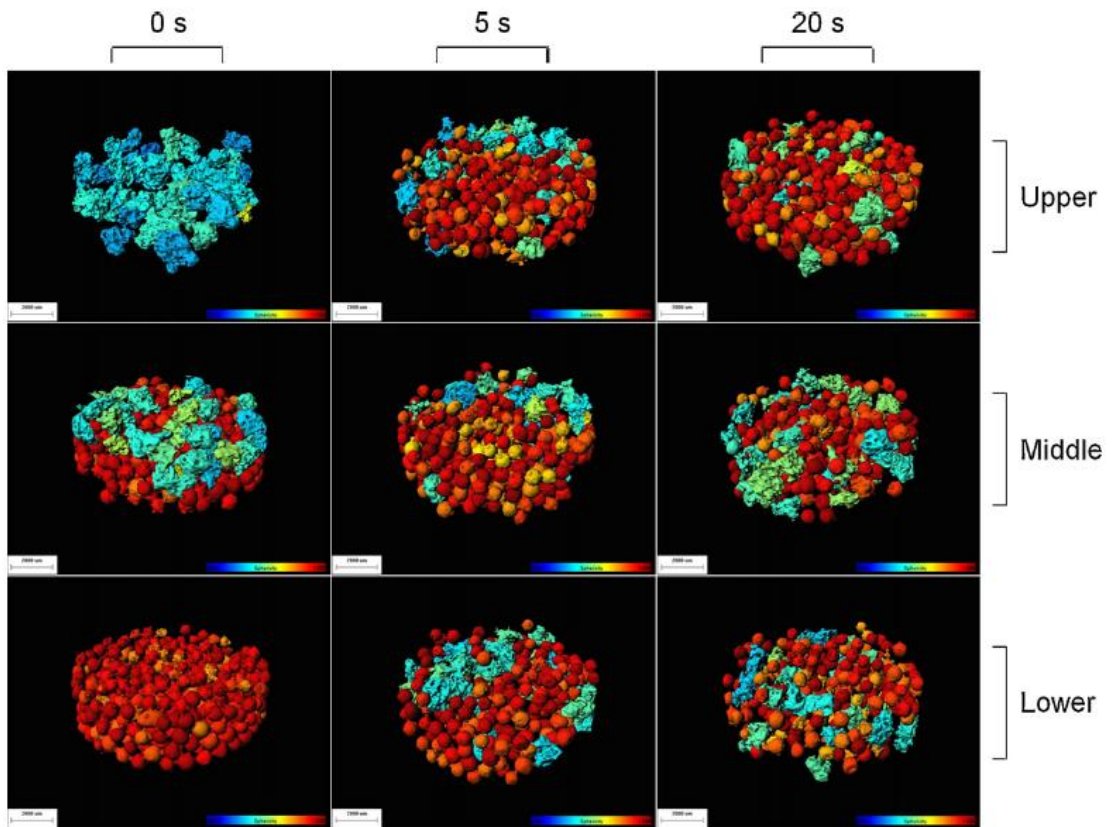


(b)

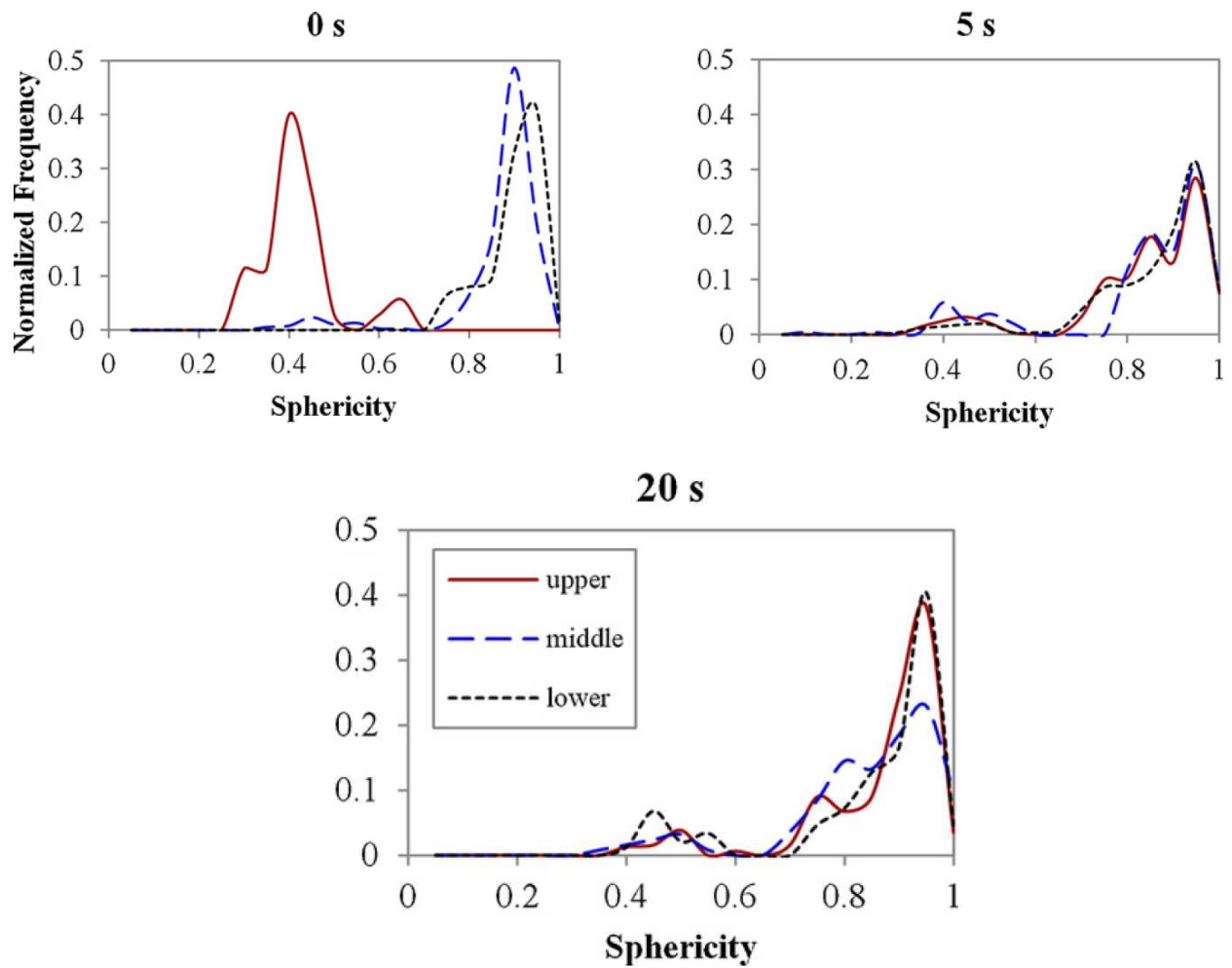
**Fig. 9.** (a) Average enthalpy changes of top, middle and bottom samples in the mixer and (b) % RSD of top, middle and bottom samples of microcrystalline cellulose-Atenolol blend at different time points, (Reprinted from Bharvada et al. [70]).



(a)

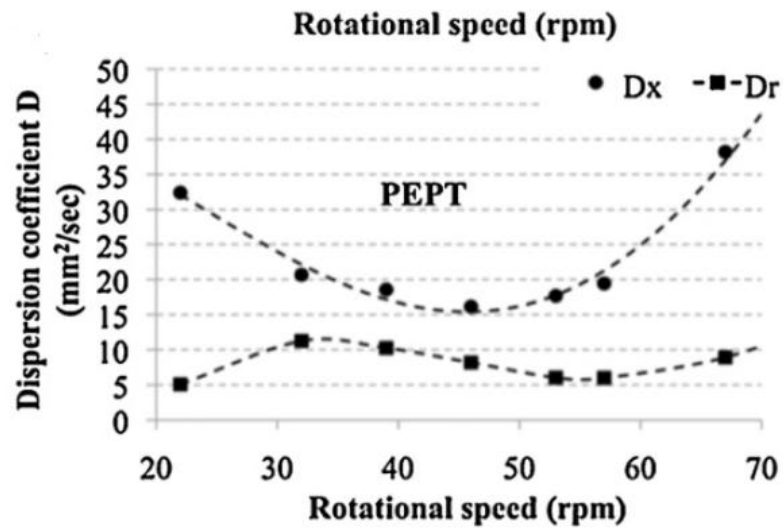


(b)

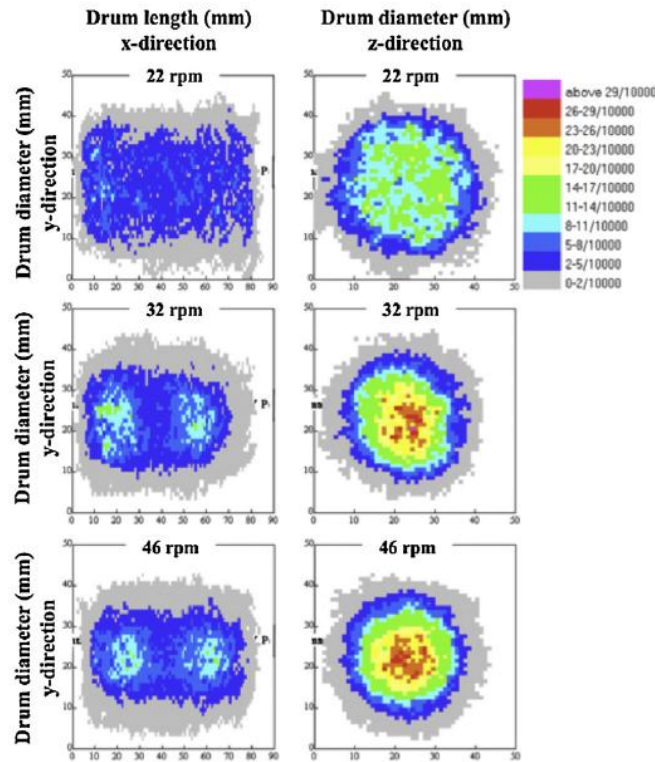


(c)

**Fig. 10.** (a) The schematic of mixing process, (b) images taken at different times of rotation and (c) evaluation of the mixing performance by normalized frequency distribution, (Reprinted from Liu et al. [73]).



(a)



(b)

**Fig. 11.** (a) Comparison of dispersion coefficients,  $D_x$  and  $D_r$ , as a function of rotation speed and (b) occupancy plots for 20 *min* measurement time, (Reprinted from Marigo et al. [81] with permission from Elsevier).

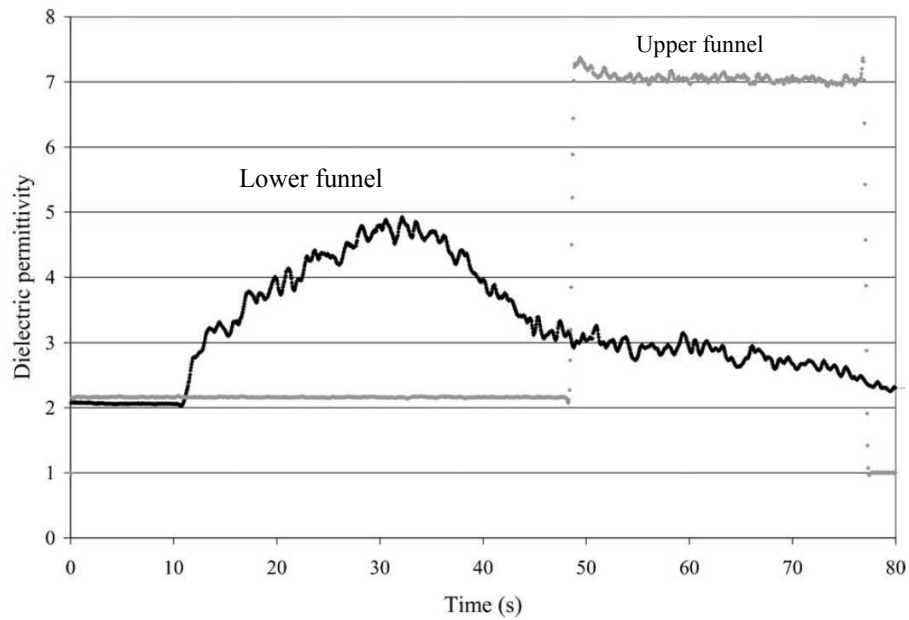
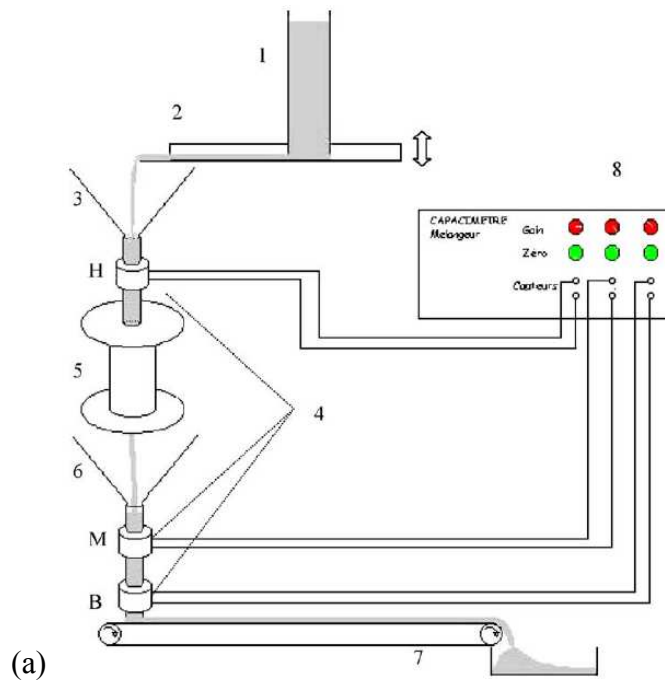
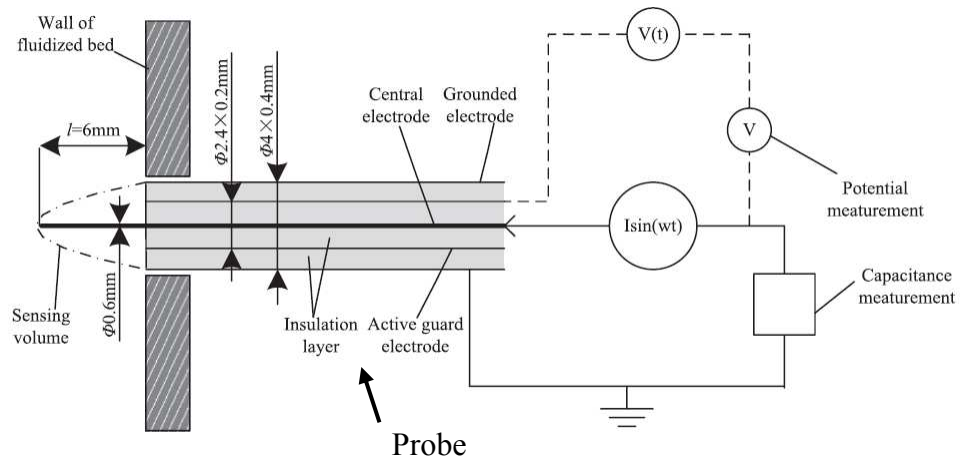
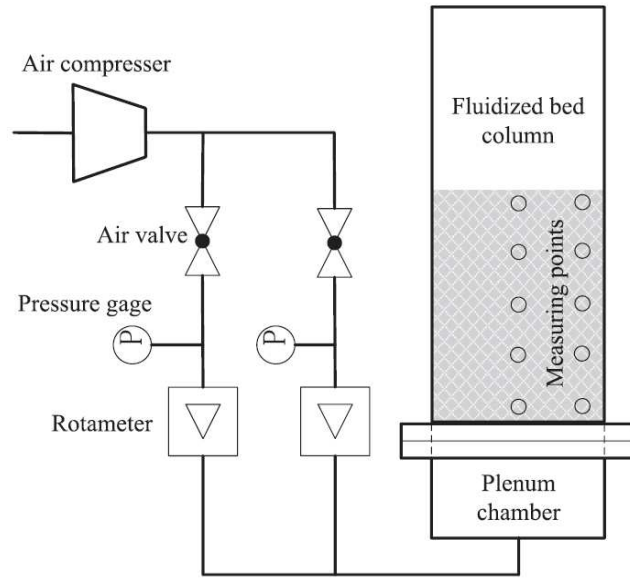


**Fig. 12.** (a) Schematic of the experimental rig comprising the initial mixture (1), vibrating channel (2), upper funnel (3), sensors (4), static mixer (5), lower funnel (6), belt conveyor (7) and capacimeter (8), (b) discharge profiles through a funnel, (Reprinted from Ehrhardt et al. [85]).



(a)

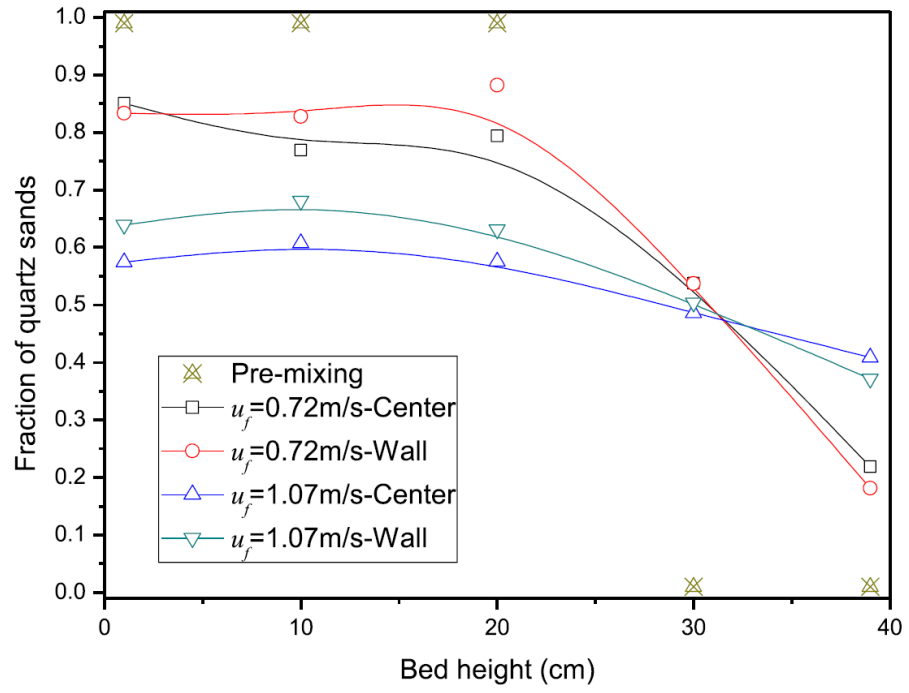


**Fig. 13.** (a) Schematic of fluidization experiment and the structure of capacitance probe and (b) fraction distribution of sand in polypropylene plastic and quartz sand mixture, (Reprinted from Huang et al. [86]).



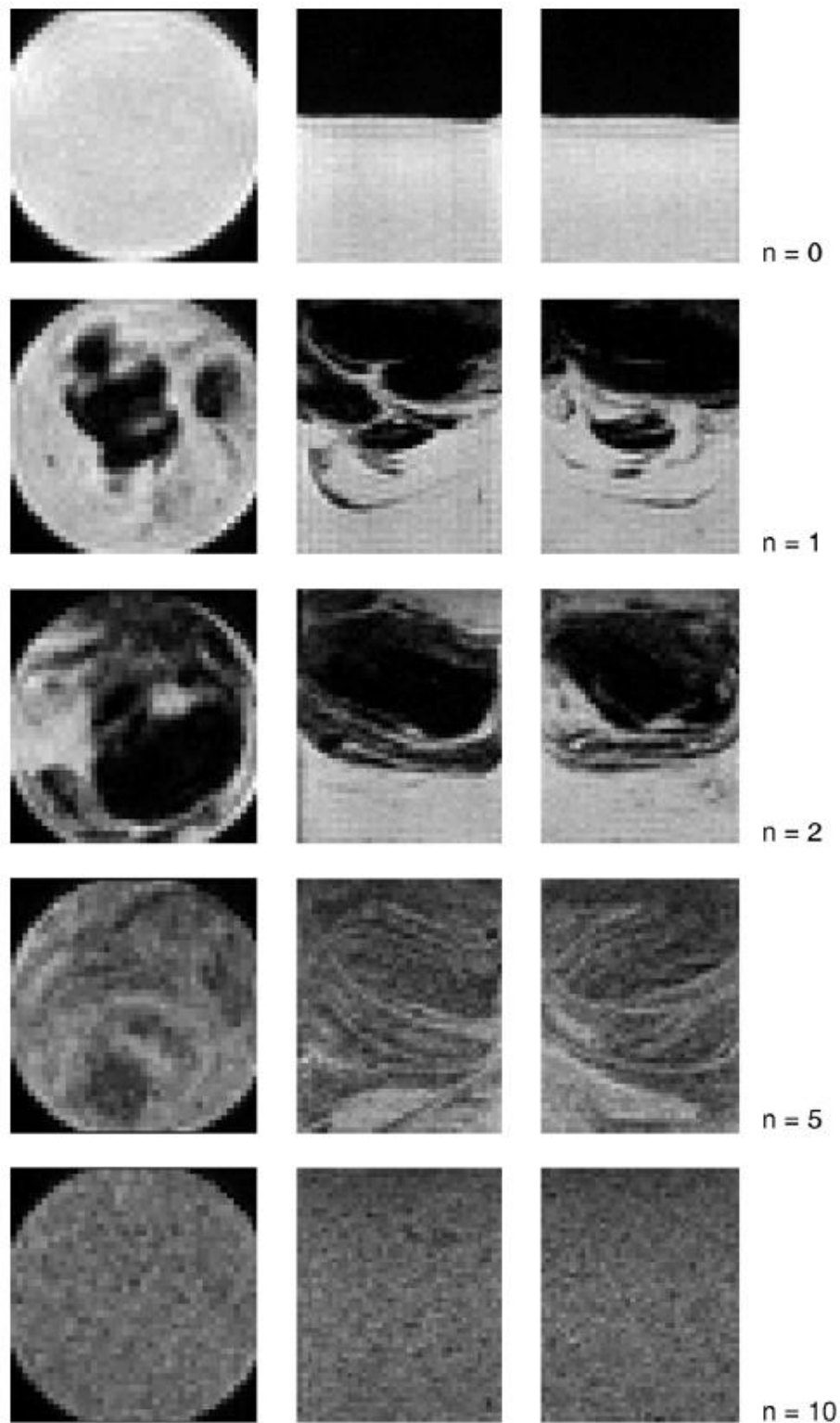
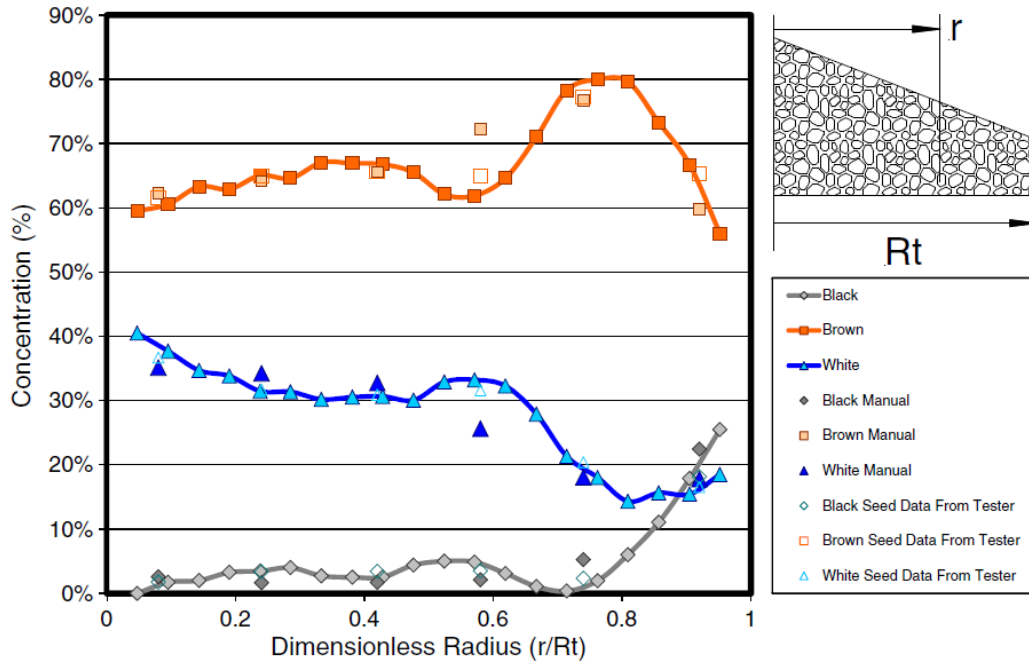
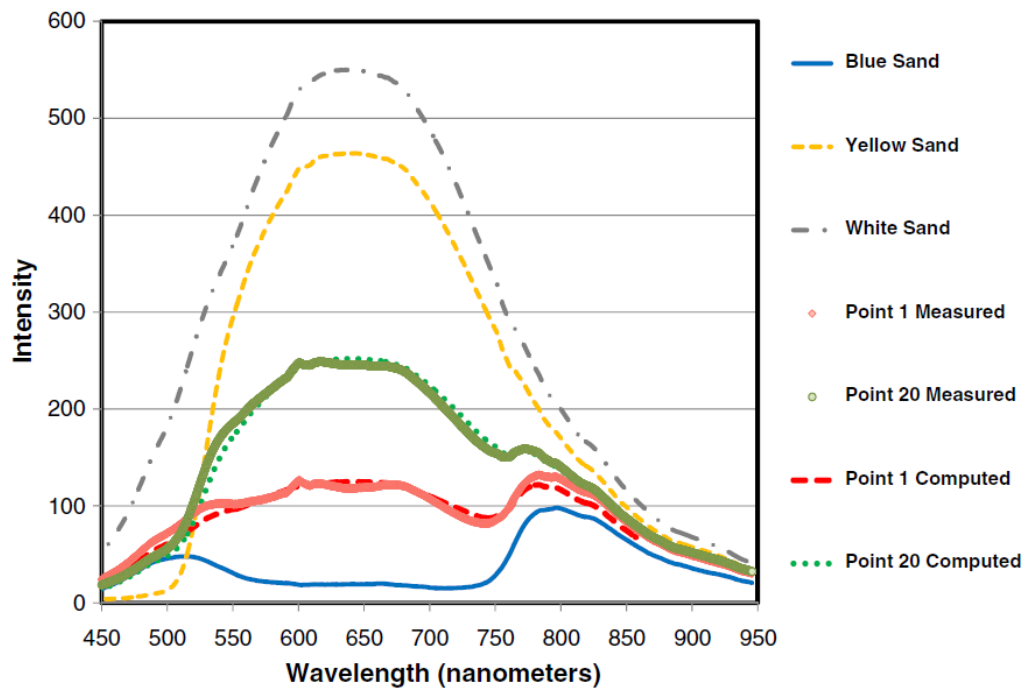


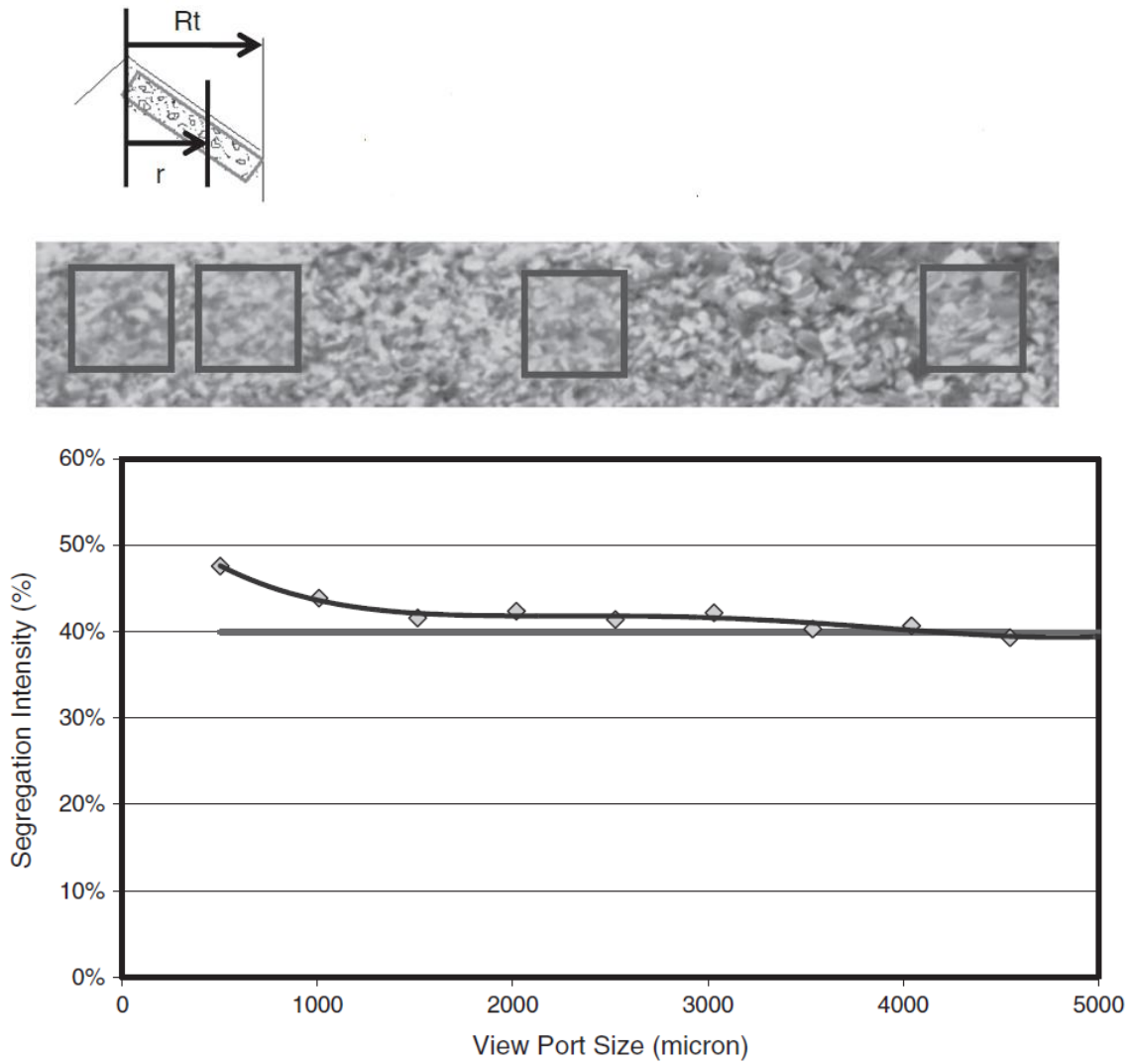
**Fig. 14.** MRI slices through a cylindrical powder sample at different time steps, (Reprinted from Hardy et al. [88]).



(a)

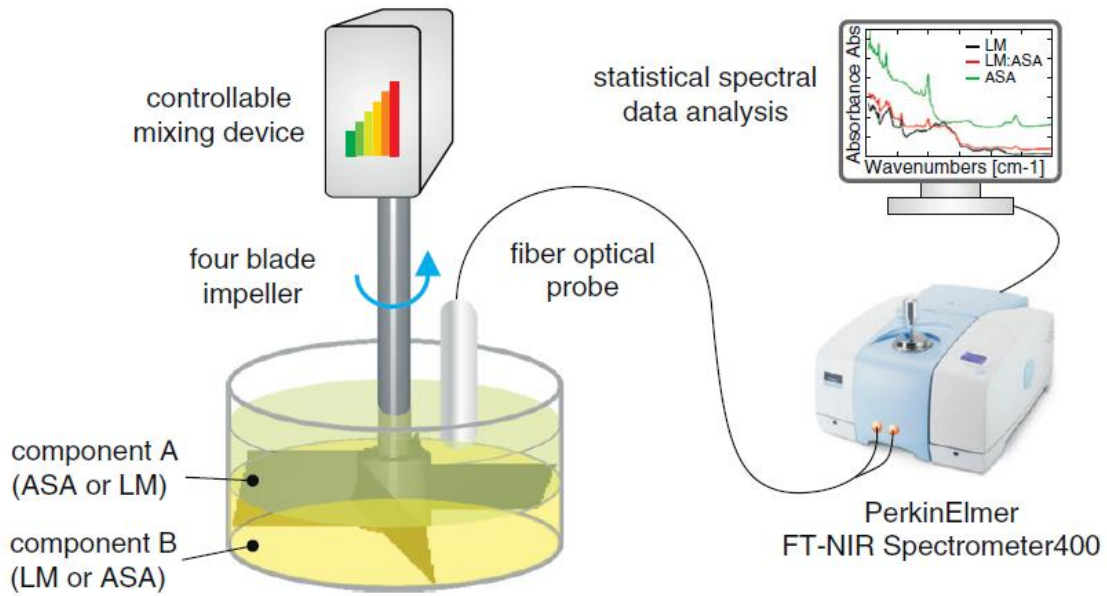


(b)

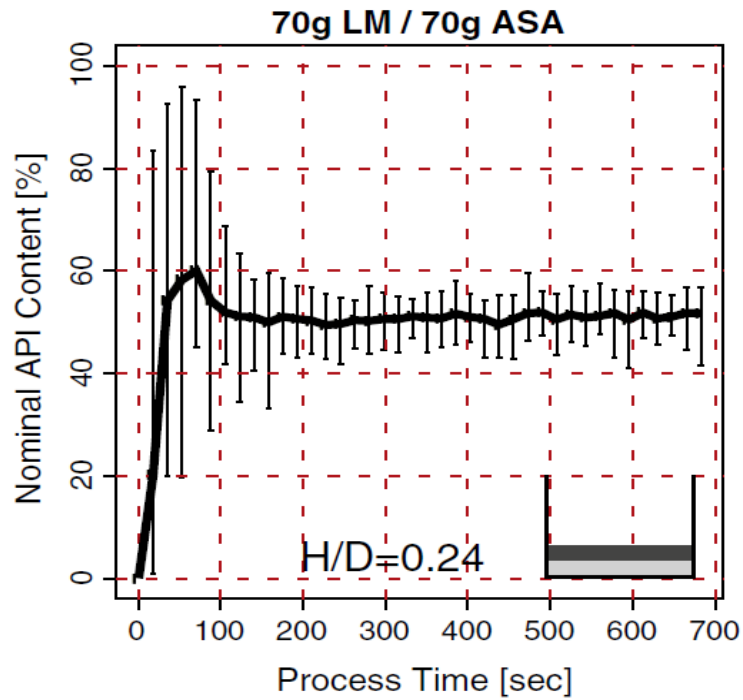


(c)

**Fig. 15.** (a) Concentration profiles of segregation for a mixture of three bird seeds and (b) spectra of pure components and mixture and (c) segregation intensity as a function of viewport size, (Reprinted from Johanson [116]).

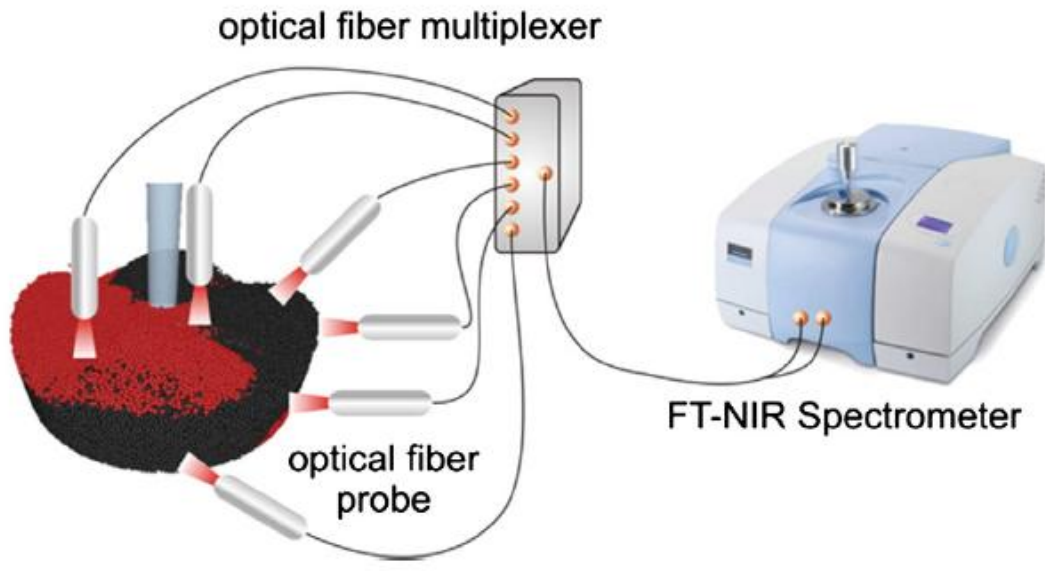


(a)

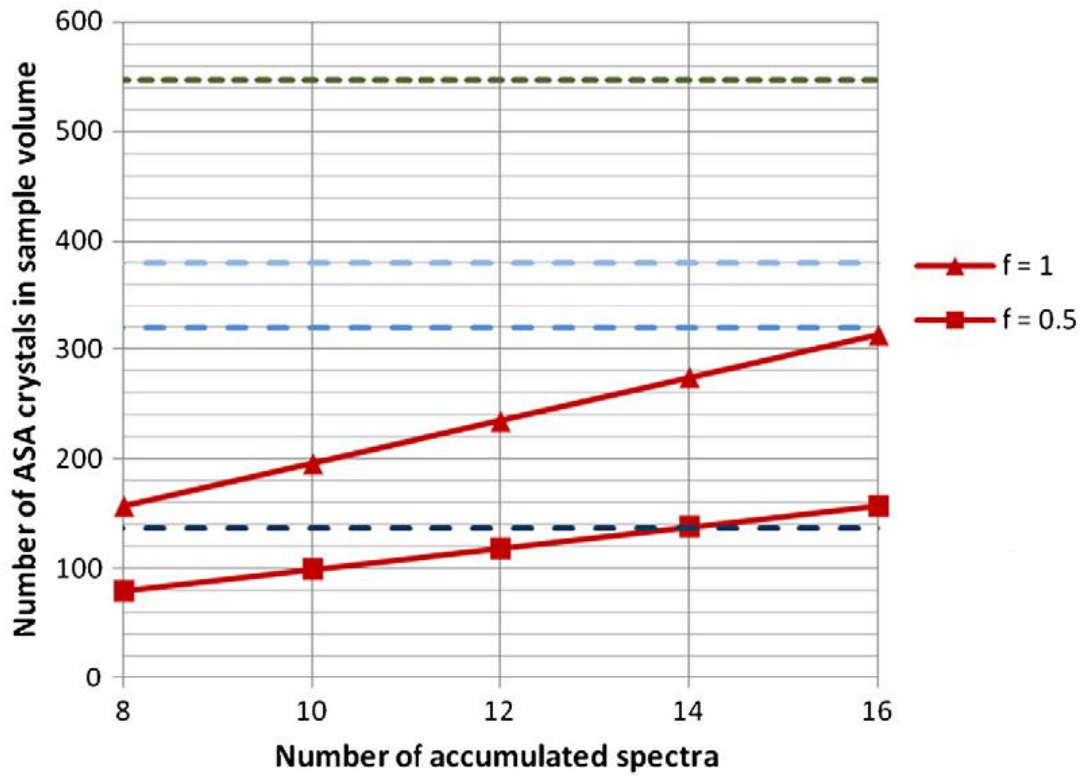


(b)

**Fig. 16.** (a) Experimental of an in-line NIR setup with a four-bladed mixer connected to a controllable mixing device and (b) blending plots for the mixer, light grey represents acetyl salicylic acid (ASA) and dark grey shows  $\alpha$ -lactose Monohydrate, (Reprinted from Koller et al. [119]).



(a)



(b)

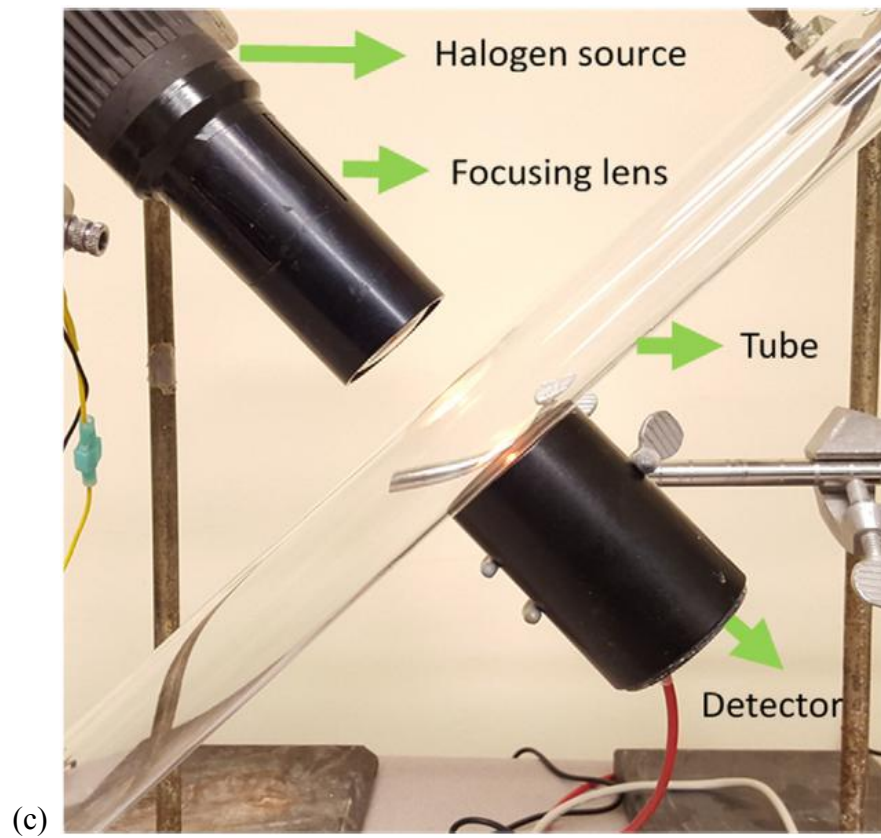


**Fig. 17.** (a) Schematic of multi-probe spectroscopy setup, (b) dependence of the sample volume size to the number of accumulated spectra and the moving speed in front of the sensor window ( $f = 1$  is the tip speed of the blade,  $f = 0.5$  is half of this speed) and (c) continuous blend monitoring of powder streams using transmission NIR, (Reprinted from Scheibelhofer et al. [121] and Reprinted from Alam et al. [122]).

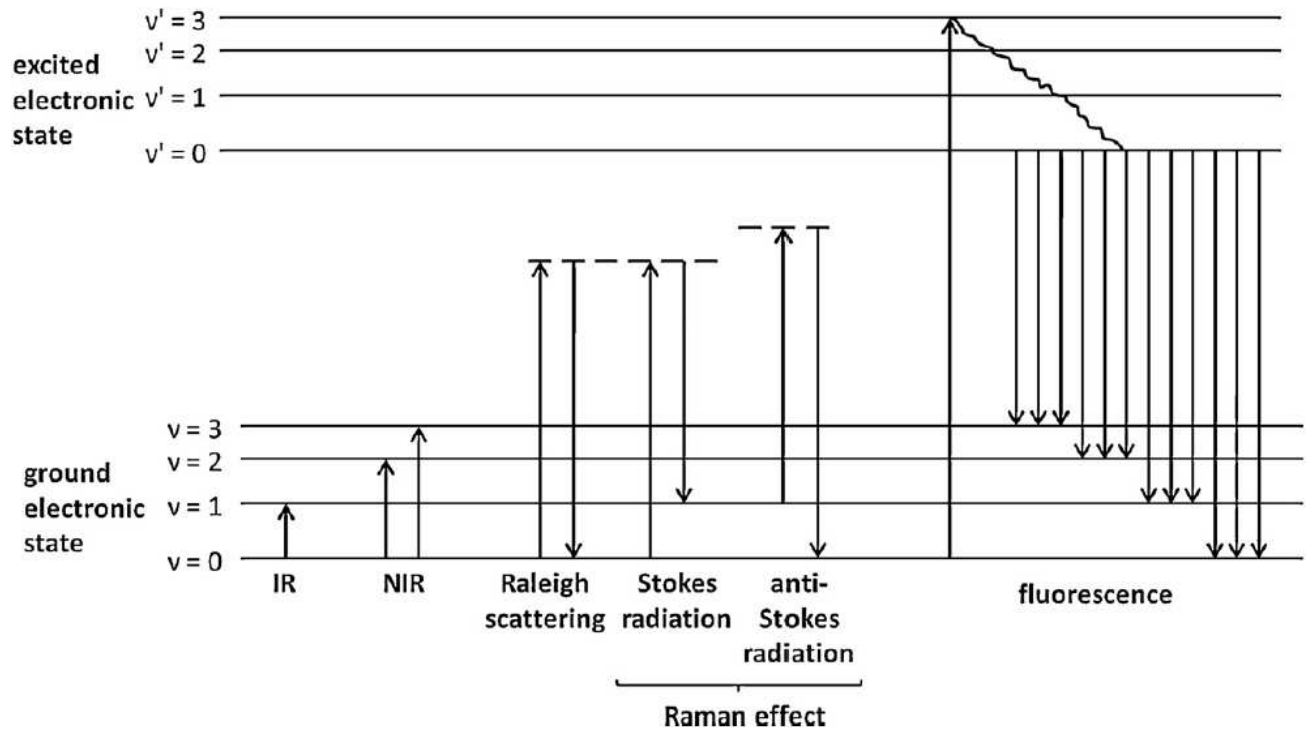


**Fig. 18.** IR and NIR absorption, the Raman effect and fluorescence, (Reprinted from De Beer et al. [25]).

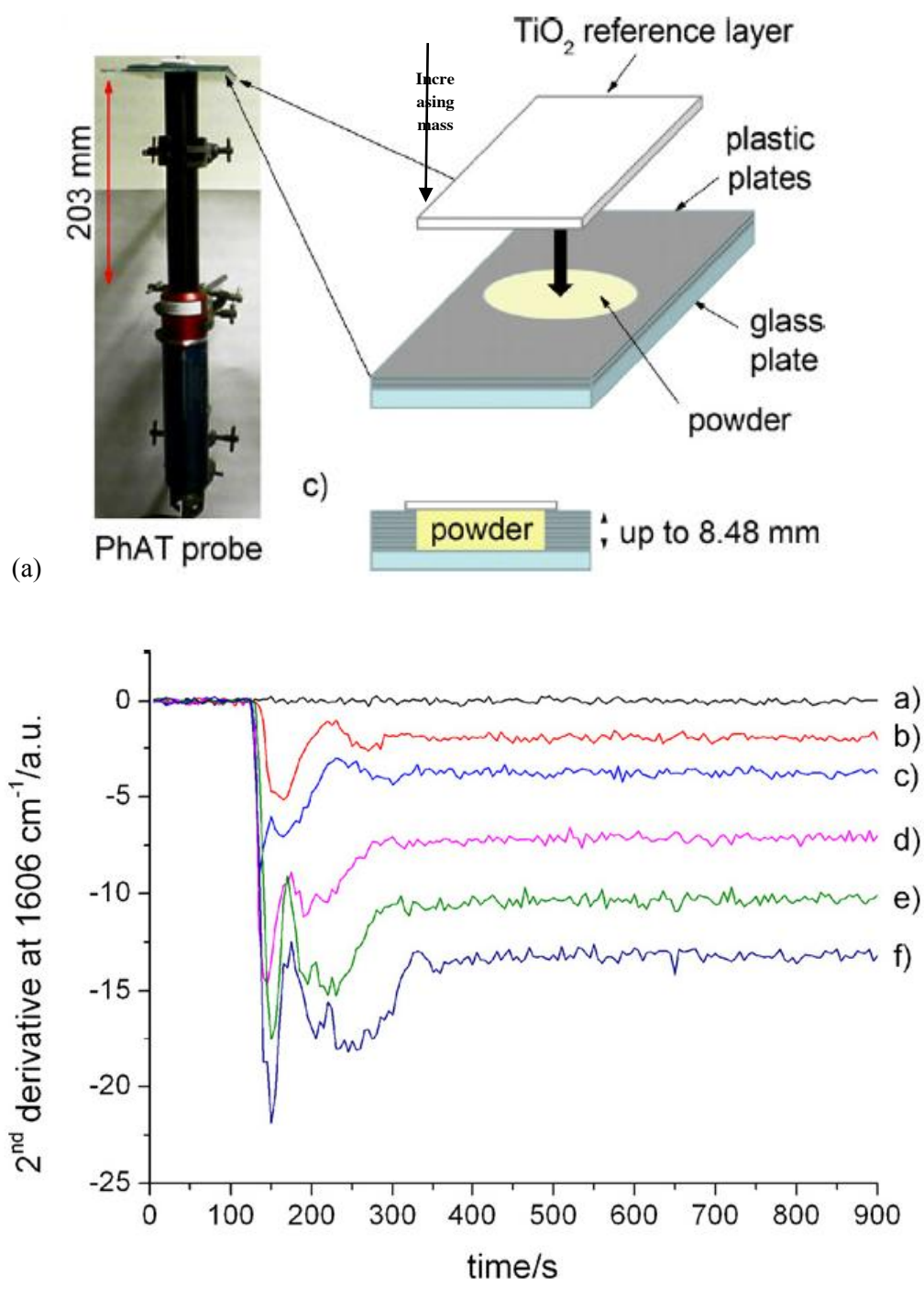
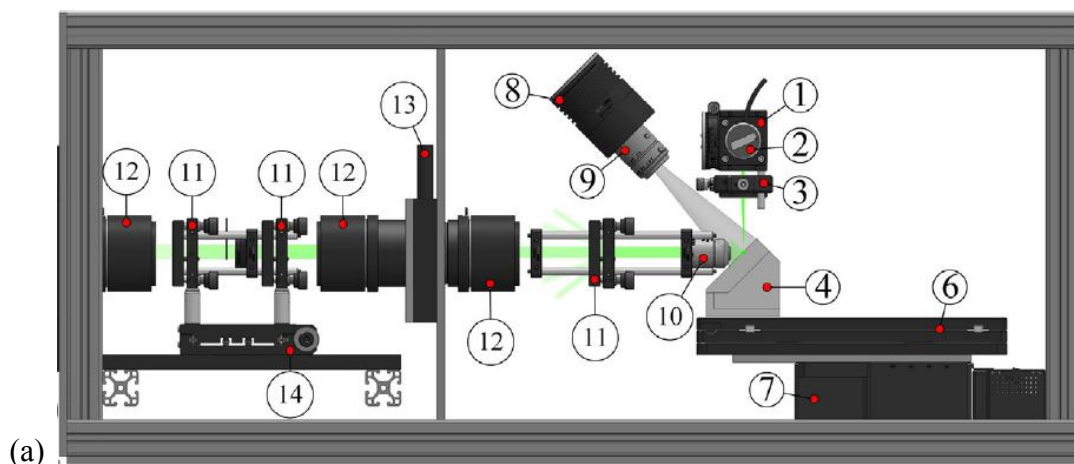


**Fig. 19.** (a) Schematic of Raman PhAT probe and sample set up and (b) Raman PhAT probe mixing profiles at  $1606 \text{ cm}^{-1}$  for the case of the addition of different amounts of aspirin to Avicel, (Reprinted from Allan et al. [125]).





(1) UV fused silica broadband plate splitter, (2) power meter, (3) plano-convex lens, (4) aluminum block, (5) square pin stub holder, (6, 7) motorized X-Y-Z stage, (8) illuminating lamp, (9) monitoring camera, (10) microscope, (11) narrow-band notch filters, (12) Nikon lenses, (13) manual slit, (14) filters.

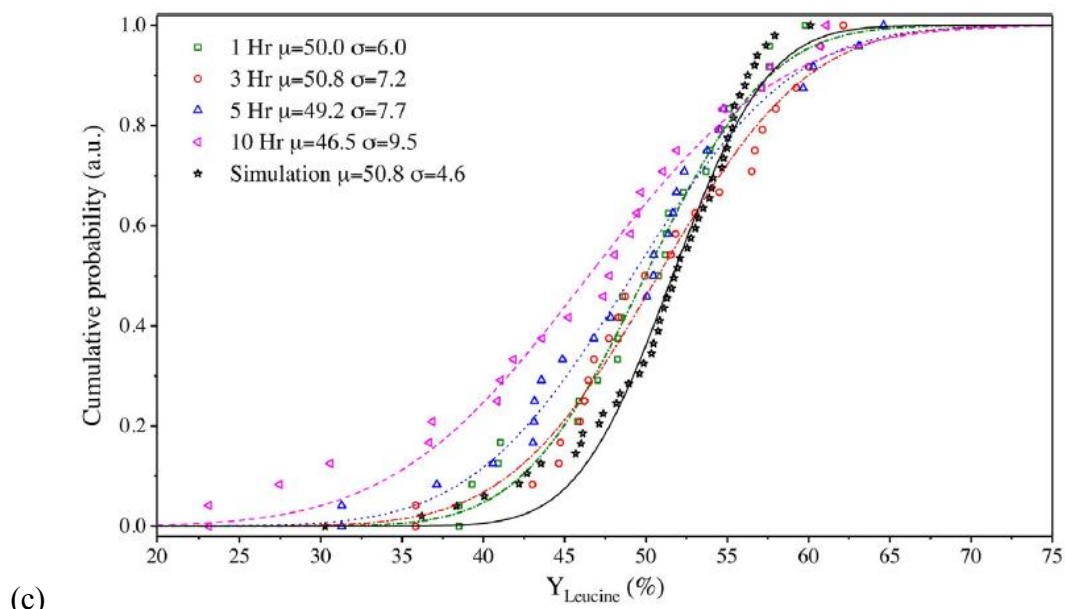
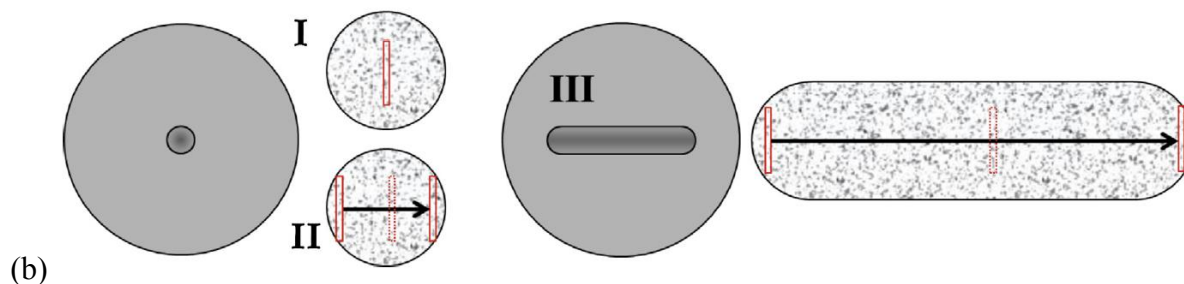
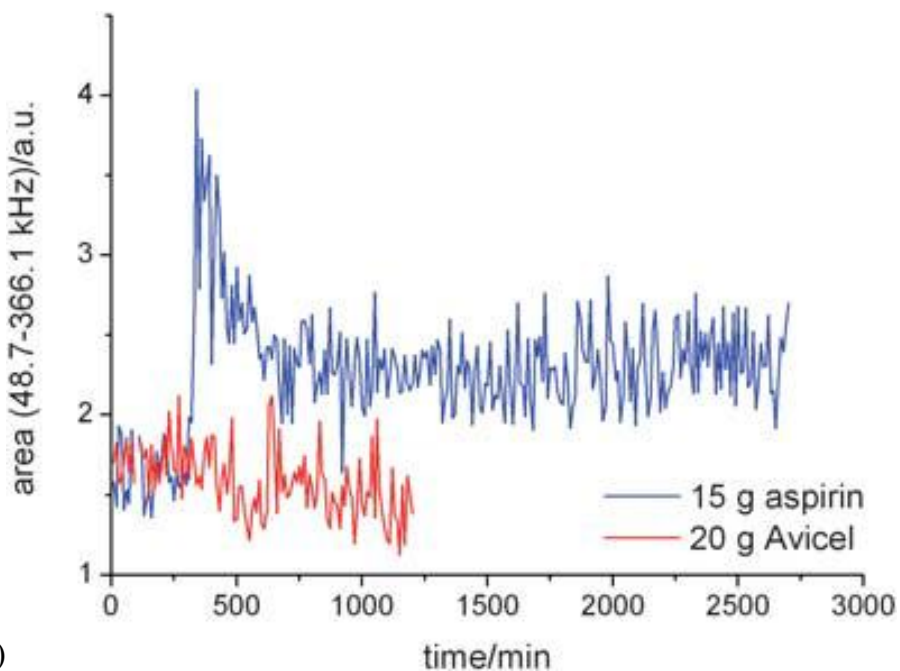
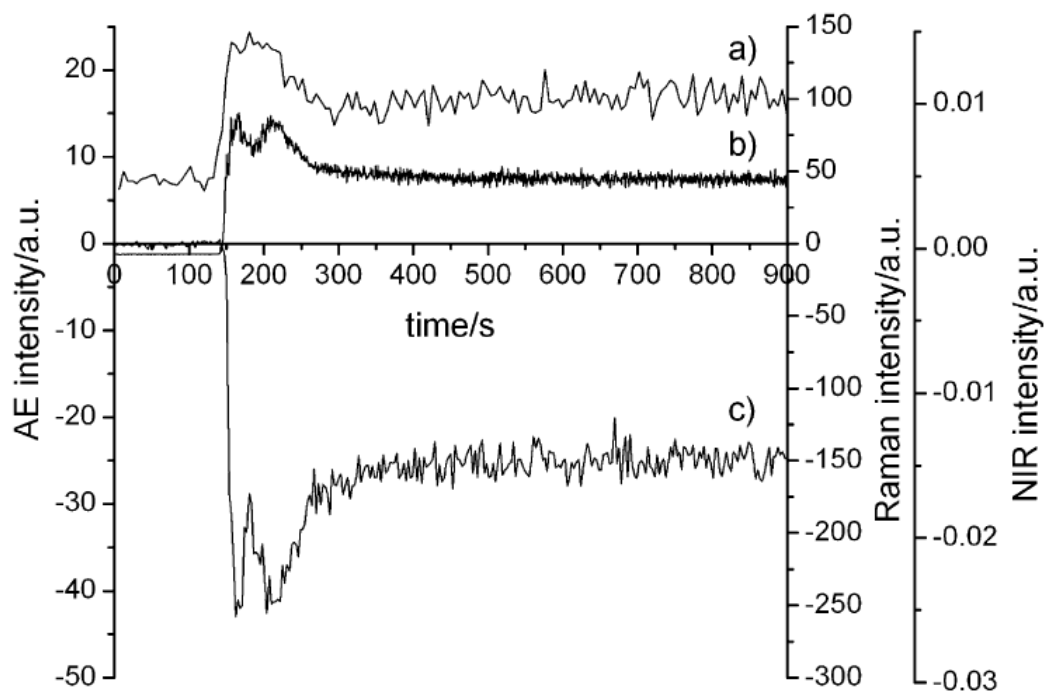


**Fig. 20.** (a) Dispersive macro-Raman Set-up, (b) different sampling methods: single spot (I), scanning across the cavity (II), scanning along the groove (III) and (c) cumulative distributions of the measured leucine mass fraction during mechanical mixing, (Reprinted from Wang et al. [126]).

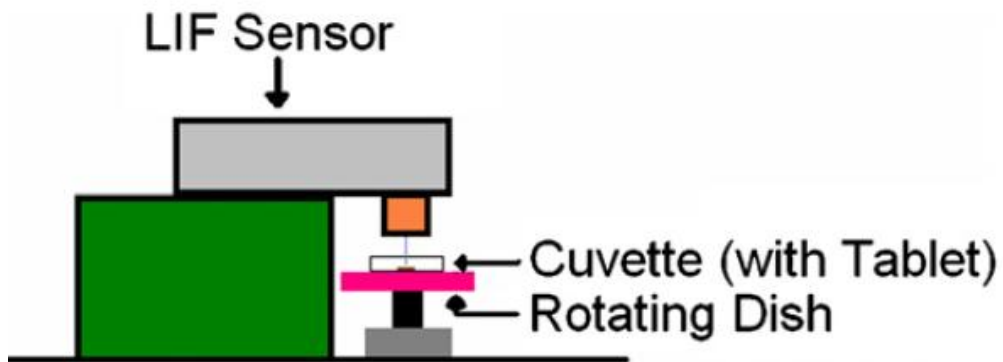


(a)

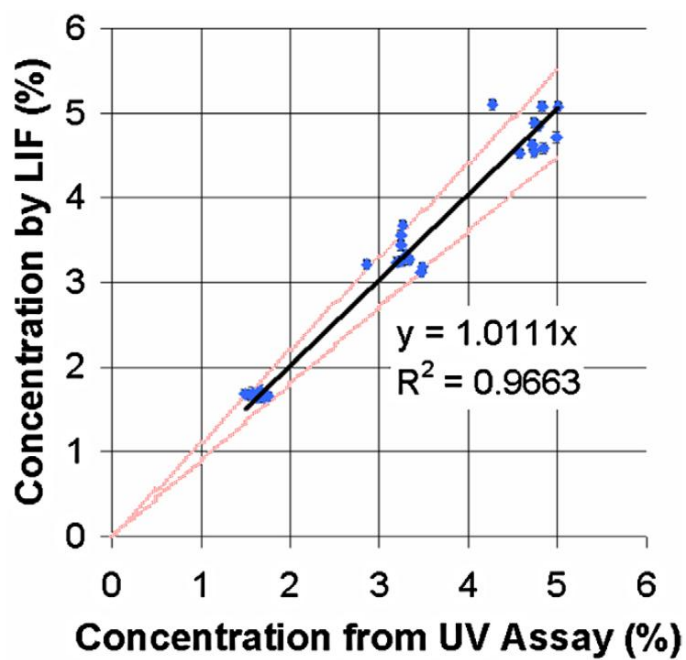


(b)

**Fig. 21.** (a) Acoustic emission mixing profiles and (b) mixing profiles for the addition of 30 g aspirin to 75 g Avicel, (Reprinted from Allan et al. [125, 132]).



(a)



(b)

**Fig. 22.** (a) LIF instrument and (b) triamterene concentration obtained using LIF and UV analysis, (Reprinted from Domike et al. [135]).

**Table 1.** Research works based on image analysis for powder blend uniformity evaluation.

<b>Objectives</b>	<b>Instrument for the image analysis</b>	<b>Reference</b>
<p>Investigation of a double cone system for the mixing of glass beads of different colours:</p> <p>Mixing performance has been done by computing the concentration of each species in each discretized square</p> <p>MATLAB software was used to determine the number of particles in discretized images</p>	<p>Camcorder at the rate of 40 frames per second</p>	<p>[52]</p>
<p>-Investigation of the component distribution of counterfeit Viagra and Cialis tablets using image processing:</p> <p>Bhattacharyya distance was performed as a measure of mixture quality</p>	<p>Video Spectral Comparator (A high resolution VSC 5000)</p>	<p>[53]</p>
<p>-Evaluation of the segregation in pseudo-2D beds using a state-of-the-art digital colour camera:</p> <p>Sample colour variance was performed as a measure of mixture quality</p>	<p>A digital image analysis technique (AT-200 GE)</p>	<p>[54]</p>
<p>-Investigation of the component distribution of dropping glass beads with two different sizes using image analysis method:</p> <p>Image obtained by the camera was converted to an indexed image using MATLAB software</p> <p>Two indices (<math>I_L</math> and <math>I_H</math>) were used to distinguish</p>	<p>Nikon D70 digital camera</p>	<p>[55]</p>

between the segregation and stratification mechanisms.		
<p>-Segregation analysis of horizontally shaken monolayers of different binary mixtures on a vibrating tray:</p> <p>The position of individual components was estimated using image processing, developed in MATLAB software</p>	CCD Nikon camera	[56]
<p>-Evaluation of the mixing time of coloured particles in a rotary drum:</p> <p>RGB colour analysis was provided using image Processing Toolbox provided by MATLAB software</p> <p>Degree of particle mixing was described using variance method</p>	Video camera at a frame rate of 25 fps	[57]
<p>-Evaluation of the effect of paddle rotational speed on the mixing performance of the agitation process in a electrophotographic system:</p> <p>The beads velocity field during agitation was used to describe the mixing extent</p>	High speed camera (MotionPro HS-4)	[58]
<p>- Investigation of the mechanism of dead zone formation:</p> <p>The effect of different mixing parameters (size, packing of particles, speed and shape of the mixer)</p>	Canon EOS 600D camera	[59]

on the degree of mixing was evaluated.		
--	--	--

**Table 2.** Summary of different tomographic techniques for powder mixing assessment.

No.	Objective	Materials	Technique	Reference
1	Mixing investigation of binary mixtures of free flowing particles in a Turbula® mixer	Sugar beads	MRI	[93]
2	Characterization of the kinematics of mixing/size segregation of dried binary mixtures	Poppy seeds and sugar beads	MRI	[94]
3	Investigation of the solid concentration changes during granular flow in a cylindrical model silo	Different type of sands	ECT	[95]
4	Evaluation of the size segregation in a cold fluidized bed at atmospheric pressure	Spherical glass particles	ECT	[96]
5	Evaluation of the mixing and segregation in a fluidized bed	Ground walnut shell particles and glass beads	μCT	[97]
6	Assessment of the mixing in an industrially static	Glycerol	Combined PEPT and	[98]

	mixer geometry		MRI	
7	Estimation of the spatial distribution of components throughout the tablets	Potassium chloride, spray-dried lactose	$\mu$ CT	[99]
8	Investigation of the axial mixing and segregation of fuel at different operational conditions of bubbling fluidized bed	Tracer particles with solid density representing biomass char	Magnetic particle tracking (MPT)	[100]

**Table 3.** Current researches investigating the powder blend uniformity using NIR system.

No.	Objective	Instrument	Blending materials	Reference
1	End-point determination of a pharmaceutical blending	Sentronic GmbH NIR spectrometer	API (Active Pharmaceutical Ingredient), crospovidone, lactose, and microcrystalline cellulose	[103]
2	Application of Near Infrared hyperspectral imaging for the evaluation of the spatial distribution of drugs in tablets	OPOTEK Inc. NIR system	Tolmetin sodium dehydrate, anhydrous lactose, magnesium stearate	[104]
	Evaluation of the effects	FT-NIR spectrometer	Aspirin, lactose,	[105]



3	of granule cohesion and size on the in-homogeneity tendency of pharmaceutical powders using NIR spectroscopy, bench scale sifting and fluidization segregation testers		microcrystalline cellulose, magnesium stearate	
4	Application of an in-line NIR spectroscopic method for the measurement of drug content of tablets during a continuous tableting process	Visio NIR	Acetaminophen, lactose and magnesium stearate	[106]
5	Implementation of a multi-point fiber optic based on NIR set-up to control the drug concentration at the discharge of a continuous mixer, comparison between in-line and off-line measurements	Multipoint NIR system	Acetaminophen, magnesium stearate and Avicel PH-200	[107]
6	Investigation of an in-line NIR spectroscopy for content uniformity analysis in an industrial tablet press	NIR spectrometer	API, EX1 (excipient1) and EX2	[108]

7	Non-contact monitoring of the blending process in pharmaceutical powder blends	NIR spectrometer	APAP, Avicel, Lactose	[109]
8	Evaluation of powder blend uniformity of a cohesive model formulation using a real-time NIR spectroscopy and an at-line NIR chemical imaging approach	Integrated Corona NIR spectrometer from Zeiss	Naproxen (API), microcrystalline cellulose, croscarmellose and free-flowing mannitol	[110]
9	Rapid determination of four structurally similar active pharmaceutical ingredients using a developed at-line Near Infrared method	A Bruker multi-purpose FT-NIR analyzer	Four APIs, microcrystalline cellulose as excipient	[111]
10	Investigation of the mixing performance of a laboratory-scale Resonant Acoustic® Mixer (LabRAM). The effect of process parameters (fill level, acceleration, and blending time) was considered	Transform Near-Infrared (FT-NIR) spectrometer	Micronized acetaminophen, granulated acetaminophen and caffeine	[112]

<b>11</b>	Evaluation of the blend mixing in a continuous/dynamic drug product manufacturing process	Fourier transform spectrometer	Acetaminophen, microcrystalline cellulose, mannitol, croscarmellose sodium, magnesium stearate	[113]
<b>12</b>	Investigation of NIR spectroscopy for overall quantitative analysis of all ingredients of laundry detergents	Bruker Multi Purpose Analyzer	Washing powder ingredients	[114]
<b>13</b>	Evaluation of NIR spectroscopy technique for the quality control of semi-solid pharmaceutical formulations	NIR spectrometer	Nonionic hydrophilic cream, Salicylic acid and Erythromycin	[115]

**Table 4.** Powder uniformity assessment techniques with their advantages and disadvantages.

<b>Method</b>	<b>Advantage</b>	<b>Disadvantage</b>
UV-visible absorbance spectrophotometry	<p>Simple to implement: Spectrophotometers are fairly straightforward instruments with very few moving parts</p> <ul style="list-style-type: none"> <li>- Fast analysis</li> <li>- Low cost maintenance</li> </ul>	<ul style="list-style-type: none"> <li>-Material is not recoverable using this method as it is dissolved in a solution (wet technique)</li> <li>-The sensitivity of a spectrophotometer is often inadequate at low concentrations</li> </ul>

		<ul style="list-style-type: none"> <li>-Absorption results can be influenced by other parameters, e.g. impurities, temperature and pH, leading to inaccurate results</li> <li>-Not a green method, as it produces liquid waste</li> <li>-Separate measurement of multi component fractions is not applicable</li> <li>-Error due to off-line sampling and disturbance of the powder bed (invasive)</li> </ul>
<p style="text-align: center;">High-Performance Liquid Chromatography</p>	<p style="text-align: center;">Accurate and sensitive for multi component quantification</p>	<ul style="list-style-type: none"> <li>-Costly and time consuming</li> <li>-Material is not recoverable using this method as it is dissolved in a solution (wet technique)</li> <li>-Not a green method, as it produces liquid waste</li> <li>-Error due to off-line sampling and disturbance of the powder bed (invasive)</li> </ul>
<p style="text-align: center;">Image analysis</p>	<p style="text-align: center;">- Simple to use</p>	<p style="text-align: center;">-No information on 3D</p>

	<ul style="list-style-type: none"> <li>-Green method (dry technique)</li> <li>- Low cost</li> <li>-Possible for blend uniformity assessment of multicomponent mixtures (providing that particles differ in colour)</li> <li>-Sample analysis can be performed non-intrusively</li> </ul>	<p>structure of powder mixtures (this method is surface sensitive). Nevertheless, if coupled with the slicing technique, the internal structural analysis of mixture could be provided</p> <ul style="list-style-type: none"> <li>-Cannot be used for uniformity assessment of powder components with the similar colours</li> <li>-Because of lighting conditions, the raw images need background correction</li> </ul>
<p style="text-align: center;">Electrical conductivity method</p>	<ul style="list-style-type: none"> <li>-Providing information on the whole volume of powder mixture</li> <li>-Easy to use</li> <li>-Low cost</li> <li>-Good for uniformity analysis of conductive materials</li> </ul>	<ul style="list-style-type: none"> <li>-Only applicable for blend uniformity assessment of a conductive material in the mixture of powders</li> <li>-Cannot be used for multicomponent mixing assessment</li> </ul>
<p style="text-align: center;">Tribo-electrification method</p>	<ul style="list-style-type: none"> <li>-Providing information on the whole powder mixtures</li> <li>-Easy to use</li> </ul>	<ul style="list-style-type: none"> <li>- Error due to off-line sampling and disturbance of the powder bed (invasive)</li> <li>-Unreliable tool because it</li> </ul>

	<ul style="list-style-type: none"> <li>-Economic</li> </ul>	<p>may be exposed to the variations in humidity, temperature and other environmental factors</p> <ul style="list-style-type: none"> <li>-Cannot be used for multicomponent mixing assessment</li> </ul>
Thermal analytical method	<ul style="list-style-type: none"> <li>-Easy to use and Low cost</li> <li>-Providing information on the whole powder mixture</li> <li>-Good for the determination of the end-point of mixing</li> </ul>	<ul style="list-style-type: none"> <li>-Error due to off-line sampling and disturbance of the powder bed (invasive)</li> <li>-Measurement must be performed quickly after sampling to reduce the heat exchange effect</li> <li>-This method should be checked on several powder systems with complex thermal event to judge whether it is suitable for powder uniformity assessment in general</li> </ul>
X-ray microtomographic method	<ul style="list-style-type: none"> <li>-Providing the three-dimensional structure of the objects non-invasively</li> <li>-Higher special resolution as compared to other tomographic techniques</li> </ul>	<ul style="list-style-type: none"> <li>-Expensive</li> <li>-Cannot be readily used for multicomponent mixing assessment</li> <li>-Safety issues due to X-rays</li> <li>-Material with similar structural properties cannot be</li> </ul>

		differentiated easily
Positron emission particle tracking	<ul style="list-style-type: none"> <li>-Produces a three-dimensional image of a process</li> <li>-Non-invasive uniformity evaluation of powders is achievable</li> </ul>	<ul style="list-style-type: none"> <li>-Expensive</li> <li>-This method mainly provides the tracking of a single particle as a representative of other particles</li> <li>-Cannot be used for multicomponent mixing assessment</li> <li>-Erroneous locations could be spotted using this technique due to scattering of gamma rays</li> </ul>
Electrical capacitance tomography	<ul style="list-style-type: none"> <li>-Providing the 3D cross-sectional view of a stream non-intrusively</li> <li>-Applicable in many harsh conditions such as high-pressure or high temperature</li> </ul>	<ul style="list-style-type: none"> <li>-Expensive</li> <li>-Hard to detect the exact component distribution due to low spatial resolution</li> <li>-This method is applicable just for powders with noticeable variation in permittivity or dielectric constant</li> <li>-Cannot be used for multicomponent mixing assessment</li> </ul>
Magnetic resonance imaging tomography	<ul style="list-style-type: none"> <li>-Providing information on 3D powder mixtures by constructing</li> </ul>	<ul style="list-style-type: none"> <li>-Expensive</li> <li>-Many particles get visible by</li> </ul>

	<p>cross-sectional images of raw data non-invasively</p>	<p>magnetic field via getting coated by detectable substances. This could change the surface properties of particles such as flowability</p> <p>-Cannot be readily for multicomponent mixing assessment</p>
Near-infrared spectroscopy	<p>-Fast chemical imaging technique</p> <p>-On-line/continuous monitoring of samples is possible using this technique</p> <p>-Applicable for multicomponent mixing assessment</p> <p>-Reasonable in price</p>	<p>-Overlapped spectra cause the minor component detection difficult</p> <p>-Light penetration to the sample is limited and therefore composition characterisation of the bulk of powders is hard to be achieved.</p>
Raman spectroscopy	<p>-Less overlapped spectra resulting in precise minor component detection (high spatial resolution)</p> <p>-Applicable for multicomponent mixing assessment</p>	<p>-Sometimes, interference by florescence may cause erroneous results</p> <p>-Expensive</p>
Acoustic emission spectrometry	<p>-Non-invasive/on-line particulate blend monitoring</p> <p>-Economic and easy to use</p> <p>-For on-line monitoring, no need of optically transparent window in the</p>	<p>-Representative for changes in powder composition at wall, rather than in the bulk of materials</p>



	process	
Fluorescence spectroscopy	<p>-Low cost and fast in data acquisition</p> <p>-Sensitivity of the method is higher than the absorption spectroscopy</p>	<p>-Sensitive to fluctuations in pH and temperature.</p> <p>-Applicability of the method depends on the strength of fluorescence of the studied component as compared to the fluorescence of other components within the mixture</p>